Aus dem Institut für Chirurgische Forschung
(im Walter-Brendel-Zentrum für Experimentelle Medizin, WBex)
der Ludwig-Maximilians-Universität München
Vorstand Prof. Dr. med. Ulrich Pohl

Endothelial cell-specific deletion of the mitochondrial thioredoxin reductase impairs vascular remodelling

Dissertation zum Erwerb des Doktorgrades der Humanbiologie (Dr. rer. biol. hum.)
an der Medizinischen Fakultät der

Ludwig-Maximilians-Universität zu München

Vorgelegt von
Julian Kirsch

aus
Melbourne, Australien

2014

Mit Genehmigung der Medizinischen Fakultät

der Universität München

Berichterstatter:	Prof. Dr. med. Ulrich Pohl
Mitberichterstatter:	Priv. Doz. Dr. Kai Hell
	Prof. Dr. Jens Waschke
Mitbetreuung durch den promovierten Mitarbeiter:	Dr. med. vet. Heike Beck
Dekan:	Prof. Dr. med. Dr. h.c. M. Reiser, FACR, FRCR
Tag der mündlichen Prüfung:	15.05.2014

Table of Contents

Index of Tables

Index of Figures

1 Introduction

1.1 Reactive Oxygen Species

For many years, reactive oxygen species (ROS) were viewed as detrimental and as undesirable due to their capacity to cause significant harm when their levels are too high, a condition termed oxidative stress. Since these readily reactive molecules, including superoxide anion (O_2^-•), hydrogen peroxide (H_2O_2), hydroxyl radicals (HO•) and peroxynitrite anions ($ONOO^-$), were initially only regarded as an exhaust of cellular energy production, ROS were quickly categorised as harmful: they were shown to deactivate proteins, cause damage to DNA and ultimately lead to cellular apoptosis. Furthermore, levels of ROS were found to positively correlate with processes of aging as well as with a wide array of diseases, ranging from diabetes and cancer to neurodegeneration and cardiovascular pathologies.

It is therefore not surprising that a great deal of effort has been invested in understanding how ROS are produced and how to decrease oxidative stress. As research progressed, it became apparent that the role of reactive oxygen species went beyond solely being a nuisance. Rather, elucidation of the cellular machinery which maintains ROS within a narrow range of concentrations enabled researchers to understand that ROS participate in vital cellular processes such as signalling, and regulation of transcription factors and proper protein function.

1.1.1 Regulation of Reactive Oxygen Species

For these reasons, it is essential for a cell to tightly control intracellular levels of ROS. In order to avoid excessive concentrations of ROS, endogenous or nutritional antioxidants such as glutathione, cysteine, uric acid, coenzyme Q, ascorbic acid (vitamin C), α-tocopherol (vitamin E) or carotenoids are commonly available. Furthermore, cells are equipped with a range of highly efficient antioxidant enzymes, including superoxide dismutases (SOD), catalases, peroxiredoxins (Prx), the glutathione peroxidases and glutathione reductase, and the thioredoxin systems. The latter family of enzymes, together with glutathione, are now considered the major regulators of cellular redox states [1]. Dysfunctionality or lack of any of these antioxidants can lead to detrimental effects associated with oxidative stress.

1.2 Mammalian Thioredoxin System

In mammals, enzymes belonging to the Thioredoxin family have been identified at distinct cellular locations. The most extensively researched enzymes, the oxidoreductases thioredoxin 1 (Txn1) and

thioredoxin reductase 1 (Txnrd1) are predominately present in the cytosol while the mitochondrial equivalents, thioredoxin 2 (Txn2) and thioredoxin reductase 2 (Txnrd2), have only recently gained attention. Cytosolic and mitochondrial thioredoxin systems have much in common; their main activity is focussed on maintaining proteins in a reduced state. An additional member of the thioredoxin family – TGR – was identified in the testes and its function differs from the cytosolic/mitochondrial equivalents in regard to its substrates, as TGR can reduce both thioredoxins and glutathione [2].

1.2.1 Thioredoxins

Irrespective of their site of expression, thioredoxins share a conserved -Cys-Gly-Pro-Cys- active site, enabling them to function as disulfide oxidoreductases [3]. Initially, Txn was described as a hydrogen donor for ribonucleotide reductase, thus affecting DNA synthesis [4]. Today, it is well established that thioredoxins participate in a much wider context of cellular redox regulation by reversible oxidation and reduction of the cysteine residues in their active site and are now considered the major protein disulfide reductase in a cell [3]. In their reduced state (Txn-$(SH)_2$), Txns can reduce disulfide bonds in proteins, thereby taking the oxidative burden upon themselves (Txn-S_2). A lack of either Txn has been described to be embryonically lethal, thus emphasizing their vital importance [5, 6]. This apparent importance is further manifested by the now well established plethora of roles of Txn.

Thus, it has been shown that the cytosolic thioredoxin 1 (Txn1) can affect DNA transcription, for example by inducing NFκB transcriptional activity via reduction of a disulfide bond in the p50 subunit [7]. However, the opposite effect on NFκB transcriptional activity has also been reported [8]. These authors suggest that the activity-enhancing effect on NFκB is possibly due to Txn1 affecting the DNA-binding capacity of the transcription factor, whereas the inhibitory effect is due to Txn1 preventing the liberation of NFκB from its inhibitor, IκB. Txn1 can also affect the transcriptional activity of the glucocorticoid receptor by directly affecting the receptor's DNA binding domain and by stabilising the steroid-binding conformation of the ligand-binding domain [9, 10].

Txn1 can also exert growth-promoting effects and as such has been shown to increase the proliferation of a range of solid tumour lines, possibly by increasing the susceptibility of receptors for autocrine growth factors [11]. In line with this finding, Txn1 has been shown to be upregulated in a number of human cancers and also to inhibit drug-induced apoptosis in a manner requiring functional redox activity [12, 13].

In contrast to the disadvantages on tumour progression, beneficial effects of Txn1 in the cardiovascular system have been reported. Thus, increased levels of Txn1 have been shown to prevent cardiac hypertrophy and to adapt transgenic mouse hearts to ischemia as well as protect from subsequent reperfusion injury [14,15]. In line with these findings, the endogenous inhibitor of

Txn1, Thioredoxin-interacting protein (TXNIP), has been implicated in a range of cardiovascular diseases [16]. In this study, the authors showed that physiological fluid shear stress decreases TXNIP, resulting in effective Txn1 reductive capacity and protection from vascular inflammation and subsequent initiation of atherosclerosis. In a follow-up study, the authors also showed that the opposite holds true: increased TXNIP-dependent inhibition of Txn1 occurs at atheroprone sites exposed to disturbed flow [17].

Less is known on the protective or harmful effects of the mitochondrial equivalent of Txn1, Txn2. Since mitochondria are required for energy production and can also regulate critical cellular events, such as progression to cell death, the maintenance of homeostatic levels of ROS in mitochondria is vital. Damdimopoulos and colleagues demonstrated that Txn2 can modulate the response to the mitochondria-targeting cytotoxic compounds etoposide and rotenone, and that Txn2 is beneficial in the maintenance of a suitable mitochondrial membrane potential ($\Delta\Psi m$) [18].

In the cardiovascular system, overexpression of Txn2 has been shown to improve vasodilatory capacity, and to blunt blood pressure increases and reduce ROS production in response to chronic Angiotensin II infusion [19]. Interestingly, in this study the authors describe that the decrease in ROS production was not limited to mitochondrial sources: overexpression of Txn2 also attenuated the usual Angiotensin II-induced increases in NADPH oxidase subunit expression, thus altering the production of ROS in the cytosol and implying a cross-talk between mitochondria and NADPH oxidase-dependent ROS production. Furthermore, in mice Txn2 is downregulated in ECs during hind-limb ischemia and this occurs in parallel to increased ROS, leukocyte infiltration, activation of the transcription factor apoptosis signal-regulating kinase 1 (ASK1), and induction of apoptosis [20]. Endothelial-specific overexpression of Txn2, on the other hand, improved recovery, thereby demonstrating a vital role of this mitochondrial antioxidant in vascular remodelling [20].

1.2.2 Thioredoxin Reductases

In order for either Txn to regain their reducing capacity, they themselves must be reduced by their respective reductases. This occurs in a NADPH-dependent manner, as depicted in Figure 1-1. Txnrds are selenoproteins that must form homodimers to exert their reducing effects [21]. Txnrds consist of three domains: a NADPH domain, a flavin adenine dinucleotide (FAD) domain which receives reducing equivalents from NADPH, and an interface domain linking the two dimer subunits [22]. In addition to the N-terminal active site which receives electrons from NADPH, the C-terminus includes a selenocysteine (Sec) residue at its active site (-Gly-Cys-Sec-Gly-), thereby producing a reversible selenenylsulfide/selenolthiol [23]. Once the C-terminal selenolthiol motif has been formed, mammalian Txnrd can exert its reductive capacity upon a much wider range of substrates as is the case for Txnrds of bacteria or plants [23]. Apart from their main substrate Txn, Txnrds can also reduce glutaredoxin 2,

the endoplasmic reticulum calcium-binding proteins CaBP1 and CaBP2 and protein disulfide isomerase [23-25]. Furthermore, Txnrds can modulate the cytolytic activity of the antibacterial peptide granulysin, and Txnrd1 has been shown to reduce the glucose-responsive protein Thioredoxin-like 1 [23, 26, 27]. All these proteins share a certain sequence homology to Txn; a certain degree of diffusion of substrate specificity is thus not surprising. In addition to these aforementioned proteins, Txnrds have also been reported to directly reduce certain non-proteins substrates, such as selenium-containing compounds, dehydroascorbate (resulting in the reconstitution of ascorbate), cytochrome c and ubiquinone (Coenzyme Q10) [23, 28-30]. In the case of the latter two compounds, both constituents of the electron transport chain (ETS), Txnrds possibly play vital roles in mitochondrial health and could therefore also impact on the mitochondrial contribution to the progression to apoptosis. The wide range of substrates that can be reduced by Txnrds is possibly due to its two active sites, the N-terminal FAD motif and the C-terminal Sec-containing sequence, which can both accept substrates, further exemplifying the importance of these enzymes in the maintenance of cellular integrity.

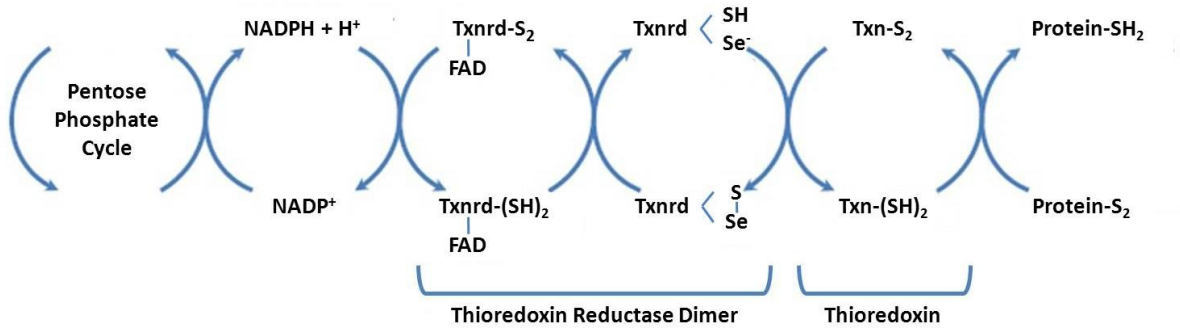

Figure 1-1: General outline of thioredoxin system functionality. NADPH functions as electron donor to FAD which passes the electrons to the N-terminal redox active site of one Txnrd subunit. Subsequently, electrons are transferred to the C-terminal Gly–Cys–Sec–Gly active site of the other Txnrd subunit. Finally, oxidised Txn (Txn-S_2) is reduced by the second Txnrd subunit. Reduced Txn (Txn-$(SH)_2$) can then in turn reduce disulfide bonds in proteins. Image adapted from Holmgren & Lu 2010 [3].

It is therefore not surprising that systems lacking these enzymes or expressing only dysfunctional Txnrds are implicated in several pathological conditions. However, due to their considerable catalogue of substrates, it is difficult to differentiate between a direct influence of Txnrds and the oxidative defect of one of the substrates. A simplified view would be to expect that dysfunctional Txnrd leads to effects mirroring those of a lack of a certain substrate's activity. For example, the phenotype of mice lacking Txnrd1 would be identical to that of mice lacking Txn1. This, however, is not the case. While Txn1-deficient embryos die at the time of implantation (embryonic day 6.5) and

the inner cell mass fails to proliferate *in vitro* [5], mice lacking Txnrd1 on the other hand survive until embryonic day 10.5, albeit with growth retardation and developmental abnormalities in a variety of organs [31]. Thus, considering individual Txnrds as simple hydrogen donors for a limited number of substrates is insufficient when attempting to understand the precise role of these enzymes.

The downside of the functional antioxidative activity of Txnrds, regardless of substrate-dependent or independent effects, is however, that these reductases have been reported to be upregulated in a number of cancers. In support of this notion, Txnrd1 deletion in Lewis Lung Carcinoma cells not only retarded tumour growth, these cells rather resembled normal cells [32]. This finding is not surprising, considering that tumours grow in an environment of constant hypoxia, which is a stimulus for the production of ROS, a concept which will be discussed in more detail below [33]. Txnrd1 could thus favour tumour growth by decreasing the oxidative burden and for this reason Txnrd1 is being considered as a target for the treatment of cancer. In recent years, however, it has become evident that, at least for Txnrd1, the involvement of Txnrd1 in cancer progression is more complex than initially anticipated. Indeed, a recent study demonstrated a protective effect of Txnrd1 on chemically-induced liver cancer [34].

In comparison to the involvement of Txnrd1 in cancer, reports on this enzyme's function in the vascular compartment are limited. Pharmacological inhibition of Txnrd1 has been reported to attenuate the endothelium-dependent vasodilatory capacity of isolated mouse aorta in response to acetylcholine [35]. The authors suggested that this was due to the lack of the antioxidant effects of Txnrd1, leading to inactivation of nitric oxide (NO) as well as its ability to reverse protein S-nitrosylation. Of course, via its reducing capability, Txnrd1 may affect processes in the vasculature requiring functional activity of its array of substrates.

1.2.3 Mitochondrial Thioredoxin Reductase

Txnrd2 shows a high degree of sequence homology to Txnrd1 (84% for human Txnrd1 and Txnrd2), with the exception of an N-terminal extension on Txnrd2. This extension has been identified as a mitochondrial import sequence [36]. The similarity between the two enzymes is exemplified in Figure 1-2.

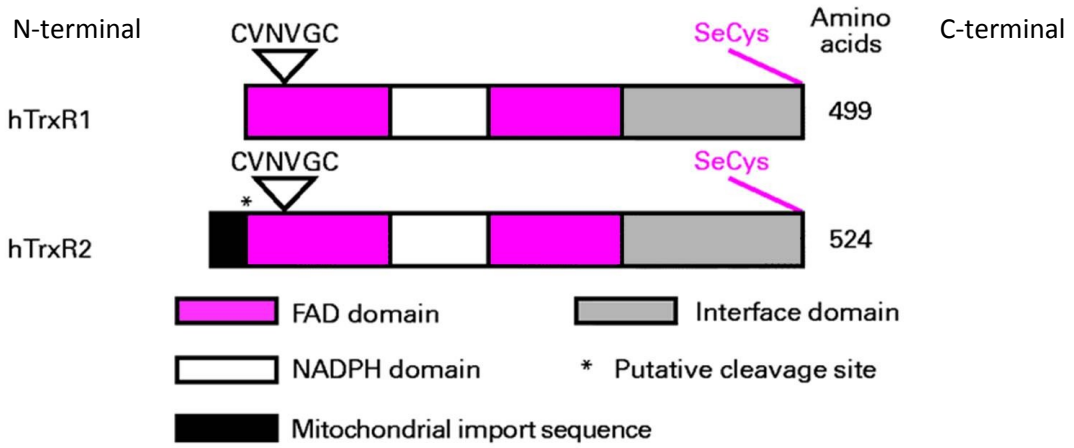

Figure 1-2: Domain structures of the human cytosolic and mitochondrial thioredoxin reductases. Triangles indicate the catalytic active sites of the reductases. Adapted from Mustacich et al., 2000 [36].

In comparison to Txnrd1, investigation of the role of Txnrd2 is less advanced. A recent study in our laboratory showed that a lack of Txnrd2 in mouse embryonic fibroblasts (MEFs) transfected with the pro-oncogenes c-myc and Ha-ras resulted in significantly smaller tumour volume when implanted subcutaneously in C57BL/6 mice. Tumour proliferation was impaired due to poor neovascularisation and a failure to stabilise HIF-1α [37]. In the cardiovascular system, Txnrd2 was shown to be indispensable for correct heart development as mice lacking Txnrd2 specifically in cardiomyocytes die shortly after birth due to dilated cardiomyopathy [38]. In a follow up study in inducible cardiomyocyte-specific Txnrd2 knockout mice, cardiac ischemia/reperfusion injury led to mitochondrial swelling, and increased cardiomyocyte death, functional impairment and larger infarct size relative to wildtype counterparts [39]. Resembling these findings, non-functional Txnrd2 with mutations in the highly conserved FAD domain have been shown to be present in some human patients with dilated cardiomyopathy, a form of congestive heart failure [40]. The importance of Txnrd2 in the heart is also revealed in embryos with a ubiquitous deletion of the enzyme. These embryos die prenatally (gestational day 13) and present profound defects in heart development and function. Furthermore, embryos with a ubiquitous lack of Txnrd2 suffer from significant impairments in haematopoiesis as well as severe anaemia and growth retardation compared to their wildtype or heterozygous counterparts [6, 38]. Thus, like its cytosolic counterpart, Txnrd2 is indispensable for normal development. Interestingly, the defects observed in mouse embryos with ubiquitous deletion of Txnrd2 do not resemble those in Txn2-deficient mouse embryos. A lack of Txn2 results in massive apoptosis, an open anterior neural tube, and ultimately lethality at gestational day 10.5, which coincides with the time point of mitochondrial maturation and the initiation of oxidative phosphorylation. Possibly, the maintenance of mitochondrial functionality beyond E10.5 is

compensated by other enzymes, such as Txnrd1 or by GSH-dependent redox activity [38]. In addition, the oxidative stress burden could also be relieved by other enzymes, e.g. mitochondrial glutathione reductase. Together these results suggest that Txnrd2 may also inhabit roles beyond Txn2 reduction. However, despite its similarity to Txnrd1, the catalogue of confirmed substrates for Txnrd2 is considerably smaller, with Txn2 considered the most efficiently reduced substrate. Whether this is due to structural differences of key residues around the redox active site of Txnrd2 or because of a different pH in mitochondria remains to be explained [21]. Possibly the identification of Txnrd2-specific substrates is solely limited due to the reduced variety of target candidates in the mitochondria compared to the cytosol.

1.3 Vasculature

Blood vessels serve to transport blood and its constituents pumped from the heart to the tissues and organs throughout the body. In mammals, the Aorta carries the bulk of blood expelled from the heart to the body, branching into muscular and adaptive arteries and ever smaller arterioles until the smallest vessels – the capillaries – are reached. Traversing the thin walls of the capillaries the transported oxygen, nutrients and other compounds move into the tissue and the exchange of metabolites for elimination occurs. The venous system, consisting of vessels with thinner, more distensible and less muscular walls then carries the blood back to the heart via small venules, larger veins and the venae cavae.

Blood vessels are constantly exposed to dynamic changes in volume, speed of flow and, due to their closed nature, pressures. For these reasons it is essential for blood vessels to be able to adapt. Short-term responses include vasodilatation and vasoconstriction and long-term adaptation to changed haemodynamics is achieved by alterations in vessel wall composition and thickness. To understand how these processes are initiated and regulated, the structure of blood vessels and signalling processes involved must be considered.

1.3.1 Structure of blood vessels

Depending on vessel type (artery or vein) and size (artery vs. arteriole vs. capillary) blood vessels consist of up to three layers: the tunica intima (innermost), tunica media (middle) and the tunica adventitia (outer layer), as displayed in Figure 1-3. The intima consists of endothelial cells (ECs) and the basal lamina, while the media is composed of contractile vascular smooth muscle cells (VSMCs) surrounded by collagen and elastin fibres, the latter constituting the boundary of this layer in form of the external elastic lamina. Finally, the adventitia, consisting mainly of connective tissue, tethers the

vessel to the surrounding tissue [41]. The smaller a vessel the fewer layers of muscle cells it contains in its wall. Thus, a capillary, for example, consists only of a single layer of ECs and the basal lamina, lacking smooth muscle cells altogether.

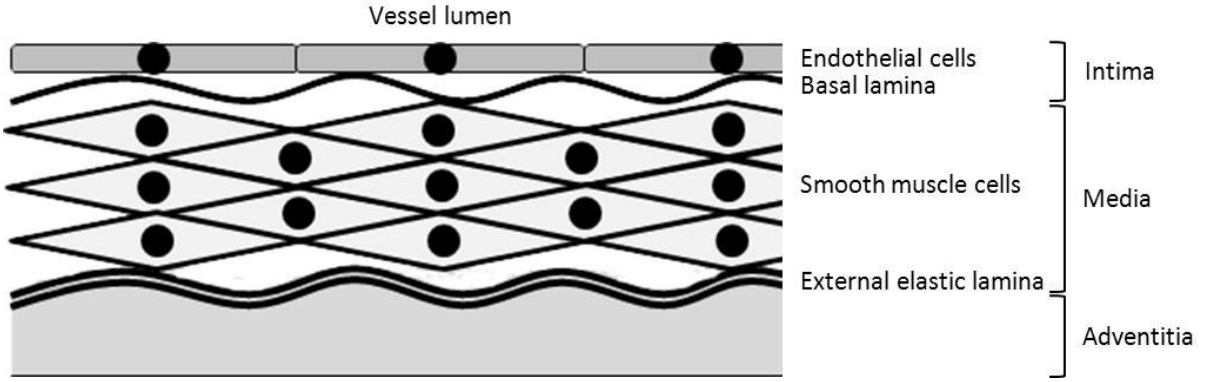

Figure 1-3: Wall structure of a blood vessel. Image adapted from Rowley et al., 2008 [42].

1.3.1.1 Endothelial Cells

Endothelial cells form the inner lining and are thus present in every blood vessel, from capillary to artery and vein. Therefore, they are directly exposed to the blood and its constituents, and as such regulate the transvascular movements of small molecules, can change vascular permeability as required, for example to allow the infiltration of leukocytes into the tissue, and can influence cells in other layers as well as circulating blood components in a paracrine and endocrine manner [43]. ECs are critical in maintaining vessel patency; a deregulation of coagulation via ECs can lead to thrombosis and atherosclerosis. Furthermore, ECs are exposed to haemodynamic forces in response to which they can produce and release vasoactive substances such as NO, leading to smooth muscle relaxation and vasodilatation. A dysfunctional endothelium can thus result in the development of hypertension, thereby initiating a myriad of possible pathological conditions ranging from heart failure to renal dysfunction.

While every cell of the vessel wall experiences stretch, for example to accommodate a change in pressure, ECs are the only cells of the vasculature exposed to changes in flow velocity, and as such are the sensors of fluid shear stress (FSS). FSS is the longitudinally acting force exerted on the endothelium by the friction the blood flow produces and has been proposed as an initial stimulus for vascular remodelling, the adaptation of the vessel wall to changes in haemodynamic forces and metabolic demands [44, 45]. How the endothelium senses FSS and which receptors and/or transducers are responsible is still under investigation. Structures on the apical surface of the endothelium, such as ion channels, G-Protein coupled receptors and receptor tyrosine kinases have been implicated as

well as integrins and focal adhesion kinases at the cell/matrix interface or proteins present within cell-cell junctions, such as PECAM1 [46].

1.3.1.2 Vascular smooth muscle cells

Vascular smooth muscle cells are responsible for the contractility of blood vessels and are therefore critical for the dynamic changes in vessel diameter and thus vessel conductance. The main function of a mature VSMC is contraction but these cells can also acquire a synthetic phenotype in which they significantly contribute to adaptive responses of blood vessels due to their plasticity and the production of matrix components [47]. As discussed in the above section, VSMCs especially require ECs to regulate their response to alterations in FSS.

1.3.2 Remodelling of blood vessels

In order to accommodate biomechanical changes, blood vessels can respond quickly, for example by vasodilatation or contraction. If an alteration in a biomechanical variable persists, however, long-term adjustments of the vessel wall must occur. Thus, capillaries can regress if they are no longer required or angiogenesis, the sprouting of new capillaries, can occur in order to maintain or establish perfusion to tissues requiring more oxygen and nutrients or to remove excess metabolites that could otherwise accumulate and be damaging. Likewise, arterioles must respond to chronic changes, for example by arteriogenesis, the remodelling of the vessel wall.

1.3.2.1 Angiogenesis

Sprouting of new capillaries is a process that can be as favourable as it can be damaging, depending on the tissue and the reason for capillary growth. A diabetic patient with an underperfused limb, for example, could benefit from the establishment of additional capillary networks. In cancer, on the other side, angiogenesis precedes the excessive growth of tumours by supplying vital blood-borne molecules. For these reasons, angiogenesis has received considerable attention and laboratories investigating numerous disease states have focussed efforts on elucidating the mechanisms involved.

The initiation of angiogenesis is generally believed to occur in response to hypoxia [48]. Low levels of oxygen stabilise the transcription factor Hypoxia-inducible factor-1α (HIF-1α) which, in turn, increases the transcription of members of the family of vascular endothelial growth factors (VEGF), the most important being VEGF-A [49]. Binding to and activation of its tyrosine receptor kinase VEGFR2 then stimulates EC proliferation, migration and sprouting, all hallmarks of angiogenesis [50]. Of course, these processes must be tightly regulated and depend not only of the release of VEGF-A in response to HIF-1α stabilisation and subsequent activation of VEGFR2. Rather, the formation of new capillaries requires the presence of at least a provisional scaffold favourable for migrating ECs which is created

by the extravasation of plasma proteins and activation of matrix metalloproteinases, the proteolytic release and activation of bound VEGF isoforms from the extracellular matrix, loosening of EC-cell contacts, and a cascade involving the activation or deactivation of compounds regulating further sprouting, such as angiopoietin 1 (Ang1), other members of the VEGF family, fibroblast and platelet-derived growth factors, angiostatin and endostatin [49, 50]. Ultimately, the vessels must mature by forming a functional lumen and fuse with the existing vessels which also requires a finely tuned coordination of VEGF isoforms, Ang1 and integrins as well as become stabilised by the recruitment of perivascular cells, in particular pericytes, to the basolateral surface [49].

Since ROS, apart from their detrimental effects at high, dysregulated levels, participate in important signalling cascades, it is not surprising to find several reports in the literature describing their contribution to the initiation and regulation of angiogenesis. The molecular background of ROS-mediated effects on vascular remodelling will be discussed in detail in the following section.

1.3.2.2 Arteriogenesis

In contrast to angiogenesis, where new capillaries sprout from an existing network in response to hypoxia, arteriogenesis as such does not involve the *de novo* formation of vessels. Rather, pre-existing vessels grow to larger conductance vessels in order to maintain or improve compromised tissue perfusion and meet a tissue's metabolic demands following the gradual obstruction of a major feeding vessel as is the case, e.g. in coronary heart disease. Arteriogenesis occurs naturally in slowly progressing peripheral artery occlusion or other cardiovascular diseases characterised by occlusion of main blood vessels. For this reason some patients experience no or only mild symptoms despite significant occlusions of essential vessels [51]. Today, pharmacological stimulation of arteriogenesis is being investigated as a possible therapeutic option to overcome limitations in the treatment of occlusive vascular diseases, either to minimise invasive surgery or as an alternative to standard therapies where contraindications or untreatable lesions prevent successful restoration of tissue perfusion [51].

A simplified view would be to condense the stimulatory mechanisms involved in arteriogenesis to changes in haemodynamic forces, such as a drop in pressure across a vessel's length, increased FSS and cyclic stretch. However, the regulation and progression of arteriogenesis requires a finely tuned molecular machinery and the participation of a multitude of other factors and perivascular cells. Initial investigations of arteriogenesis were hampered by the expectation that the regulation will share similarities with angiogenesis [51]. In contrast to angiogenesis, however, arteriogenesis has been shown to occur independently of a drop in O_2 tension and subsequent hypoxic signalling, and does not involve, at least directly, an increase in VEGF [52]. Rather, it has been suggested that an increase in

FSS is the main driving force, at least in the initial phases of arteriogenesis. Increasing evidence supports the suggestion that the occlusion of a conduit vessel indeed causes an increase in flow velocity in collateral vessels due to the sudden pressure drop between the prestenotic high pressure bed and the poststenotic low pressure bed [53]. It is well established that FSS can initiate complex signalling cascades, leading to a multifaceted response of the whole vessel. However, the effects of FSS on arteriogenesis upon flow obstruction in other vessels are often incomplete. Indeed, investigations on this topic consistently report that, while the remodelling of collateral vessels can provide a certain degree of compensation for stenosis, re-perfusion to levels equivalent to pre-stenotic values is rarely achieved. Rather, collateral development ceases before optimal adaptation is achieved [54]. This is most likely due to the flow-mediated dilation elicited by endothelial autacoids released upon the increase in FSS: release and subsequent relaxation of VSMCs leads to an increase in vessel diameter which is inversely proportional to FSS by the third power, ultimately producing a drop in FSS [53, 55]. This endothelial-initiated dilation is mediated by NO, prostacyclin PGI_2, endothelium-derived hyperpolarising factor (EDHF) and hydrogen peroxide (H_2O_2) [56]. Increased FSS results in a sustained production and release of NO from ECs until the subsequent vasodilatation is sufficient to return FSS to homeostatic levels [56]. This prolonged effect is in stark contrast to NO release upon receptor stimulation and is suggested to occur via the phosphorylation of specific serine residues of endothelial nitric oxide synthase (eNOS) by phosphatidylinositol 3-kinase and the serine kinase Akt [57]. While the identity and exact mode of action of EDHF is still extensively debated, it appears as a common denominator that involves potassium and possibly calcium-dependent potassium channels, ultimately hyperpolarising and relaxing vascular VSMCs [56]. Finally, ROS can also exert vasodilatory effects [58, 59]. During flow-mediated dilatation of human coronary resistance arteries, superoxide ($O_2^-\bullet$) production in the electron transport chain (ETC) complexes I and III of EC mitochondria increases, leading to augmented production and release of H_2O_2 [58]. The dilatation of vessels subsequent to the release of H_2O_2 has been suggested to occur via a mechanism involving calcium-dependent activation of eNOS, release of NO, increase in soluble guanylyl cyclase and formation of cyclic guanosine monophosphate (cGMP) [59].

Of course FSS, a mechanical force experienced only by the endothelium, may be the major player in the initiation of arteriogenesis but cannot serve as the only stimulus for a blood vessel to remodel. Other, non-endothelial factors also play a role, such as the effect on wall tension as a result of flow-mediated dilation and the infiltration of inflammatory cells, especially monocytes [45, 60].

Principally, a homeostatic level of wall tension provides optimal conditions for VSMCs. The Law of Laplace describes the relation of wall tension (T), pressure (P), radius (r) and wall thickness (w) ($T = P \times r / w$) and must be considered in this setting: an increase in vessel radius, as

occurs during flow-mediated vasodilatation, invariably increases wall tension. In order to maintain this radius but also return wall tension to homeostatic values, an increase in wall thickness occurs [61]. As increases in FSS result in the dilation of vessels, the impact of flow on wall tension must also be considered in arteriogenesis. Indeed, prolonged periods of vasodilatation resulting from augmented tissue perfusion requirements ultimately lead to outward remodelling, i.e. an increase in luminal diameter, and this has been shown to occur both *in vitro* and *in vivo* [62]. For example, isolated resistance vessels receiving the calcium channel blocker amlodipine for three days to cause prolonged vasodilatation developed an increase in passive diameter [63]. *In vivo*, Unthank and colleagues reported that the diameters of collaterals had significantly increased in a model of mesenteric arteriole occlusion within one week [64]. In a parallel study, the authors could also show that this increase in luminal diameter was greatest at sites exposed to the highest levels of flow and, most importantly in the concept of arteriogenesis, that this was accompanied by significant increases in cross-sectional medial area [65]. The observed increase in medial thickness was produced via both endothelial and VSMC proliferation, ultimately returning the ratio of medial thickness : luminal radius to normal levels and thus also homeostatic wall tension.

In addition to the generation of endothelial autacoids and vasodilatation discussed above, FSS has also been reported to alter the expression of numerous genes in ECs [66]. Moreover, the expression of adhesion molecules, in particular the intercellular adhesion molecule-1 (ICAM-1) and the vascular cell adhesion molecule-1 (VCAM-1) are reported to be upregulated in ECs upon increased FSS, whereas the latter has also been reported to decrease upon FSS [60, 67-69]. Similarly, the expression of the chemokine monocyte chemotactic protein-1 (MCP-1) has also been reported to increase in collateral vessels on both the mRNA as well as on the protein levels in response to FSS [60, 70]. Together with the adhesion molecules ICAM-1 and VCAM-1, MCP-1 is now considered a vital component of pro-arteriogenic processes by attracting and facilitating the transmigration of monocytes [67]. However, this is a topic of substantial debate as the increased levels of FSS characteristic for arterioles are certainly not an environment favourable for cellular adhesion processes. Regardless of the site of attachment and transmigration, evidence supports the involvement of monocytes in arteriogenesis: Infusion of MCP-1 during hind-limb ischemia can significantly improve arteriogenesis [54]. Furthermore, in the same study it was shown that the inhibition of ICAM-1 by a monoclonal antibody against the adhesion molecule significantly attenuated the beneficial effect of exogenous MCP-1. It is likely that the pro-arteriogenic properties of monocyte infiltration are due to their production and release of growth factors, especially tumour necrosis factor alpha (TNF-α) and basic fibroblast growth factor (bFGF) [70].

Unlike the shear stress-dependent expression of ICAM-1 and VCAM-1, MCP-1 expression is not increased in ECs upon increased FSS. Actually, in isolated human umbilical vein ECs the expression of

MCP-1 mRNA decreased upon exposure to FSS [60, 66]. It rather appears that the increased wall tension upon flow-induced dilation is the driving force for increased MCP-1 expression. Demicheva and colleagues showed that cyclic stretch, as a surrogate for increased wall tension, increased MCP-1 expression on the mRNA and protein levels in both ECs as well as VSMCs *in vitro* [60]. In isolated vessels, MCP-1 mRNA was increased 24 hours after the onset of arteriogenesis and even remained high after seven days [60]. Furthermore, the authors could identify the VSMCs as the main source of MCP-1 protein expression. Finally, it was demonstrated that the cyclic stretch-induced upregulation of ICAM-1, VCAM-1 and MCP-1 was mediated by the increased activity of the stress-responsive transcription factor activator protein 1 (AP-1) [60]. A possible pathway how the signals produced by growth factors, wall tension and FSS are integrated into an arteriogenic response was presented by Eitenmuller and colleagues in 2006 who provided evidence for the involvement of three potential signalling pathways. They showed a marked increase in phosphorylation of Ras and ERK as well as an upregulation of Ras protein levels, a pathway which translates growth factor signals to cellular proliferation processes. Furthermore, they described the involvement of the Rho pathway and especially RhoA which is commonly involved in cytoskeletal rearrangement, processes invariably engaged with cellular mobility and thus collateral development. Finally, they also discussed the somewhat enigmatic involvement of NO in the transmission of growth signals – after all, NO is well-known for its antiproliferative effects. However, NO is at least required to mediate the flow-dependent dilation following alterations in FSS and the authors suggest that NO can participate in the pro-arteriogenic processes by activating the Rho pathway [71].

Finally, in the later stages of arteriogenesis, the surrounding matrix structures must give way to the growing structures and also provide support for the expanding vessel. This is achieved by the initial breakdown of elastic lamina and restructuring of the matrix constituents, achieved most likely via the increased expression and activity of various matrix metalloproteinases (MMPs), in particular MMP-2 and MMP-9 [72, 73].

Considering the variety and this by far not exhaustive description of factors implicated in the initiation and progression of the processes involved in arteriogenesis and the delicacy of its regulation, it is not unexpected that ROS participate or can deregulate collateral vessel development. As for angiogenesis, the implication of ROS in arteriogenesis will be introduced in the following section.

1.4 Reactive oxygen species in vascular remodelling

In vivo, low levels of H_2O_2 have been shown to activate proliferative responses in ECs via the activation of the angiogenic transcription factors NFκB, AP-1 and ets-1 [74, 75]. VEGF genes have binding sites for NFκB and AP-1 in their promoter sequences which is in line with findings showing that H_2O_2 dose-dependently increases VEGF mRNA [76]. A number of cancer cells have been reported to constitutively generate H_2O_2 *in vivo* and this can have a considerable influence on angiogenesis, both via the induction of VEGF transcription as well as through the inhibition of the tumour suppressor PTEN [77-79]. Such a H_2O_2-dependent increase in VEGF production has also been reported to occur in macrophages, cells that migrate to sites of inflammation where angiogenesis is usually required [80].

A possible molecular link between oxygen radicals and angiogenesis has recently been described and involves the stabilisation of HIF-1α. This oxygen-dependent transcription factor is rapidly ubiquinated under normoxia by the E3 ubiquitin ligase complex which is under control of the von Hippel-Landau tumour suppressor protein (pVHL) [81, 82]. Under normoxic conditions, proline residues in HIF-1α are hydroxylated by the prolyl hydroxylase 2 (PHD2). This hydroxylproline residue is recognised by pVHL, leading to rapid degradation of HIF-1α. PHD2 requires the presence of the essential cofactors O_2, Fe^{2+} and 2-oxoglutarate in order to hydroxylate HIF-1α and is therefore considered an influential oxygen sensor [82]. Thus, if oxygen concentrations in the cytosol decrease (due to tissue hypoxia or increased O_2 consumption by the mitochondria for oxidative phosphorylation), PHD2 cannot destabilise HIF-1α, leading to its accumulation, transmigration to the nucleus and, ultimately, transcription of its more than 100 target genes, including other transcription factor which can further amplify the effects of HIF-1α [83].

One of the other essential co-factors for PHD2 performance, Fe^{2+}, is susceptible to oxidation by ROS. An increase in its positive charge (Fe^{3+}) renders it unavailable for PHD2 catalytic activity [84]. In situations with little available oxygen it appears plausible that ROS production decreases so the charge of Fe^{2+} should remain favourable for PHD2 activity. Paradoxically, despite a decrease of oxygen availability during hypoxia, ROS production increases as a stress response [85]. This occurs in a biphasic manner, the first, quick effect possibly involving a deregulation of the mitochondrial complex III of the ETC, leads to an increase in ROS, oxidation of Fe^{2+} to Fe^{3+} and inhibition of PHD2 catalytic activity, ultimately resulting in HIF-1α stabilisation and transcription of target genes. A second, time-delayed production of ROS via NADPH oxidase activation has been suggested to occur in response to the resulting increase in VEGF-A levels and binding to VEGFR2 [85].

While this regulatory system involving PHD2 and its oxygen and ROS-sensitive co-factors appears sound, and evidence, such as the activation of hypoxic signalling by exogenous H_2O_2 during normoxia, strongly supports the system discussed above, recent studies have shown that post-translational

modification of HIF-1α is more complex. For example, the HIF asparaginyl hydroxylase Factor inhibiting HIF (FIH) can be modified by peroxides at significantly lower levels than required to affect PHD2, suggesting a much lower sensitivity of PHDs to peroxide-dependent regulation. On the other hand, levels of ROS sufficient to inhibit PHD2 activity have no effects on FIH, suggesting that ROS do not play, at least not a direct role in HIF-1α stabilisation [86]. In support of this, it was recently communicated that the production of ROS from isolated mitochondria actually decreases in response to hypoxia and that this occurs in an O_2 concentration-dependent manner [87].

Both the cytosolic thioredoxin system and the mitochondrial equivalent potentially participate in angiogenesis. As mentioned previously, Txn1 has a dual role in the regulation of NFκB, a transcription factor affecting numerous angiogenic genes. Reduced Txn1 also directly interferes with the activity of ASK1 and elevated levels of oxidative stress can lead to the dissociation of the reduced Txn1 from the ASK1 signalosome, thereby enabling it to participate in apoptotic pathways [88, 89]. Txn1 has also been reported to modify the activity of MMPs and their inhibitors, both enzymes required for the rearrangement of the extracellular scaffold supporting the newly formed vessels [90].

In the previous section, the implication of Txnrd1 in a number of cancers was introduced. While cancer cells themselves express increased levels of Txnrd1 and strategies to combat tumour growth by inhibiting Txnrd1 are being developed, reports on an involvement of Txnrds on angiogenesis per se are few. A recent report using gold compounds as inhibitors of Txnrd1 showed an antiangiogenic effect in developing zebrafish [91]. However, whether this effect was due to Txnrd1 inhibition in endothelial or other cells of the vasculature remains elusive. Furthermore, at which level angiogenesis was impaired (e.g. ROS, PHD2 or HIF-1α) was not investigated. To date, no reports on the possible direct involvement of Txnrd2 on angiogenesis have been published.

In summary, the net output of ECs in response to an angiogenic stimulus cannot be explained solely by viewing only oxygen availability, production of ROS or the synthesis of proteins required for cellular migration, tube formation and stabilisation of immature vessels. Rather, it seems an integrated and highly regulated response occurs, ideally leading to a response that is beneficial to the tissue but also to the organism as a whole.

Since many of the pathways and mediators implicated in vascular remodelling are impacted upon by their redox status, it is not surprising to find that ROS can participate in and/or modulate vascular growth in collateral vessels [92]. However, the literature on the involvement of ROS on arteriogenesis is more limited than in the angiogenic situation, possibly due to the biomechanical nature of this type of vascular remodelling or the contribution of so many different cells. Of course, many of the effects

ROS exert on ECs discussed above in the context of angiogenesis may also be implicated in arteriogenesis. Additionally, there are some reports on the impact of ROS specifically on arteriogenesis. As described, FSS is thought as an initial stimulus for arteriogenesis and, despite this being a biomechanical force, numerous molecules are altered in response to changes in flow characteristics. More specifically, Laurindo et al. measured an increase in ROS production in ECs exposed to alterations in flow in intact rabbit aortas by electron spin resonance spectroscopy [93]. In particular H_2O_2 was found in subsequent studies to increase in response to alterations in FSS [58, 59]. Interestingly, the effects of H_2O_2 also extend beyond the ECs as it has been shown to be released from ECs exposed to FSS and can thus also affect VSMCs [94]. This is of particular importance in the context of remodelling of the vascular wall as H_2O_2 from endothelial sources increases placenta growth factor (PLGF) mRNA and protein expression in VSMCs. Furthermore, PLGF favours the recruitment of monocytes to the vascular wall, which inhabit central roles in the progression of arteriogenesis [95].

Above, the transcription factor AP-1 was described as being activated by H_2O_2. Activation of AP-1 leads to the production of vascular growth factors, such as ICAM-1 [60]. Thus, changes in FSS may not only initiate arteriogenesis via the subsequent vasodilation but also by increasing the synthesis and release of growth factors essential for vascular remodelling.

Furthermore, ROS have been implicated in the regulation of MMP gene expression and activation [96]. Indeed, elevated ROS have been described to increase the deposition of matrix proteins [97]. Since ROS are released from sheared ECs and react with thiol groups, such as those present in the propeptide domain of MMPs, it is possible that increases in H_2O_2 may modulate the extracellular matrix composition and/or structure by altering the activity of MMPs [98]. Interestingly, in the media of VSMCs exposed to increasing concentrations of H_2O_2 a biphasic effect on MMP-2 activation was observed: while low doses (4 µM) lead to an increase in MMP-2 activity, concentrations above 10 µM H_2O_2 inactivated MMP-2 [98]. This further supports the presumption that ROS participate in many processes as long as they are maintained at tolerable concentrations.

The detrimental effects of excessive ROS can be observed in many processes in aging, as ROS levels increase with senescence [99, 100]. Therapeutically this is of particular importance as many cardio-vascular diseases commonly occur in older individuals and the increased production of ROS can impair patient recovery. Accordingly, in a mesenteric collateral development model in the rat, vascular remodelling was impaired in older animals and this could be improved by the administration of antioxidants [101, 102]. Hypertension, often associated with oxidative stress, has also been shown to impair arteriogenesis in the same rat model of mesenteric collateral growth. Here the administration of antioxidant therapy also ameliorated the detrimental effects of excess ROS [103, 104]. Since ROS can

participate in numerous signalling pathways, can act as second messengers and regulate the activity of several proteins, it is near impossible to identify a single mechanism by which excess ROS can impair arteriogenesis. One possibility is the reduced bioavailability of NO, required for example for the vasodilatory response to increased FSS, which occurs through its rapid oxidative inactivation by excess $O_2^-\bullet$, resulting in a blunted vasodilatory capacity and the production of peroxynitrite ($ONOO^-$) [105]. Additionally, excessive production or inadequate antioxidative defense against ROS as seen with increasing age, can lead to the uncoupling of eNOS. Possibly caused by the oxidation of the eNOS cofactor Tetrahydrobiopterin (BH_4) by $ONOO^-$, uncoupled eNOS produces $O_2^-\bullet$ rather than NO, thereby increasing the oxidative burden even more [106].

As for the involvement of the thioredoxin family in arteriogenesis, little is known. As mentioned previously, overexpression of Txn2 improves arteriogenesis in a murine hind-limb ischemia model [20]. Models investigating other vascular remodelling processes such as pathological changes in response to hypertension or the development of atherosclerosis also provide support for the involvement of these endogenous antioxidants in vascular remodelling. Thus, overexpression of Txn2 also resulted in a blunted vasoconstrictive effect of Angiotensin II [19]. In a similar study, Txn2 transgenesis produced an attenuated basal mean arterial blood pressure as well as end diastolic and end systolic pressures. In this study, increases in NO bioavailability and improved endothelium-dependent vasodilation were also observed. Additionally, these transgenics, when crossed with Apolipoprotein E-deficient mice, displayed fewer atherosclerotic lesions than their wildtype counterparts [107].

1.5 Endothelial mitochondria in vascular remodelling

Considering that mitochondria are one of the main sources of ROS in a cell and these radicals, as described above, can both participate in fundamental cellular processes but also cause detrimental damage, it is necessary to consider the contribution of this organelle in processes involved in vascular remodelling. While in most cells mitochondria are highly dependent on O_2 to meet energy needs by the synthesis of adenosine triphosphate (ATP) via the ETC, endothelial mitochondria produce up to 75% of their ATP via anaerobic glycolysis [108]. In contrast to other, highly aerobic cells, mitochondria constitute only 5% of the mass of an EC [109]. Since the energy production via the ETC is only of minor relevance, the capacity of endothelial mitochondria to produce ROS and thus participate in other processes such as signalling or apoptosis was, to a certain degree, neglected [110]. Presently, however, endothelial mitochondria have been implicated in a range of pathological conditions of the vasculature such as atherosclerosis, diabetes and reperfusion injury, thereby highlighting the need to better understand the role of these organelles in the otherwise anaerobic endothelium [109]. Of course,

as a producer of ROS, mitochondria can contribute to all the effects discussed above on oxidative signalling and stress. In addition, mitochondria have been described to be able to substantially modulate intracellular Ca^{2+} handling. Ca^{2+} inhabits central roles in many processes, ranging from eNOS activation and concomitant NO syntheses and vasodilatation to its function as a second messenger, and is therefore of considerable importance in the endothelium. Endothelial mitochondria, initially thought as a passive sink for Ca^{2+}, actually actively participate in cellular Ca^{2+} homeostasis, the extent of which can be modulated by mitochondrial ROS [109, 110]. For example, extracellular H_2O_2 has been shown to increase mitochondrial Ca^{2+} concentration in excess of the increase in the cytosol of ECs. Furthermore, this appears in part to be due to an impairment of the mitochondrial Ca^{2+}/Na^+ exchanger which expels Ca^{2+} from the organelle, leading to an accumulation of Ca^{2+}. Considering that mitochondria can pass Ca^{2+} to the endoplasmic reticulum (ER) to replenish its stores, oxidative interference with the mitochondrial Ca^{2+}/Na^+ exchanger can also severely limit ER function, leading to both mitochondrial and ER dysfunction [111, 112].

A determinant of the electrochemical potential gradient driving molecules such as Ca^{2+}, other ions and proteins from the cytosol into the mitochondria is the mitochondrial membrane potential (ΔΨm) [110]. The ΔΨm resides around -180 to -220 mV and is the product of the reductive movement of protons via the ETC complexes across the inner membrane into the intermembrane space from where they are harvested by ATP synthase to produce ATP [113]. As such, the charge of the ΔΨm can be indicative of mitochondrial health. Consequently, a decrease in the ΔΨm can attenuate the accumulation of Ca^{2+} (and other molecules) in the mitochondria in addition to the reduction in Ca^{2+} funnelling to the ER due to the oxidative stress-impaired Ca^{2+}/Na^+ exchanger [110].

It is commonly reported that a decrease in ΔΨm increases O_2^{-}• production from mitochondrial sources. Interestingly, it has now also been described that the charge of the ΔΨm in the mitochondria of kidney tumour cells was sensitive to intracellular H_2O_2 concentrations, suggesting that an increase in H_2O_2 may also disrupt the membrane potential [114].

Despite these findings, much of the role of mitochondria specifically in ECs remains to be fully elucidated. Studies investigating the modification of mitochondrial ROS production in ECs support a role for these organelles in vascular signalling, health and disease. Focus has been directed to the roles of the ETC, the NADPH oxidases and the antioxidant enzymes SOD or catalase in the endothelium. Knowledge on the participation of the mitochondrial thioredoxin system in the defence against oxidative stress as well as in signalling processes is rather scarce and even less is known within the EC. Since this enzyme system, together with the glutathione system, is now considered the main H_2O_2 detoxifying axis in mitochondria, it is necessary to begin to elucidate its contribution in ECs [115].

1.6 Intention of the present work

Until now research has mainly focussed on the Thioredoxins and the cytosolic form of Txnrd, Txnrd1. Especially the involvement of the cytosolic Txn system in cancer has received a lot of attention. Less effort has been directed to the thioredoxin systems in cardiac and especially vascular contexts. Thus, Txn1 has been shown to prevent cardiac hypertrophy and protect from reperfusion injury, its suppressor TXNIP has been implicated in the initiation of atherosclerosis, and Txn2 has been reported to decrease angiotensin II-induced ROS production and improve arteriogenesis and angiogenesis when overexpressed. On the other hand, less is known on the participation of the corresponding reductases in vascular processes [14-17, 19, 20]. Nonetheless, a report on the inhibition of Txnrd1 portrayed an increase in protein S-nitrosylation and blunted endothelium-dependent vasodilatation in mouse aortic rings, suggesting an important involvement of Txnrds in the vascular compartment [35].

In previous studies, our cooperation partner Marcus Conrad, together with us, has been able to demonstrate that Txnrd2 is essential for embryogenesis, in particular in heart development and function as well as in haematopoiesis [38]. In subsequent studies, the investigation of Txnrd2 was advanced using fibroblasts isolated from Txnrd2 knockout mouse embryos. In these studies, the effect of Txnrd2 on cellular proliferation, oxidative stress, interaction with other antioxidants as well as tumour growth and tumour angiogenesis were explored [37, 116].

In regard to Txnrd2 function, studies have converged mainly on cancer and, to a lesser degree, cardiac physiology. Vascular implications of Txnrd2 function remain unexplored.

Therefore, using embryonic endothelial progenitor cells (eEPCs) lacking Txnrd2 and inducible endothelium-specific Txnrd2 knockout mice, the present study aims to unravel the role of the mitochondrial Txnrd in endothelial physiology, vascular homeostasis and vascular remodelling processes with the following hypotheses:

- Txnrd2 deletion leads to increased oxidative stress in eEPCs

- Mitochondrial health, represented by $\Delta\Psi m$, is impaired in Txnrd2-lacking eEPCs

- Endothelial-specific deletion blunts both angiogenesis as well as arteriogenesis in a mouse model of hind-limb ischemia

2 Methods and Materials

2.1 Materials

ANTIBODIES	COMPANY
anti-α-Tubulin	Sigma-Aldrich GmbH, Taufkirchen, Germany
Rabbit anti-ß-actin	Sigma-Aldrich GmbH, Taufkirchen, Germany
Rabbit anti-BiP	New England Biolabs GmbH, Frankfurt/Main, Germany
Rat anti-CD31	Acris Antibodies GmbH, Herford, Germany
Rat anti-CD45	BD, Franklin Lakes, USA
Mouse anti-GAPDH	Merck-Millipore GmbH, Schwalbach/Ts., Germany
anti-goat IgG H&L chain specific	Merck KGaA, Darmstadt, Germany
Rabbit anti-HIF-1α	Acris Antibodies GmbH, Herford, Germany
Rabbit anti-IRE-1α	New England Biolabs GmbH, Frankfurt/Main, Germany
anti-mouse IgG H&L chain specific Peroxidase Conjugate	Calbiochem, Nottingham, UK
Mouse anti-Nitrotyrosine	Abcam, Cambridge, UK
Rabbit anti-PDI	New England Biolabs GmbH, Frankfurt/Main, Germany
Rabbit anti-PHD2	New England Biolabs GmbH, Frankfurt/Main, Germany
anti-rabbit IgG, H&L chain specific Peroxidase Conjugate	Calbiochem, Nottingham, UK
Peroxidase AffiniPure Goat Anti-Rat IgG (H+L)	Dianova GmbH, Hamburg, Germany
anti-rat IgG H&L Cy3-Conjugate	Dianova GmbH, Hamburg, Germany
anti-Txnrd2 monoclonal antisera #1C4	Dr. Elisabeth Kremmer, Helmholtz Centre, Munich, Germany

The monoclonal antibody against Txnrd2 was previously produced in collaboration with Dr. Elisabeth Kremmer and Dr. Tamara Perisic (Helmholtz Centre, Munich). By immunising rats with the Txnrd2-specific peptide (VKLHISKRSGLEPTVTG) coupled to ovalbumin (OVA)/ Keyhole limpet hemocyanin (KHL) (Peptide Specialty Laboratories, Heidelberg, Germany), more than 30 hybridoma clones were obtained and immunoreactivity screened by western blotting. For this study, the supernatant of the hybridoma clone #1C4 was used.

CELL CULTURE REAGENTS	COMPANY
ß-Mercaptoethanol	Invitrogen, Karlsruhe, Germany
Dimethyl sulfoxide	AppliChem GmbH, Darmstadt, Germany
Dulbecco´s Modified Eagle Medium high glucose (4.5g/l glucose)	Invitrogen, Karlsruhe, Germany
Fetal calf serum	Biochrom AG, Berlin, Germany
Gelatine from porcine skin	Sigma-Aldrich GmbH, Taufkirchen, Germany
L-Glutamine, 200mM, liquid	Invitrogen, Karlsruhe, Germany
MEM non-essential amino acids (100x)	Invitrogen, Karlsruhe, Germany
Penicillin-Streptomycin Solution, 100mM	Invitrogen, Karlsruhe, Germany
Trypsin 0.05% (1x) EDTA 4Na, liquid	Invitrogen, Karlsruhe, Germany

CHEMICALS	COMPANY
2-Propanol	Carl Roth GmbH & Co. KG, Heidelberg, Germany
3-Morpholinopropanesulfonic acid	AppliChem GmbH, Darmstadt, Germany
Acetic Acid 100%	Carl Roth GmbH & Co. KG, Heidelberg, Germany
Acetone	Carl Roth GmbH & Co. KG, Heidelberg, Germany
Adenosine	Sigma-Aldrich GmbH, Taufkirchen, Germany
Agarose low EEO	AppliChem GmbH, Darmstadt, Germany
Aqua ad iniectabilia	B. Braun Melsungen AG, Melsungen, Germany
Bovine serum albumin (albumin fraction V)	AppliChem GmbH, Darmstadt, Germany
Bromphenol blue	Sigma-Aldrich GmbH, Taufkirchen, Germany
Calcium chloride dihydrate	Sigma-Aldrich GmbH, Taufkirchen, Germany
CellROX	Life Technologies, Darmstadt, Germany
CheLuminate-HRP PicoDetect	AppliChem GmbH, Darmstadt, Germany
Collagenase A	Roche Applied Science, Mannheim, Germany
Dimethyl sulphoxide	Carl Roth GmbH & Co. KG, Heidelberg, Germany
Disodium hydrogenphosphate	AppliChem GmbH, Darmstadt, Germany
dNTPs for PCR, premixed	GE Healthcare, Freiburg, Germany
Ethylenediaminetetraacetic acid	AppliChem GmbH, Darmstadt, Germany
Eosin G, 0.5%	Carl Roth GmbH & Co. KG, Heidelberg, Germany
Ethanol	Merck KGaA, Darmstadt, Germany
Forene®	Abbott GmbH & Co KG, Wiesbaden, Germany

Gel Red	Biotrend, Cologne, Germany
Glucose	AppliChem GmbH, Darmstadt, Germany
Glycerol	Sigma-Aldrich GmbH, Taufkirchen, Germany
Goat Serum	Sigma-Aldrich GmbH, Taufkirchen, Germany
Haematoxylin solution, acidic	Carl Roth GmbH & Co. KG, Heidelberg, Germany
Hydrochloric acid	Merck KGaA, Darmstadt, Germany
JC-1	Life Technologies, Darmstadt, Germany
Magnesium chloride	AppliChem GmbH, Darmstadt, Germany
Magnesium sulphate heptahydrate	AppliChem GmbH, Darmstadt, Germany
Methanol	Carl Roth GmbH & Co. KG, Heidelberg, Germany
Nonfat dried milk powder	AppliChem GmbH, Darmstadt, Germany
Page Ruler™ Prestained Protein Ladder	Fermentas GmbH, St. Leon-Roth, Germany
Paraformaldehyde	Merck KGaA, Darmstadt, Germany
peqGOLD 100 bp DNA ladder	Peqlab, Erlangen, Germany
Phenol/Chloroform/Isoamyl alcohol	Carl Roth GmbH & Co. KG, Heidelberg, Germany
Ponceau S	Sigma-Aldrich GmbH, Taufkirchen, Germany
Potassium acetate	Merck KGaA, Darmstadt, Germany
Potassium chloride	AppliChem GmbH, Darmstadt, Germany
Potassium cyanide	Sigma-Aldrich GmbH, Taufkirchen, Germany
Potassium dihydrogen phosphate	Merck KGaA Darmstadt, Germany
Roti-Histol	Carl Roth GmbH & Co. KG, Heidelberg, Germany
Sodium Nitroprusside (SNAP)	Biotrend Chemikalien GmbH, Cologne, Germany
Sodium chloride	AppliChem GmbH, Darmstadt, Germany
Sodium deoxycholate	Sigma-Aldrich GmbH, Taufkirchen, Germany
Sodium dodecyl sulfate	Sigma-Aldrich GmbH, Taufkirchen, Germany
Sodium fluoride	Merck KGaA, Darmstadt, Germany
Sodium hydroxide	Merck KGaA, Darmstadt, Germany
Sodium orthovanadate	Enzo Life Sciences GmbH, Lörrach, Germany,
Sodium phosphate monobasic monohydrate	AppliChem GmbH, Darmstadt, Germany
Sodium pyruvate	Sigma-Aldrich GmbH, Taufkirchen, Germany
SuperSignal® West Femto Substrate	Thermo Fischer Scientific, Bonn, Germany
Tamoxifen	Sigma-Aldrich GmbH, Taufkirchen, Germany
Tris	AppliChem GmbH, Darmstadt, Germany
Triton X-100	AppliChem GmbH, Darmstadt, Germany
Tween 20	AppliChem GmbH, Darmstadt, Germany

VectaMount AQ Aqueous Mounting Medium	Linaris GmbH, Dossenheim, Germany
Vectashield HardSet Mounting Medium with DAPI	Linaris GmbH, Dossenheim, Germany

ENZYMES	COMPANY
Protease/Phosphatase Inhibitor Cocktail (100X)	New England Biolabs GmbH, Frankfurt/Main, Germany
Proteinase K	Roche Applied Science, Mannheim, Germany
Taq DNA polymerase	Qiagen GmbH, Hilden, Germany

KITS AND DISPOSABLES	COMPANY
8 – 16% Precise Tris-Glycine gels, 10x10 and 8x10 cm Cassettes	Perbio, Thermo Fischer Scientific, Bonn, Germany
BCA™ Protein Assay Reagent A/B	Thermo Fischer Scientific, Bonn, Germany
Delimiting Pen	Dako, Hamburg, Germany
Parafilm M®	Pechiney Plastic Packaging Company
Perma-Hand Silk Suture	Ethicon, Neuss, Germany
Polypropylene tubes	Greiner Bio-One, Frickenhausen; Germany
QIAshredder	Qiagen GmbH, Hilden, Germany
Reverse Transcription System	Promega GmbH, Mannheim, Germany
RNase-Free DNase Set	Qiagen GmbH, Hilden Germany
RNeasy Mini Kit	Qiagen GmbH, Hilden, Germany
Silk braided suture (7-0)	Pearsalls Ltd, Somerset, UK
SuperFrost® Plus slides	Thermo Fischer Scientific, Bonn, Germany
Tissue-Tek® O.C.T. ™	Sakura, Zoeterwonde, Netherlands
Vectastain ABC-Kit Elite Rat IgG	Linaris GmbH, Dossenheim, Germany

OLIGONUCLEOTIDES FOR GENOTYPING	SEQUENCE
TR2_Del_for	5´-CACGACCAAGTGACAGCAATGCTG-3´
TR2_Del_rev	5´-CAGGCTCCTGTAGGCCCATTAAGGTGC-3´
TR2_Flox_for	5´-CAGGTCACTAGGCTGTAGAGTTTGC-3´
TR2_Flox_rev	5´-TTCACGGTGGCGGATAGGGATGC-3´
CRE 1	5´-GCCTGCATTACCGGTCGATGCAACGA-3’
CRE 2	5´-GTGGCAGATGGCGCGGCAACACCATT-3’

All DNA-oligonucleotides were obtained from Eurofins MWG Operon, Ebersberg, Germany.

2.2 Animals

Mice lacking Txnrd2 were established as described previously for other organs [39]. In brief, inducible endothelial-specific deletion of Txnrd2 was achieved by crossing mice expressing LoxP-flanked Txnrd2 (flox) with mice expressing Cre recombinase (Cre) under control of the VE-Cadherin promoter. Induction of the knockout was achieved through i.p. administration of Tamoxifen (20 mg/ml in neutral oil (medium chain triglycerides)) for 5 consecutive days for a total of 5 mg Tamoxifen per mouse. The induction was allowed to proceed for at least two weeks before experiments were performed.

2.2.1 Genotyping

The genotype of the Mice undergoing experimental procedures was established prior to their import from the animal holding facility to the laboratory by digesting of and the extraction of DNA from tail clippings.

DNA was precipitated by immersing the tail clipping in 500 µl Lysis buffer containing Proteinase K in a Thermomixer (Eppendorf, Germany) set to 55°C and 700 rpm overnight. The following morning the temperature was increased to 85 °C for one hour to inactivate Proteinase K, followed by the addition of 500 µl Phenol/Chloroform to the homogenate, vortexing and centrifugation (14,000 rpm, 6 minutes), after which an upper and a lower phase appeared in the supernatant. The upper phase was transferred to an eppendorf tube containing 2.5 volumes of 100% Ethanol and 5M NaCl, shaken and centrifuged (15,000 rpm, 10 minutes, 4°C). Having discarded the supernatant, the pellet was washed twice in 70% Ethanol and subsequently dried in a Thermomixer at 55°C. Finally, the pellet was dissolved in TE buffer and stored at -20°C until analysed by PCR (discussed below).

Tail lysis buffer

EDTA	10 mM
Tris-HCl, pH 7.6	10 mM
SDS	0.5%
NaCl	10 mM
Proteinase K	15 µl/ ml lysis buffer

After completion of experimental procedures and sacrificing of the mice, tail clippings were additionally obtained to ensure, by the method described above, the correct genotype of the mice.

Furthermore, to confirm the successful deletion of Txnrd2 specifically in the endothelium, kidneys were removed, homogenised and digested in Collagenase A (2 mg/ml) for one hour at 37°C. The homogenate was centrifuged (1300 rpm, 10 min, 4°C) and the pellets washed twice by resuspension in 2% FCS in PBS and centrifugation. To isolate the ECs from the other cells present in the homogenate, the pellets were incubated with a rat anti-mouse CD31 antibody (1:100 in 2% FCS/PBS in a thermo shaker set to 4°C and 700 rpm for one hour). After an additional three washing steps, the CD31 antibody was conjugated to anti-rat-coated microbeads (concentration 1:5, Miltenyi Biotech, Bergisch Gladbach, Germany) by incubation in a thermo shaker set to 4°C and 700 rpm for one hour. Subsequently, samples were again washed three times by centrifugation and the homogenate applied to MACS® cell separation columns placed in a magnet (Miltenyi Biotech, Bergisch Gladbach, Germany). As the homogenate passes through the magnets, the CD31/microbead-labelled ECs are retained within the columns and the unwanted cells discarded. Once the entire volume had passed the columns, the magnets were removed and the retained ECs were flushed out of the columns. After a final centrifugation step, the EC-pellet was lysed in RIPA buffer and the presence of Txnrd2 determined by western blot as described below.

2.3 Hind-limb ischemia

Occlusive artery disease is a common hallmark in a variety of diseases, such as myocardial infarction and stroke, which are characterised by an acute occlusion of conduit arteries and a resulting lack of perfusion to the downstream tissue. If perfusion is to be re-established in such conditions, blood flow must be restored. This can occur either by dissipation of the cause of the occlusion, for example by fibrinolytic processes. Another possibility to re-establish perfusion is for the blood to bypass the blocked vessel through other, pre-existing – collateral – arterioles.

Collateral arterioles bud off from the artery upstream of the site of occlusion and re-enter downstream. At the onset of occlusion, collateral arterioles experience the drop in downstream pressure in the artery as a pressure gradient across their length. As a result, blood flow through the collateral arterioles increases, thereby inducing a cascade of haemodynamic-sensitive responses.

At a constant vessel diameter, an increase in flow is associated with an increase in FSS, the tension the viscous blood exerts on the endothelial layer of a vessel wall. While the impact of increased FSS on collateral artery remodelling is highly debated, another result of increased blood flow is pressure-induced vasodilatation. Vasodilation stretches the vessel wall constituents: VSMC and ECs, but also extracellular matrix structures and the elastic lamina. In response, vascular wall cells proliferate in order to distribute the stretch-induced burden and re-establish homeostatic conditions. Invasion of inflammatory cells, especially monocytes, adds another stimulus for VSMC proliferation, thereby further enhancing the adaptive response.

In the end, collateral arterioles of an occluded artery act as natural bypass vessels and can compensate, at least to a certain degree, the decrease in perfusion [117].

Tissues downstream of the occlusion and dependent on vessel patency to maintain oxygen homeostasis can be subject to hypoxic conditions if perfusion is impaired for longer durations. Hypoxia is considered the main driving force for angiogenesis [49], the budding of new capillaries within an existing network.

2.3.1 Surgery

Hind-limb ischemia was induced by unilateral ligation of the right femoral artery as described in detail elsewhere [118]. Briefly, Mice were anaesthetised by subcutaneous injection of Midazolam, Fentanyl and Medetomidine (Midazolam (5 mg/kg; Ratiopharm, Ulm, Germany), Fentanyl (0.05 mg/kg; CuraMed, Karlsruhe, Germany), and Medetomidine (0.5 mg/kg; Pfizer, Karlsruhe, Germany)) and a Laser Doppler measurement performed (described below) to establish baseline hind-limb perfusion. Subsequently, both thighs were shaved and the femoral artery located. Through a small incision the femoral artery was isolated from the corresponding nerve and vein as well as connective tissue. Occlusion was performed on the right femoral artery by tying a thread around it just below the deep femoral branch. An in-animal sham-control was performed on the contralateral limb by placing the thread around the isolated femoral artery without tying a knot. Finally, the skin was closed with a surgical suture thread and animals allowed to recover in solitary cages after having received a mixture of Atipamezole, Naloxone and Flumazenil (Atipamezole (2.5 mg/kg; Pfizer, Karlsruhe, Germany), Naloxone (1.2 mg/kg; Inresa, Freiburg, Germany), and Flumazenil (0.5 mg/kg; Hoffmann-La-Roche, Grenzach-Wyhlen, Germany)) subcutaneously.

2.3.2 Laser Doppler Imaging (LDI)

The extent of hind-limb perfusion was established prior to surgery, immediately thereafter as well as three and seven days after occlusion of the femoral artery. Unless mice were anaesthetised for surgery as described above, sedation was achieved by inhalation of isoflurane (Isoflurane 1 vol. %, O_2 1.5 l/min) throughout the measurement. Hind-limbs of mice were fixed with double-sided adhesive tape to a plate within a heated chamber (37°C). After an acclimatisation period of seven to ten minutes, LDI measurements of the hind-limbs were performed with the laser Doppler LDI 5061 (Moor Instruments, Remagen, Germany) connected to a PC running the corresponding Moor Software Version 3.01. Equal-sized regions of interest were placed around the paws of the mice and perfusion (reflected in terms of colours, where warm colours represent high perfusion values and cold colours symbolise little perfusion) was assessed. To standardise LDI measurements, background tissue values were subtracted and results expressed as the perfusion ratio of the occluded hind-limb relative to the sham-operated limb.

2.3.3 Tissue Harvesting & Processing

After the final LDI measurement the adductor and calf muscles of the occluded and sham-operated limb were either excised directly or after maximal dilation of vessels and/or perfusion fixation as described below. After opening the abdominal cavity, the descending Aorta was catheterised with PE tubing and the vena cava was punctured to allow blood and the administered solutions to drain. Adenosine buffer (1 ml PBS, 5 mg bovine serum albumin, 1 mg adenosine) and, if paraffin sections were to be prepared, 4% paraformaldehyde solution were subsequently administered via the aortic catheter until the solution returned via the vena cava clear from blood.

Removed muscles were embedded in either Tissue Tek and stored at -80°C for cryo preservation or embedded in paraffin following general protocols for subsequent histology and immunofluorescence studies.

2.4 Arteriogenesis

Paraffin-embedded adductor muscles were sectioned using a microtome (Biocut 2030, Reichert-Jung, Leica Microsystems, Wetzlar, Germany) in 5 – 6 µm thick slices and three sections, from each the medial, intermediate and lateral side of the muscle, placed on a microscope slide. Subsequently the slices were stained with haematoxylin and eosin as described in Table 2-1 to visualise cell nuclei and eosinophilic structures, such as cytoplasm and connective tissue. Since collateral vessels differ in their thickness across their course through the muscle, vessels at the height of the occlusion (i.e. the

intermediate section which is the narrowest area) were photographed at 400x magnification using a bright field microscope (BX41, Olympus, Hamburg, Germany) featuring a camera (Camedia C5050, Olympus) coupled to imaging software (DP-Soft v. 3.2, Olympus). Vessels were assessed for inner and outer vessel circumference using ImageJ software (1.43u, National Institutes of Health, USA). Measuring circumference allows the comparison of blood vessels irrespective of their shape and also permits the calculation of wall area, wall thickness and lumen using standard circle formulas [118].

Table 2-1: Haematoxylin and eosin staining protocol

Thaw slices at room temperature	5 min
Rehydrate slices in PBS	5 minutes
Stain with Harris haematoxylin	7 minutes
Wash in demineralized water	17 minutes
Stain with 0.1% Eosin	5 minutes
Briefly wash in demineralized water	5 intermittent washes
Dehydrate in 100% EtOH	2 minutes
Immerse in Xylene	5 minutes
Cover with mounting medium (Roti-Histol) and glass cover slips	

2.5 Angiogenesis

Cryo-conserved calf (gastrocnemius) muscles were sectioned with a cryostat (Cryotome HM 560, Microm, Walldorf, Germany) in 10 µm thick slices and three slices from the anterior, posterior and intermediate region of the muscle placed on a microscope slide. Subsequently, they were fixed in ice-cold acetone for 20 minutes and air-dried before being frozen at -20°C for storage. To assess angiogenesis, calf muscle cryosections were stained with an antibody raised against the endothelial membrane protein CD31 which, in turn, was detected with a Cy3-conjugated secondary antibody following the protocol outlined below (**Table** 2-2).

Calf muscle cryosections were photographed using a camera (AxioCam, Zeiss, Munich, Germany) coupled to a fluorescence microscope (Axiophot, Zeiss) at 20x magnification. In order to be able to compare vessel density within and between individual mice, three distinct sites per slice were selected. Angiogenesis in these areas was then assessed by measuring CD31-positive areas using ImageJ software (1.43u, National Institutes of Health, USA). Results were expressed as the area fraction of the entire image.

Table 2-2: Immunofluorescence Staining Protocol

Thaw sections at room temperature	10 – 15 min
Rehydrate in PBS at room temperature	≥ 20 min
Dry and cycle sections with liquid blocker pen	
Incubate with blocking solution 5 % BSA in PBS	30 min
Incubate with rat anti-CD31 antibody (1:400 in blocking solution) at 4°C	Over night
Wash three times in PBS	Five min each
Incubate with Cy3-conjugated goat anti-rat antibody (1:200 in blocking solution) at room temperature	Two hours
Wash three times in PBS	Five min each
Mount coverslips with Vectashield DAPI	

2.6 Flow-mediated Dilatation

To assess the vasodilatory capacity of the collateral arterioles from Txnrd2^{ECWT} and Txnrd2^{ECKO} mice in response to alterations in flow velocity, a protocol described in detail previously was applied with minor modifications [119]. In brief, male Txnrd2^{ECWT} and Txnrd2^{ECKO} mice were euthanized by cervical dislocation. After removal of the skin of the thighs, the adductor muscle was carefully dissected and removed without damaging the vessels. During the whole procedure, the tissue was superfused by 4°C cold 3-morpholinopropanesulphonic acid (MOPS)-buffered salt solution (composition below). Five hundred µm long sections of collateral arterioles without branches were carefully isolated and cleaned from connective tissue using a preparation microscope (M205A, Leica Microsystems, Wetzlar, Germany). In a temperature-controlled, MOPS-filled organ bath, collateral vessel sections were cannulated with glass micropipettes (Science Products, Hofheim, Germany) mounted on micromanipulators (World Precision Instruments, Berlin, Germany), which allowed three-dimensional adjustment of the pipettes. Via a three-way valve the open end of one pipette was connected to a silicone tube and a height-adjustable reservoir containing MOPS buffer. Initially, the reservoir was set to a height representing a transmural pressure in the vessel of 45 mmHg. The open end of the other micropipette was also connected to silicone tubing via a three-way valve to allow the outflow of the perfusion fluid (Figure 2-1). The setup was mounted on an inverted microscope (Diaphot 300, Nikon, Düsseldorf, Germany) and the vessel visualised at 20x magnification (D-APO 20 UV lens, Olympus, Hamburg, Germany) with a CCD camera (WAT-902B, Watec Newburgh, NY, USA). Inner and outer diameters of the collateral arteriole were continuously monitored with the commercial software Blood Vessel Analyser 300 (Hasotec, Rostock, Germany).

With both three-way valves open, collateral arterioles were precontracted to a level comparable to the *in vivo* situation by administration of 1 µM of the thromboxane mimetic, U46619 (Tocris, R&D Systems GmbH, Wiesbaden-Nordenstadt, Germany). To assess flow-mediated dilatation the position of the reservoir was adjusted to produce various pressures (7.5, 15, 25, 35, 45, 55 mmHg), thereby changing the flow velocity within the collateral arteriole. By continuously recording the changes in arteriole diameter, the effect of increased flow velocity on vasodilatation was assessed and analysed as the % dilation of the U46619-induced precontraction with the following formula:

$$\text{Diameter}_{\text{actual}} - \text{Diameter}_{\text{U46}} \qquad \text{Diameter}_{\text{max}} - \text{Diameter}_{\text{U46}}$$

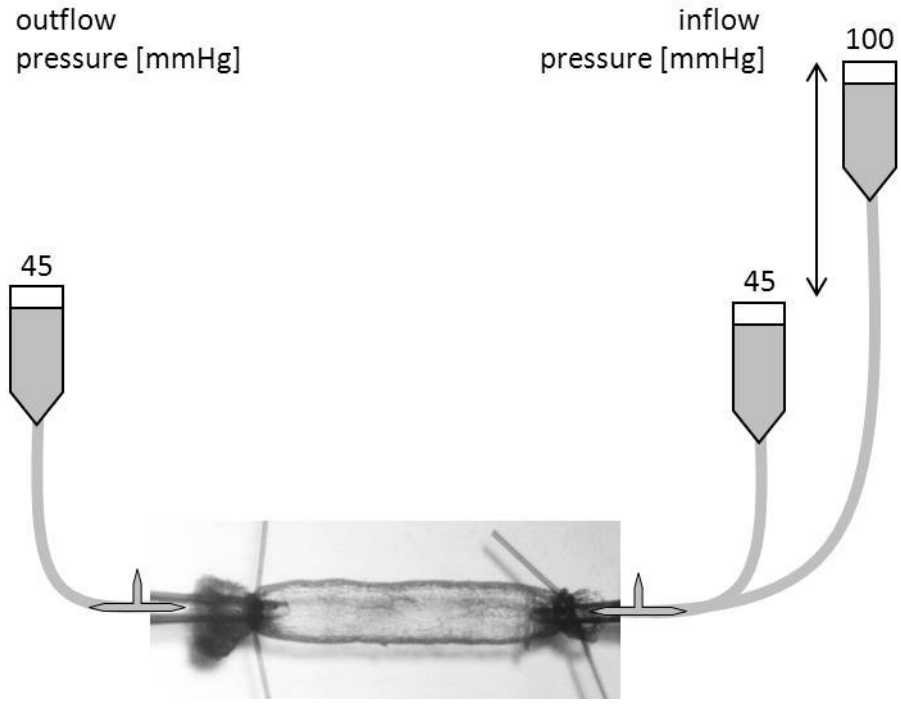

Figure 2-1: Representative setup for the measurement of flow-mediated dilatation. By changing the height of the MOPS-reservoir depicted on the right the inflow pressure into the vessel was altered. When both three-way valves were open, the change in inflow pressure resulted in an alteration of flow velocity and consequently also vessel diameter.

MOPS buffer

NaCl	145 mM	Pyruvate	2 mM
KCl	4.7 mM	EDTA	0.02 mM
$CaCl_2$ x 2 H_2O	3 mM	MOPS	3 mM
$MgSO_4$ x 7 H_2O	1.17 mM	Glucose	5 mM
NaH_2PO_4 x 1 H_2O	1.2 mM	pH	7.4

Sterile filtration

2.7 Cell Culture

All cell culture-related work was carried out under sterile conditions using an air flow bench (Steril Compact VBH 48 C2, Foster Wheeler, Corsico, Italy). Furthermore, any reagents or instruments to be introduced to the sterile area were autoclaved (Vakulab, Münchener Medizin Mechanik GmbH, Munich or Varioklav®, HP Labortechnik, Oberschleißheim, Germany) and/or disinfected with Bacillol® AF (Paul Hartmann AG, Heidenheim, Germany). Cells were cultured in a humidified incubator (APT.line™ CB210, Binder, Tuttlingen, Germany) at a constant temperature of 37°C, 5% CO_2 and 20% O_2. Cells were routinely monitored under a light microscope (IX50, Olympus, Hamburg, Germany).

2.7.1 Embryonic endothelial progenitor cells

Since primary mouse ECs are not available in ample amounts and do not allow multiple passaging, eEPCs were employed as a tool to investigate *in vitro* effects of Txnrd2 deletion.

Embryonic EPCs had been isolated from embryos of pregnant heterozygous mice according to a protocol developed by Hatzopoulos et al.[120] at embryonic day 7.5. eEPCs were cultured on 0.1% gelatine-coated plates at 37°C and 5 % CO_2 in a humidified incubator in high glucose Dulbecco´s modified eagle´s medium (DMEM) supplemented with 10 % fetal calf serum (FCS), 1 % L-Glutamine (200 mM), 1 % penicillin/streptomycin, 1 % non-essential amino acids and 0.06% ß-Mercaptoethanol (50 mM). For serial passaging, eEPCs were washed with PBS, detached with trypsin and split in a ratio up to 1:6 every two days.

To investigate oxidative stress-dependent effects, eEPCs were cultured in medium without ß-Mercaptoethanol as this compound exhibits antioxidant properties. To this end, confluent cells were washed in PBS and cultured in high glucose DMEM supplemented with 20 % FCS as well as the above additions except ß-Mercaptoethanol. Medium was changed once daily for at least four consecutive days before experiments were performed.

2.7.2 Cell Passaging and Harvesting

eEPCs were cultured to 80 – 90% confluence, washed with PBS^- and detached by adding 1 ml of Trypsin/EDTA solution per 10 cm dish. At 37°C, the proteolytic activity of trypsin and the chelating capacity of EDTA dissociate the cells within 5 minutes, a process which was checked under a light microscope. To stop the enzymatic activity of Trypsin, FCS-containing DMEM was added at a volume corresponding to at least the volume of Trypsin/EDTA. Depending on the experiment to be performed or whether cells were solely passaged to maintain growth, cells were split at ratios ranging from 1:2 to 1:6.

2.7.3 Determination of Cell Number

Cells were trypsinised and collected in an appropriate amount of DMEM. Subsequently, 100 µl of cell suspension was added to 10 ml of NaCl and analysed by a Coulter Z2 Cell and Particle counter (Beckman Coulter, Krefeld, Germany).

2.7.4 Cell Thawing and Cryo-conservation

To maintain a sufficient supply of eEPCs in liquid nitrogen, cells were routinely expanded by serial passaging and subsequently cryo-conserved. Once cells had grown to near confluence they were collected by trypsination and centrifugation (1500 rpm, 5 minutes). The pellet was resolved in freezing medium, transferred to cryo-vials and stored at -80°C overnight before being transferred to liquid nitrogen for long-term storage.

As required, cells were quickly defrosted in a water bath set to 37°C, transferred to a falcon tube containing standard DMEM as described above and centrifuged (1500 rpm, 5 minutes) to protect the cells from the DMSO in the freezing medium (see below). Following centrifugation, the pellet was resuspended in DMEM and transferred to a 10 cm dish. After 24 hours, cells were checked for viability using a light microscope and fresh medium added.

Freezing Medium

DMSO in FCS	10%

2.8 Protein Biochemistry

In order to study proteins in regard to their existence, quantity and potential post-translational modifications such as phosphorylation or nitration, western blotting experiments were performed. This technique employs Tris-Glycine SDS-PAGE electrophoresis to separate proteins depending on their molecular size. To achieve this, proteins must first be denatured by a combination of lysis buffer, heat and loading buffer. Denaturation of proteins exposes their hydrophobic regions which readily bind to SDS, thereby conferring a negative charge upon them [121]. During electrophoresis the denatured, negatively charged proteins migrate toward the anode with varying speeds, depending on their size and the acrylamide concentration of the gel matrix. Thus, in a given period of time a large protein will traverse only a fraction of the distance a small protein can travel.

2.8.1 Preparation of Protein Lysates

Cells were grown to confluence, washed twice with PBS and incubated with lysis buffer for 10 minutes on ice. Subsequently, any cells remaining attached to the dish were mechanically removed

using a rubber policeman and all cells transferred to an eppendorf tube. Depending on the protein of interest either a mild or harsh lysis buffer was employed, the main variation between buffers being the type of detergent used. The mild lysis buffer contained only one ionic detergent, sodium deoxycholate, whereas the harsh buffer, RIPA, also contains SDS as an additional ionic detergent and Triton X-100 as a non-ionic detergent.

If a mild lysis buffer was employed, samples were further processed with an insulin syringe. Following lysis with RIPA buffer, samples were additionally sonicated (five seconds, 50% pulse). To remove remaining cell debris, lysates were centrifuged (13000 rpm, 10 minutes at 4°C) and the pellet discarded. Protein quantification was then performed either directly or after storage of the samples at -20°C.

Mild Lysis Buffer	
Tris, pH 7.4	20 mM
NaCl	137 mM
EDTA	2 mM
Glycerol	10%
Sodium deoxycholate	0.1%, added freshly

Harsh Lysis Buffer (RIPA)	
NaCl	150 mM
Triton X-100	1%
Sodium deoxycholate	0.5%
Sodium dodecyl sulphate (SDS)	0.1%
Tris, pH 8.0	50 mM

Protease and phosphatase inhibitors (Protease/Phosphatase Inhibitor Cocktail (100X)) were added to the lysis buffers immediately before use

2.8.2 Protein Quantification

Quantification of sample protein content was performed with the bicinchoninic assay BCA™ Protein Assay Reagent A/B with a standard curve ranging up to 2 mg/ml using bovine serum albumin supplied with the kit. Duplicate standards and samples were incubated at appropriate dilutions for 30 minutes at 37°C with the BCA reagents (50 parts reagent A : 1 part reagent B) in 96-well plates and absorbance of the resulting BCA-copper complex detected at 550 nm with a plate reader (Infinite F200, Tecan, Crailsheim, Germany). The concentration of the samples was then calculated by linear regression of the standards and expressed in µg/ml.

2.8.3 Immunoblotting

To separate proteins solubilised in lysis buffer, SDS-Page electrophoresis was performed. Having established a sample's protein concentration, a volume corresponding to 10 to 50 µg of protein per sample was mixed with 4x or 6x loading buffer and heated to 95°C for 10 minutes to denature the

proteins. Brief centrifugation was performed to collect any precipitate formed on the walls and lid of the tubes. Samples were then loaded in 8-12 % gradient gels and proteins separated depending on their molecular weight using a Mighty Small II SE 250/SE 260 mini vertical unit (Amersham, GE Healthcare, Freiburg, Germany) connected to a power supply unit set to 300 V and 25 mA per Gel. Electrophoretic separation was performed until the samples had almost reached the bottom of the gel and the marker (PageRuler Prestained Protein Ladder, Fermentas) bands were separated sufficiently.

Gels were removed from the cassettes and the separated proteins transferred to a nitrocellulose membrane (Amersham, GE Healthcare, Freiburg, Germany) by semi-dry blotting using a custom-made blotter set to 300 V and 0.8 mA per cm^2 of membrane for 1:15 – 1:30 h. To eliminate unspecific binding of antibodies, the membrane was blocked in 5% skim milk powder in TBST for at least one hour at room temperature with gentle agitation. Primary antibodies were diluted at an antibody-dependent concentration (Table 2-3) in either 5% skim milk powder or BSA in TBST and incubated under gentle agitation either over night at 4°C or for one hour at room temperature. Following incubation with the primary antibody, membranes were washed 3 times in TBST and the HRP-conjugated secondary antibody, diluted in 5% skim milk in TBST, was incubated for 30 minutes to 2 hours at room temperature with gentle agitation. To visualise protein bands, membranes were washed 3 times in TBST and subjected to a chemiluminescent substrate (CheLuminate-HRP PicoDetect, or SuperSignal West Femto Chemiluminescent Substrate). Luminescence was detected with a Digital CCD Camera and analysed with Wasabi imaging software (Hamamatsu Photonics, Herrsching am Ammersee, Germany).

If re-probing was desired, membranes were incubated with stripping buffer for 10 – 30 minutes, washed three times and blocked with 5% skim milk in TBST for one hour before primary and secondary antibodies were added as described above.

4x Loading Buffer

Tris, pH 6.8	250 mM
SDS	8%
Glycerol	40%
ß-Mercaptoethanol	400 mM
Bromophenol blue	0.02%

Electrophoresis running buffer

Tris	124 mM
Glycerol	960 mM
SDS	0.5%

TBST	
Tris	50 mM
NaCl	150 mM
Tween 20	0.1%

Transfer buffer	
Tris	48 mM
Glycerol	39 mM
SDS	0.037%
Methanol	10 %

6x Loading Buffer	
Tris, pH 6.8	375 mM
SDS	9%
Glycerol	50 %
ß-Mercaptoethanol	9%
Bromophenol blue	0.03%

Stripping buffer	
Glycerol	0.2 M
NaCl	0.5 M
pH 2.8	

Table 2-3: Primary Antibodies for Western Blotting

Antigen	MW (kDa)	Isotype	Dilution	Provider, Cat. #
ß-Actin	42	Rabbit polyclonal IgG	1:1000 in 5% BSA	Sigma-Aldrich A2066
BiP	78	Rabbit monoclonal IgG	1:1000 in 5% BSA	Cell Signaling Technology #3177
GAPDH	36	Mouse monoclonal IgG1	1:10000 in 5% BSA	Chemicon MAB374
IRE1α	130	Rabbit monoclonal IgG	1:500 in 5% BSA	Cell Signaling Technology #3294
Nitrotyrosine		Mouse monoclonal IgG2b		Abcam ab7048
Txnrd2 (#1C4)	56	rat monoclonal	1:1 in 5% BSA	custom
PDI	57	Rabbit monoclonal IgG	1:1000 in 5% BSA	Cell Signaling Technology #3501
PHD-2	50	Rabbit monoclonal IgG	1:500 in 5% BSA	Cell Signaling Technology #4835

Secondary Antibodies for Western Blotting

Antigen	Dilution	Provider, Cat. #
Goat anti-mouse IgG HRP conjugate	1:5000 in 5% skim milk	Calbiochem 401253
Goat anti-rabbit IgG HRP conjugate	1:2000 in 5% skim milk	Calbiochem 401353
Goat anti-rat IgG HRP conjugate	1:10000 in 5% skim milk	Jackson ImmunoResearch 112-035-062

2.9 Polymerase Chain Reaction

2.9.1 Isolation of mRNA

To investigate the regulation of a range of genes, total mRNA was isolated from cells using the RNeasy Mini Kit (Qiagen). For cell lysis, 10^6 cells were incubated with a cell number-appropriate amount of RLT buffer supplemented with ß-Mercaptoethanol. RLT buffer disrupts cells based on the denaturing capacity of its constituent guanidine-thiocyanate while ß-Mercaptoethanol additionally inactivates RNAses. Following cell lysis, samples were further homogenised with QIAshredder columns (Qiagen) to remove insoluble material and reduce sample viscosity. Subsequently, Ethanol was added to each sample to improve binding conditions and passed through RNEasy Mini Spin columns (Qiagen). The columns were centrifuged at 10,000 x g during which the RNA precipitates and binds to the silica-based membrane in the columns and contaminants are removed. Finally, RNA was eluted in RNase-free water and aliquots stored at -20°C after the concentration of RNA (260/280 nm) was measured with a spectrophotometer (Eppendorf, Hamburg, Germany).

2.9.2 Synthesis of cDNA

To reverse transcribe mRNA to cDNA, a Reverse Transcription Kit (Promega) was used. First, 1 µg of RNA diluted in 5 µl dH_2O was incubated with Oligo(dT) primers at 65°C for 7 minutes. Subsequently, the remaining constituents of the Kit were added to a total volume of 10 µl and incubated for 1 hour at 37°C. Enzyme activity was halted by increasing the temperature to 97°C for 7 minutes before the mixture was diluted 1:10 with dH_2O. cDNA was then either stored at -20°C or used directly for semi-quantitative PCR.

2.9.3 Polymerase Chain Reaction (PCR)

Polymerase Chain Reaction was performed in either a Mastercycler ep gradient S (Eppendorf) or a PTC-100 Programmable Thermal Controller (MJ research Inc., St Bruno (Quebec), Canada) following the general outline listed in Table 2-4. Individual steps were adjusted according to primer and/or sample determinants. Primers were designed online (Primer3, v. 0.4.0) and, if possible, the sequence confirmed by electronic PCR (http://www.ncbi.nlm.nih.gov/sutils/e-pcr/reverse.cgi). All primers were obtained from Eurofins MWG GmbH (Ebersberg, Germany) Sample cDNA was added to a mixture containing an equal volume of primers, 10x PCR Buffer, DMSO, dNTPs, Taq Polymerase and dH_2O to a total volume of 20 µl. Following PCR amplification, product size was determined by gel electrophoresis.

Table 2-4: Model PCR protocol

Step	Time	Temperature	Cycles
Initial denaturation	3 min	94°C	
Denaturation	1 min	94°C	
Annealing	1 min	55 -65°C, according to primer pairs	30 - 35
Elongation	1 min	72°C	
Prolonged elongation	7 min	72°C	

2.9.4 Agarose Gel Electrophoresis

Agarose gels with concentrations ranging from 1% to 2.3% were prepared in TAE buffer and Gel Red (0.04 µl/ml) added. Once the gel had polymerized a DNA ladder (25-2010, Peqlab) and samples, prepared with loading buffer (Coral Load Buffer 10x, Qiagen) were applied to the gel pockets. Electrophoresis was performed within a gel chamber (Peqlab) powered at 150 Volts/500 mA (Phero-Stab 0310, Biotec-Fischer, Reiskirchen, Germany) and product fluorescence detected with a Gel Doc 1000 station (Bio-Rad, Munich, Germany).

TAE Buffer (50x)

Tris	2 M
Acetic Acid	1 M
EDTA	50 mM

2.10 Flow Cytometry

Flow cytometry is a widely employed method to analyse cells and can be applied to investigate cell number, shape, size, and granularity as well as cell surface and cytosolic expression of proteins using fluorescent antibodies. Furthermore, the fluorescent properties of a range of reagents allow flow cytometry to be used to detect changes such as in electric potentials and the production of reactive oxygen species.

A flow cytometer generally consists of a fluidics unit, an optical system and respective electronics as well as a computer to control the system and for visualisation. In principle, single cells are transported via a sheath of fluid and delivered to a laser source. The laser light is scattered as it passes through the cell and the scattering of the light is collected by specifically positioned detectors. The direction of scattered light can give an estimation of cell size (forward scatter, FSC) and granularity, e.g. number of vacuoles or organelles, (side scatter, SSC) of a cell. In addition to cell morphology, different lasers can also be employed to excite certain fluorescent antibodies or reagents. Corresponding detectors can then be used to quantify cell surface or cytosolic proteins as well as cellular markers, e.g. of cell cycling or health.

2.10.1 Quantification of reactive oxygen species

eEPCs were cultured as described above without ß-Mercaptoethanol. After four days, 10^6 cells were allowed to grow in gelatine-coated 6-well plates overnight at standard culture conditions without ß-Mercaptoethanol. Subsequently, the medium was exchanged with Medium supplemented with 5 µM of the cell-permeable redox-sensitive fluorogenic dye, CellROX (Invitrogen, Life Technologies) and incubated for 30 minutes at 37°C. Cells were then washed with PBS three times, detached with trypsin, centrifuged for five minutes at 1200 RPM and resuspended in 500 µl PBS. CellROX fluorescence (excitation 644nm, emission 665 nm; principal depicted in Figure 2-2) was then measured by flow cytometry (FL-6) using a Gallios 2/8 flow cytometer (Becton Coulter. Krefeld, Germany). Fluorescence results were divided by the values of isotype controls to correct for autofluorescence.

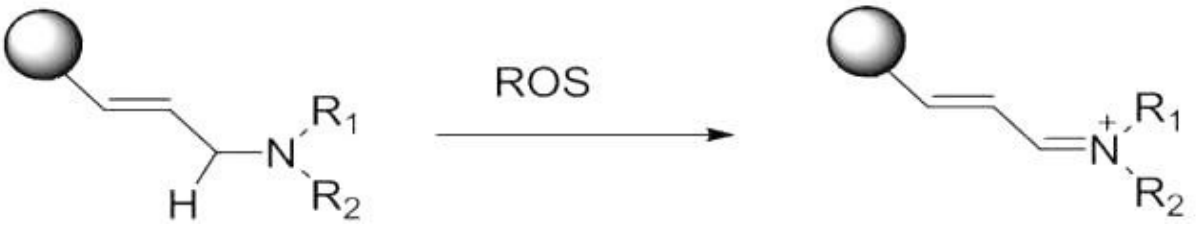

Reduced, non-fluorescent Oxidised, fluorescent

Figure 2-2: Mechanism of CellROX redox-sensitivity (Image courtesy of Life Technologies)

2.10.2 Measurement of mitochondrial membrane potential

To measure the mitochondrial membrane potential, eEPCs were cultured and pre-treated without ß-Mercaptoethanol as described for the CellROX measurement. Cells were trypsinised, centrifuged (200 rcf, five minutes) and 10^6 cells resuspended in warm PBS. Subsequently, cells were incubated with 2 µM of the MitoProbe™ JC-1 Assay Kit (Invitrogen, Life Technologies; chemical structure outlined in Figure 2-3) for 30 minutes in an incubator set to 37°C and 5% CO_2, according to the manufacturer's protocol. Like CellROX, JC-1 (5',6,6'-tetrachloro-1,1',3,3'-tetraethylbenzimidazolylcarbocyanine iodide) is a cell-permeable dye. It specifically localises to the intermembrane space of mitochondria and, when excited at 488 nm, fluoresces at either of two membrane potential-dependent wave lengths. At physiological membrane potentials (approximately -180 to -220 mV) red-fluorescent J-aggregates form which can be detected at 590 nm. As the potential becomes more positive, J-aggregates dissociate and the green fluorescence of J-monomers can be detected at 529 nm. Prior incubation with the membrane potential disruptor CCCP (carbonyl cyanide 3-chlorophenylhydrazone) for five minutes at 37°C served as a positive control. Subsequently, cells were washed twice by centrifugation (200 rcf, five minutes) and resuspended in warm PBS before the shift of fluorescence from green to red was measured by flow cytometry.

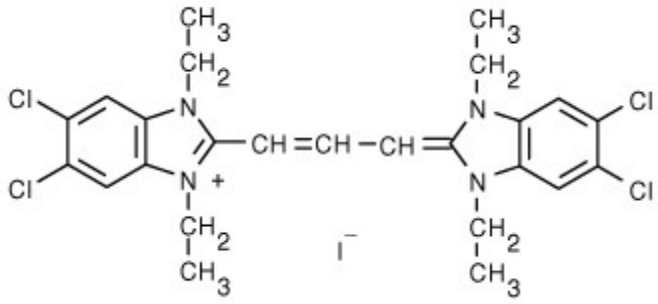

Figure 2-3: Chemical structure of the mitochondrial membrane potential marker JC-1 (image courtesy of Life Technologies)

2.11 Statistics

For statistical comparison of results, experiments were conducted at least three times. Results were compiled using Excel (Microsoft) and analysed using the statistical software SigmaPlot v. 11.0 (Systat Software, Erkrath, Germany). Statistical comparison of two groups for normally-distributed data was achieved by Student's t-test or by Rank Sum test if the data was not distributed normally. For the comparison of multiple groups, 2-way analysis of variance (ANOVA) followed by a Holm-Sidak Post-Hoc test was performed. The corresponding tests are indicated in the figure legends. In all statistical

tests, a p-value < 0.05 was considered statistically significant and data is presented as mean ± standard error of the mean (SEM) (normal distribution) or median and interquartile range (25 – 75 %) for non-normal distribution of data. If data was excluded, only data points three standard deviations (SD) above the mean were eliminated.

3 Results

3.1 Txnrd2 deletion affects cellular redox state and mitochondrial health

To assess the impact of Txnrd2 deletion *in vitro*, we used Txnrd2-deficient eEPCs as substitutes for ECs. Since the eEPCs had been previously isolated from embryos of Txnrd2-heterozygous mice, the protein level of Txnrd2 was confirmed in each clone by western blot. A representative blot confirming the lack of Txnrd2 in eEPC protein lysates is displayed in Figure 3-1 (A). Whether the deletion of Txnrd2 impacts on the cellular concentrations of ROS and ΔΨm was assessed after culturing the cells in medium lacking ß-Mercaptoethanol for four days followed by seeding of $1x10^6$ cells/well in 6-Well plates over night. The following day, ROS and ΔΨm were assessed by flow cytometry using respective markers.

3.1.1 Txnrd2 deletion increases ROS in eEPCs *in vitro*

To investigate how the deletion of Txnrd2 impacts on cellular levels of ROS, eEPCs were incubated with the Redox-sensitive dye CellROX and fluorescence intensity measured by flow cytometry. As displayed in Figure 3-1 (B), Txnrd2 deletion resulted in a significant increase in the fluorescence intensity (FL6) of CellROX ($Txnrd2^{+/+}$: 17.002; $Txnrd2^{-/-}$: 23.382 (median); $p < 0.001$, Rank-Sum test), representative of increased cellular ROS concentrations in $Txnrd2^{-/-}$ eEPCs.

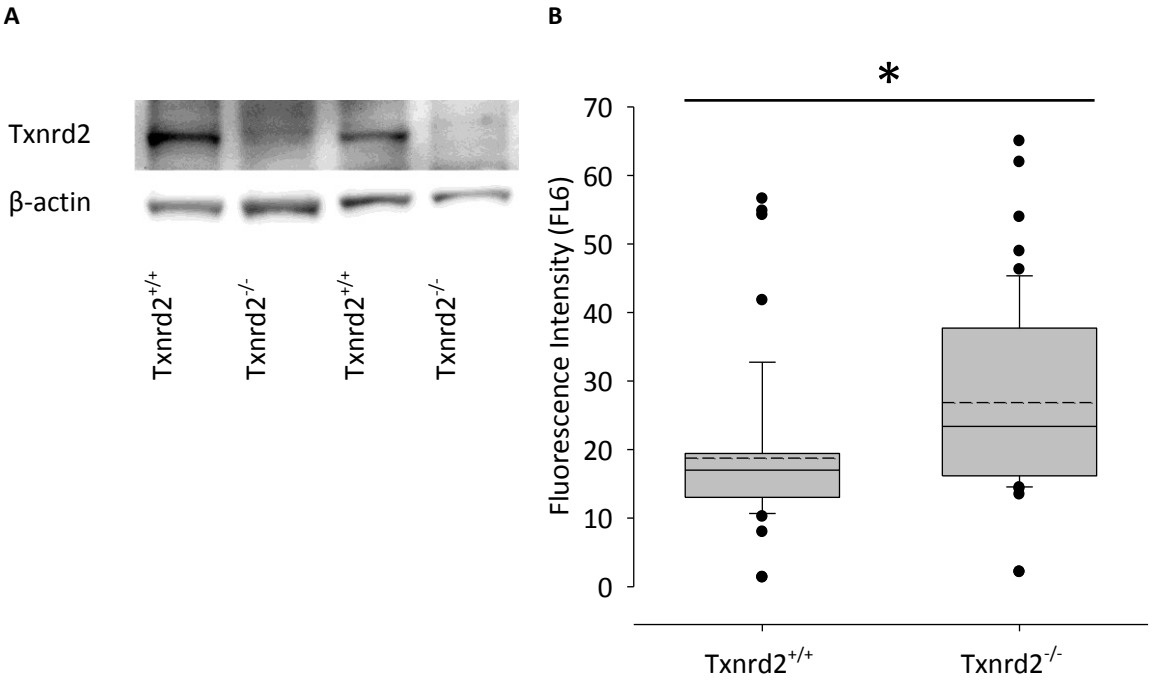

Figure 3-1: Txnrd2 deletion increases ROS levels in eEPCs. (A) Representative western blot displaying the absence of Txnrd2 in eEPCs. β-actin served as loading control. (B) The fluorescence of the redox-sensitive dye CellROX was measured by flow cytometry and the values corrected for autofluorescence using the values obtained from isotype controls not containing the dye. Dots indicate outliers, solid lines represent the median values and dotted lines the mean. * $p < 0.001$, Rank-Sum Test, n =.50 (Txnrd2 $^{+/+}$) – 51 (Txnrd2 $^{-/-}$).

3.2 Txnrd2 deletion impairs mitochondrial membrane potential in eEPCs *in vitro*

Since the eEPCs lacking Txnrd2 were subject to increased ROS levels and the mitochondrial Txn system is considered to be involved in the most important H_2O_2 detoxification processes, we sought to investigate whether this increased mitochondrial ROS burden may also affect the ΔΨm in these cells. Indeed, as depicted in Figure 3-2, eEPCs lacking Txnrd2 exhibited a significantly impaired potential of their mitochondrial membranes, indicative of impaired mitochondrial health (Txnrd2$^{+/+}$: 1.03±0.048; Txnrd2$^{-/-}$: 0.85±0.038 (mean ratio±SEM) $p < 0.01$, t-test). Txnrd2 deletion did not lead to complete loss of ΔΨm which is exemplified by incubating the cells with the potential disrupter CCCP as a positive control (Txnrd2$^{+/+}$ CCCP: 0.64±0.012; Txnrd2$^{-/-}$ CCCP: 0.65±0.028).

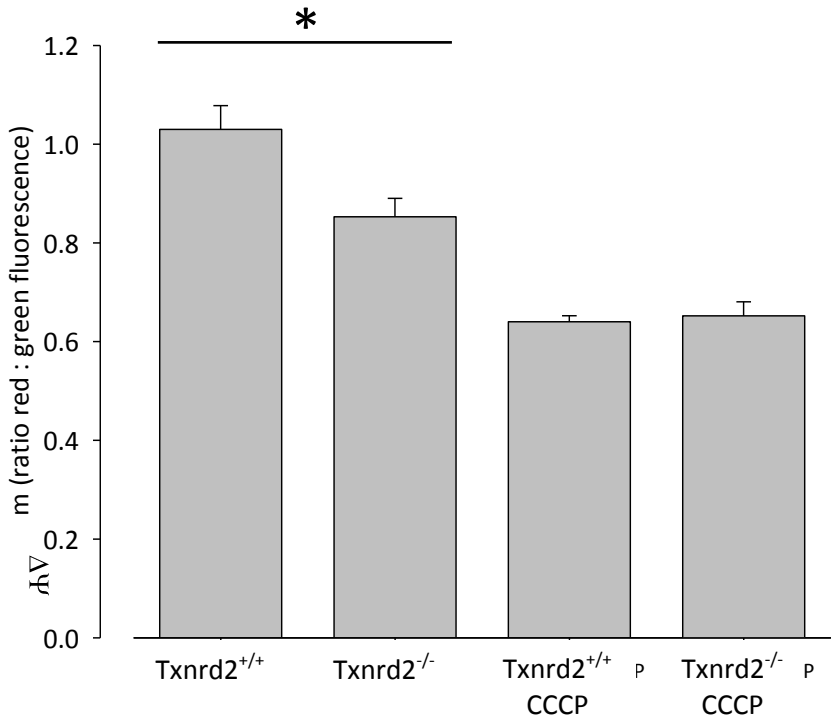

Figure 3-2: Measurement of ΔΨm in eEPCs expressing or lacking Txnrd2. The colour shift in eEPCs previously loaded with the cell-permeable, mitochondrial-specific and potential-dependent dye JC-1 was assessed by flow cytometry. CCCP was used as a negative control for JC-1. * $p < 0.01$, t-test, n = 13.

3.3 Effects of endothelial-specific deletion of Txnrd2 *in vivo*

The different genotypes of mice employed for the *in vivo* examination of Txnrd2 deletion in ECs is displayed in Figure 3-3 (A). Tamoxifen application resulted in the expected deletion of Txnrd2 in the endothelium as exemplarily shown for renal endothelial cells (Figure 3-3 B). Endothelial deletion of Txnrd2 had no impact on mouse survival following knockout induction. To investigate the role of Txnrd2 in adult ECs under forced angiogenesis as well as arteriogenesis, mice lacking the mitochondrial antioxidant specifically in the endothelium were subjected to hind-limb ischemia. By ligating the femoral artery in one leg, flow is redirected through pre-existing collateral vessels to bypass the occlusion. In the adductor muscle this is suggested to lead to an initial increase in FSS in the collateral vessels which is sensed only by ECs. Subsequently, ECs signal this alteration in flow to the underlying cells and elicit vasodilatation via the release of NO and H_2O_2, amongst others. Increased FSS, vasodilatation, infiltration of monocytes and other processes then lead to arteriogenesis of the collateral vessels. In the calf muscle the upstream obstruction of flow decreases O_2 availability and thus initiates hypoxic signalling. Hypoxia is a strong initiator of angiogenesis, i.e. the sprouting of new capillaries.

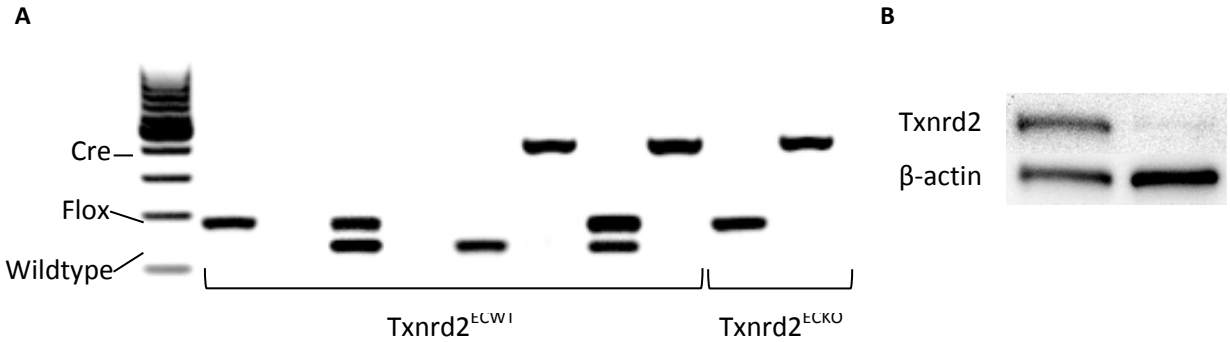

Figure 3-3: Genotyping of mouse tail clippings and confirmation of Txnrd2 deletion in ECs. (A) Various Genotypes of mice as determined by PCR from tail clippings. Only one combination (flox/flox cre^{+}) represents a Tamoxifen-inducible Txnrd2^{ECKO} mouse. (B) Representative western blot from ECs isolated from the kidneys of a Txnrd2^{ECWT} (left) and a Txnrd2^{ECKO} (right) mouse. β-actin served as loading control.

3.3.1 Re-establishment of perfusion in the murine hind-limb

As displayed in Figure 3-4, values for hind-limb perfusion were calculated as a ratio of the perfusion in the sham-operated hind-limb to that in the occluded hind-limb. These ratios were similar between wildtype and Txnrd2^{ECKO} mice prior to and immediately after occlusion. Furthermore, no difference could be observed after 3 days of recovery. However, after 7 days it became evident that perfusion recovery in the occluded hind-limb of Txnrd2^{ECKO} mice was significantly attenuated (0.471±0.0298) relative to their wildtype counterparts (0.603±0.0312 (mean±SEM); $p < 0.01$, 2-Way RM ANOVA and Holm-Sidak Post-Hoc test).

The data presented in Figure 3-4 suggest that the impairment in perfusion in Txnrd2^{ECKO} mice is only slight. However, in one Txnrd2^{ECKO} mouse, the perfusion ratio at day 7 hat attained a value close to 1.00 and this data point was thus revealed as a substantial outlier (three SD above the mean). We suspect that the ligation thread or the knot had disintegrated since the occlusion in this mouse was successful and perfusion was comparable to other mice at day three. And while a complete recovery of perfusion to baseline conditions within seven days is unlikely, we decided not to exclude this data point as a) *in vivo* results naturally tend to spread more than *in vitro* examinations due to individual differences between the animals and b) we could only speculate on the reason for the recovery and could not directly identify the cause of the drastic recovery.

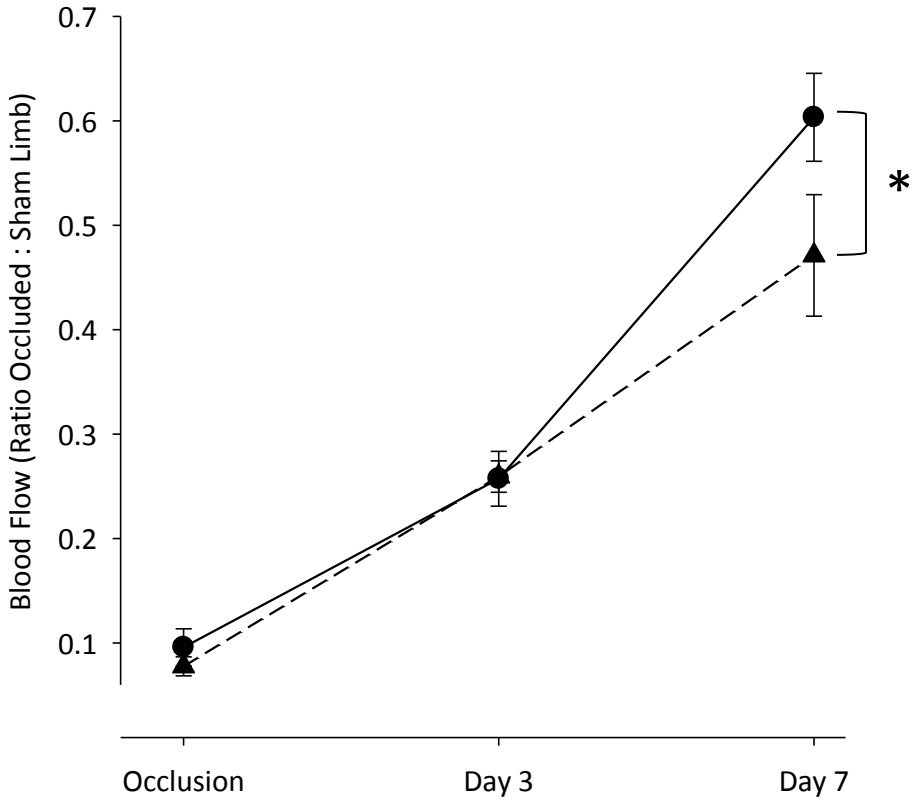

Figure 3-4: Recovery of perfusion after occlusion of the femoral artery. While no differences in perfusion ratio of sham-operated to occluded hind-limb were evident prior to, immediately after and 3 days post-surgery in Txnrd2^{ECKO} compared to Txnrd2^{ECWT} mice, recovery was significantly reduced in mice lacking Txnrd2 after 7 days. Circles with solid line: Txnrd2^{ECWT}; triangles with dashed line: Txnrd2^{ECKO}. * $p < 0.01$, 2-Way RM ANOVA and Holm-Sidak Post-Hoc test, n = 11 (Txnrd2^{ECWT}) – 12 (Txnrd2^{ECKO}).

3.3.2 Assessment of Angiogenesis

In order to elucidate the cause for the impairment of reperfusion in the Txnrd2^{ECKO} mice after hind-limb ischemia, we isolated the calf (gastrocnemius) muscles after the final LDI measurement. Ten µm thick cryo-sections of the muscle were stained with a primary antibody raised against the EC-specific surface protein CD31 coupled to a Cy3-conjugated secondary antibody. Fluorescence microscopy was subsequently performed to visualise the capillaries in the calf muscle. Capillary density was evaluated as the area fluorescently labelled by the CD31/Cy3 antibody complex relative to the whole area per field of view. Within each section photographs were taken at three distinct sites as depicted in Figure 3-5.

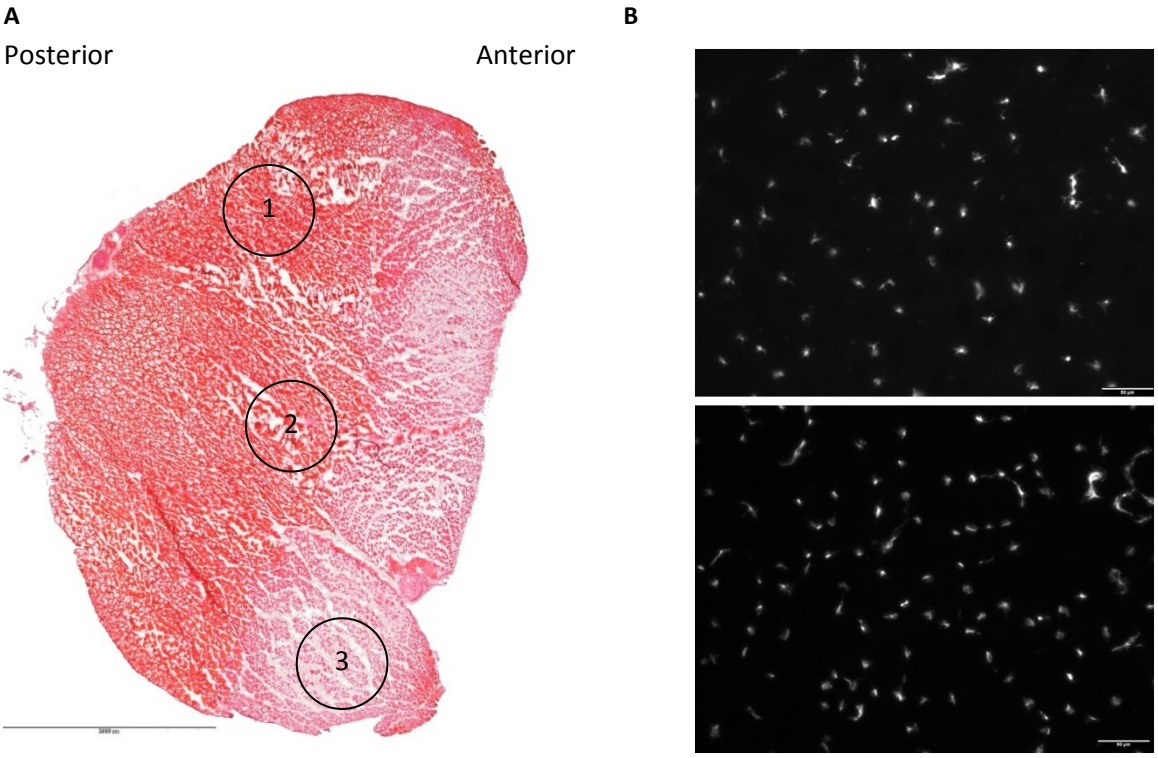

Figure 3-5: Representative images of a gastrocnemius muscle cryo-section. Muscle sections were prepared after seven days of hind-limb ischemia. (A) H&E stain of a calf muscle slice from a Txnrd2^{ECKO} mouse. Three distinct areas per slice were assessed for capillary density in the CD31/Cy3-labelled sections as indicated by the numbered circles. Scale bar: 2 mm. (B) Representative images of fluorescently labelled cryo-sections obtained from sham (upper panel) and occluded (lower panel) hind-limbs. CD31/Cy3-labelled ECs are displayed in white and the positively stained area evaluated relative to the total field of view. Scale bar: 50 µm.

As illustrated in Figure 3-6 (A), capillary density was significantly lower in the calf muscle of Txnrd2^{ECKO} mice than in Txnrd2^{ECWT} mice after seven days of hind-limb ischemia (Txnrd2^{ECWT}: 115.17, Txnrd2^{ECKO}: 108.88 (median), $p < 0.05$, Rank Sum test). Interestingly, this impairment was only present in two of the three sites analysed (Figure 3-6 B, Txnrd2^{ECWT}: 134.47; Txnrd2^{ECKO}: 116.18; Figure 3-6 C, Txnrd2^{ECWT}: 118.16; Txnrd2^{ECKO}: 108.79 (median), $p < 0.05$, Rank Sum test). In the third area no difference in capillary density was evident between the groups (Txnrd2^{ECWT}: 98.29; Txnrd2^{ECKO}: 98.76 (median), $p = 0.702$, Rank Sum test). In fact, no increase in capillary area fraction from the sham-operated limb occurred in this region, possibly due to the development of necrosis in this area in both animal groups.

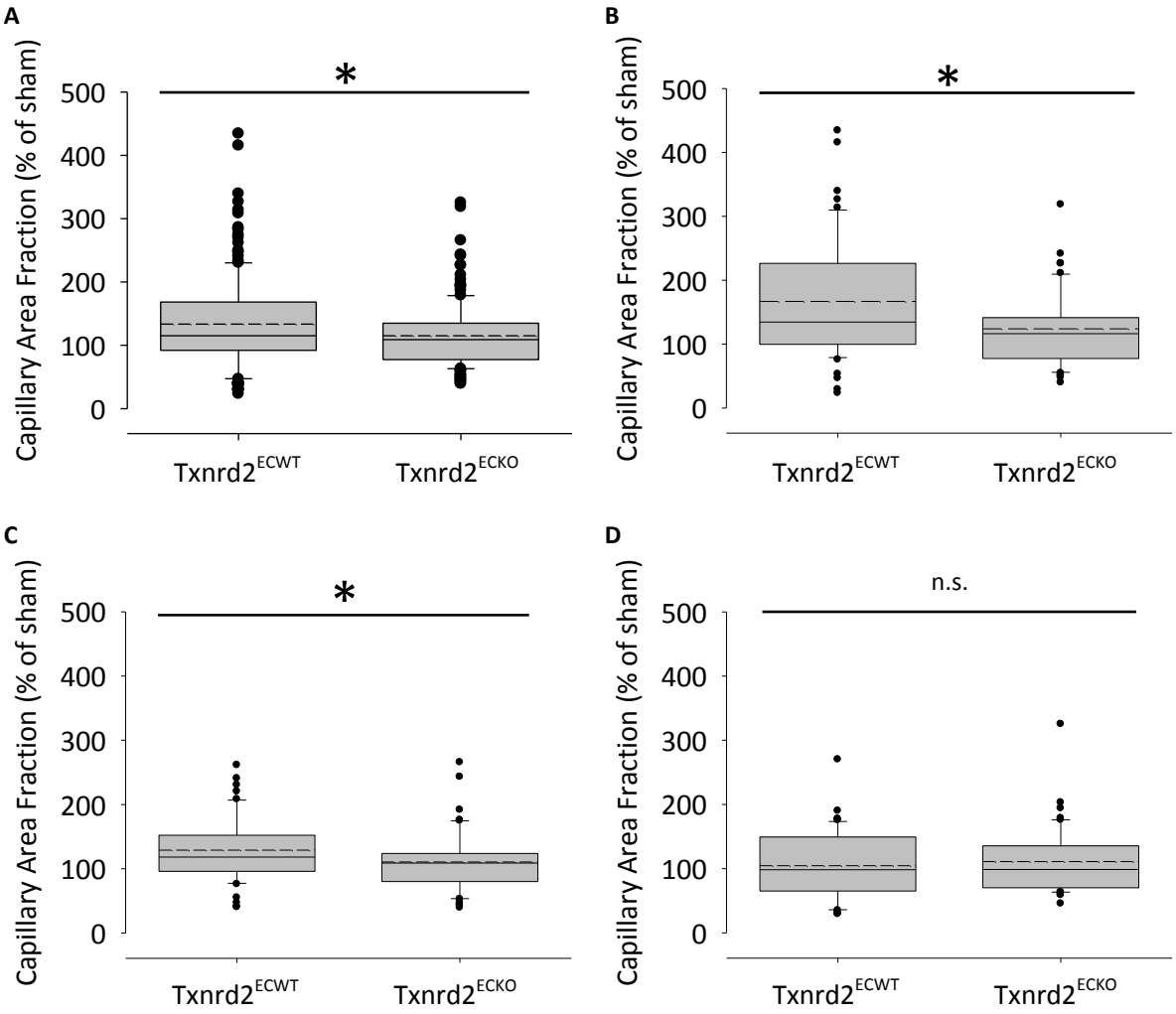

Figure 3-6: Evaluation of capillary density in the occluded hind-limb after seven days of ischemia. Angiogenesis was evaluated by comparing the increase in capillary area fraction in the calf muscle of the occluded hind-limb and expressed as the % difference from the sham-operated calf muscle. (A) There was a significantly lower density of capillaries in the calf muscle of Txnrd2^{ECKO} mice when comparing the data from all analysed sections together. This significant impairment was present in area 1 (B) and in area 2 (C). (D) No difference in the capillary area fraction exists between the two subject groups in area 3. Solid line: median; dashed line: mean; Dots: outliers. *p < 0.05; n.s. not significant; Rank Sum Test; n= 8 (Txnrd2^{ECWT}) – 9 (Txnrd2^{ECKO}).

3.3.3 Assessment of Arteriogenesis

While capillary density was indeed attenuated in the occluded hind-limb of Txnrd2^{ECKO} mice, the extent the impairment could contribute to the decrease in perfusion measured by LDI is rather small. Considering that resistance to flow is inversely proportional to the fourth power of the radius, even the sum of all new capillaries would easily be excelled by small diameter changes in the upstream collateral vessels of the adductor muscle. We therefore analysed various parameters of remodelling in the collateral arterioles of the adductor muscle after seven days of hind-limb ischemia.

Five to 6 µm thick paraffin sections of the adductor muscles were H&E stained and both the inner (C_i) and outer circumference (C_o) of the collateral vessels measured using ImageJ software. From these data, vessel wall area (A) and thickness (T) as well as luminal diameter (d) were calculated with the following formulas:

$$A = \pi \left(\frac{C_o}{2\pi}\right)^2 - \pi \left(\frac{C_i}{2\pi}\right)^2$$

$$d = \frac{C_i}{\pi}$$

$$T = \frac{C_o}{2\pi} - \frac{C_i}{2\pi}$$

As displayed in Figure 3-7, the collateral arterioles in the occluded hind-limbs were subject to substantial remodelling in both the Txnrd2^{ECWT} and Txnrd2^{ECKO} mice seven days post-ischemia. The results in Figure 3-8, however, demonstrate that while vessel wall area had increased in both groups, this effect was significantly less pronounced in the mice lacking Txnrd2 (Txnrd2^{ECWT}: 686.76 µm^2; Txnrd2^{ECKO}: 487.28 µm^2 (median), p <0.001 Rank Sum test). Interestingly, these mice had a slight but significant greater wall area at baseline in the sham hind-limb (Txnrd2^{ECWT}: 180.45 µm^2; Txnrd2^{ECKO}: 279.71 µm^2 (median), p <0.001 Rank Sum test).

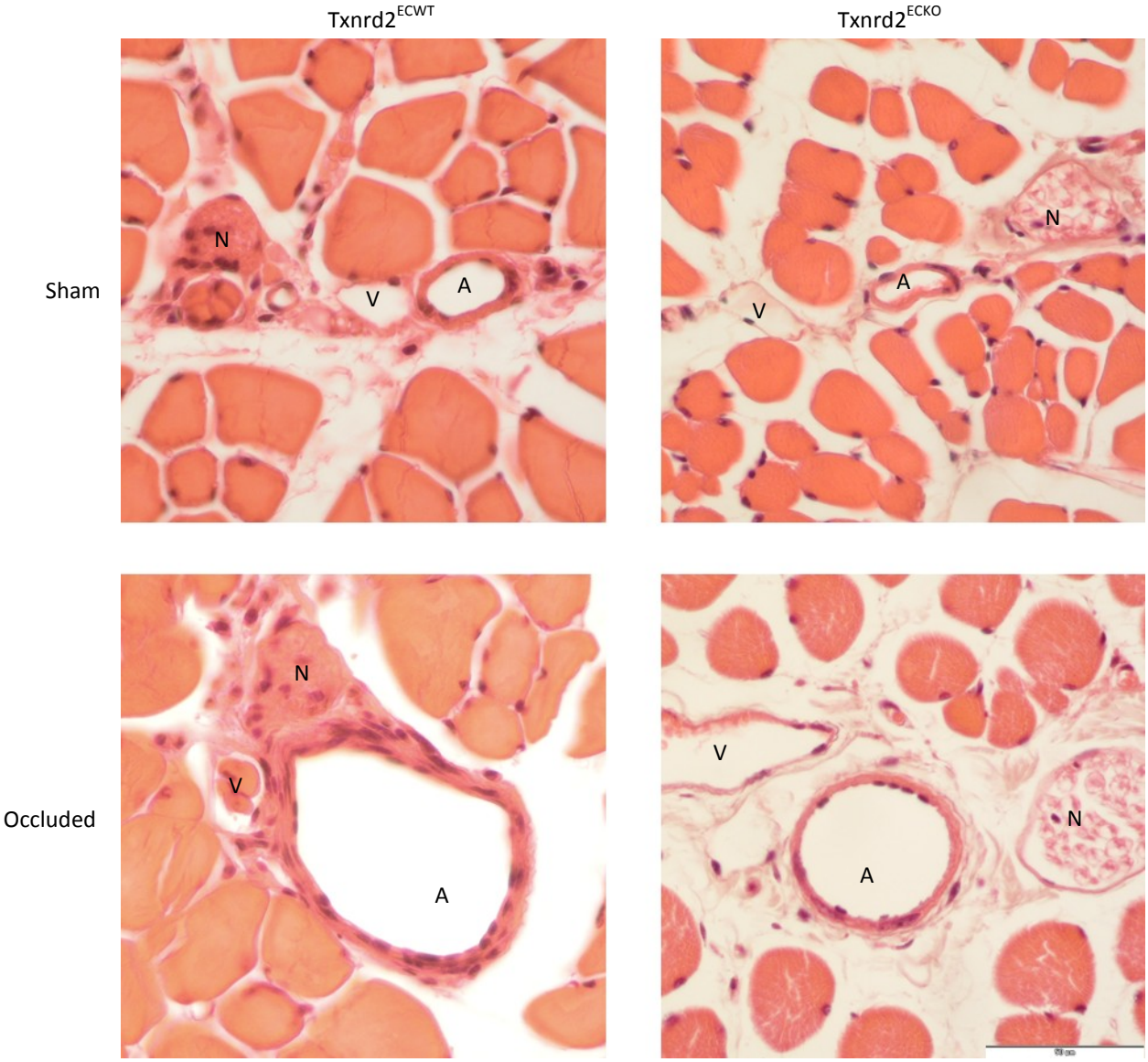

Figure 3-7: Representative images of thigh muscle paraffin sections. Muscle sections were prepared after seven days of hind-limb ischemia and the inner and outer arteriole circumference measured to assess wall area, thickness and luminal diameter. A, arteriole; N, nerve; V, venule. Scale bar: 50 µm.

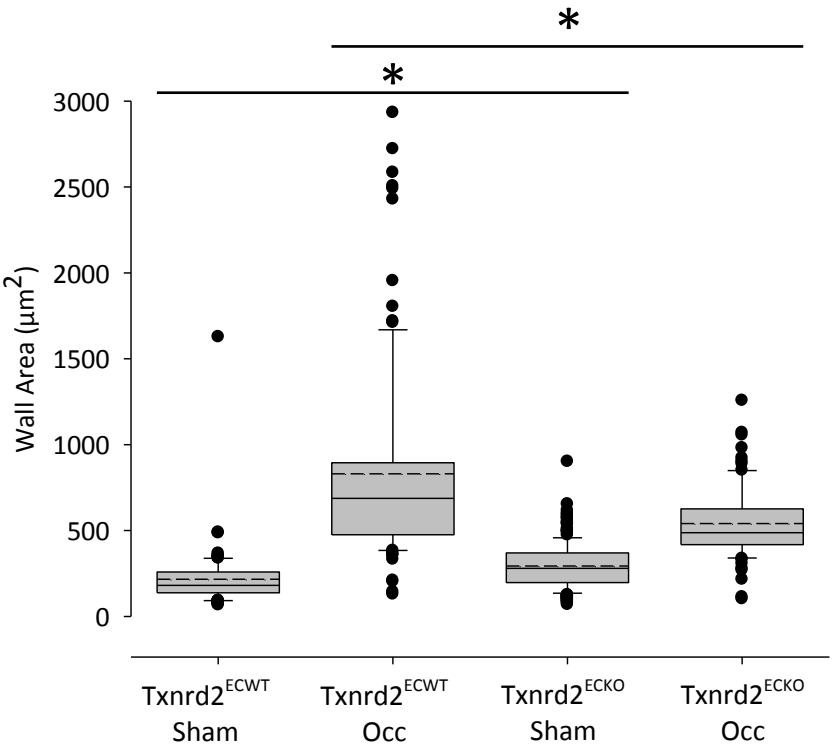

Figure 3-8: Assessment of collateral vessel wall area Collateral vessel wall area was greater in Txnrd2^{ECKO} mice than in Txnrd2^{ECWT} mice at basal levels. The increase in collateral vessel wall area in the occluded hind-limb was significantly attenuated in Txnrd2^{ECKO} mice compared to their wildtype counterparts after 7 days of hind-limb ischemia. Solid line: median; dashed line: mean; dots: outliers. *p < 0.001; Rank Sum Test; n = 3 (Txnrd2^{ECWT}) – 4 (Txnrd2^{ECKO}).

In contrast to the findings on collateral artery wall area, the walls of these vessels were found to be similarly thick in Txnrd2^{ECWT} and mice lacking Txnrd2 after seven days of hind-limb ischemia (Txnrd2^{ECWT}: 4.22 µm; Txnrd2^{ECKO}: 4.38 µm (median); p = 0.445, Rank Sum test; Figure 3-9 A). Analogous to the findings on the wall area, Txnrd2^{ECKO} mice also displayed basally thicker walls in their collaterals (Txnrd2^{ECWT}: 2.96 µm; Txnrd2^{ECKO}: 3.79 µm; p <0.001, Rank Sum test). Normalisation of the wall thickness of the collaterals in the occluded hind-limb to those in the sham-operated hind-limb, however, revealed that the increase in thickness above basal levels was significantly attenuated in the collateral vessels in the Txnrd2^{ECKO} mice after seven days of hind-limb ischemia (Txnrd2^{ECWT}: 134.95 % of sham; Txnrd2^{ECKO}: 106.93 % of sham (median); p < 0.001, Rank Sum test; Figure 3-9 B).

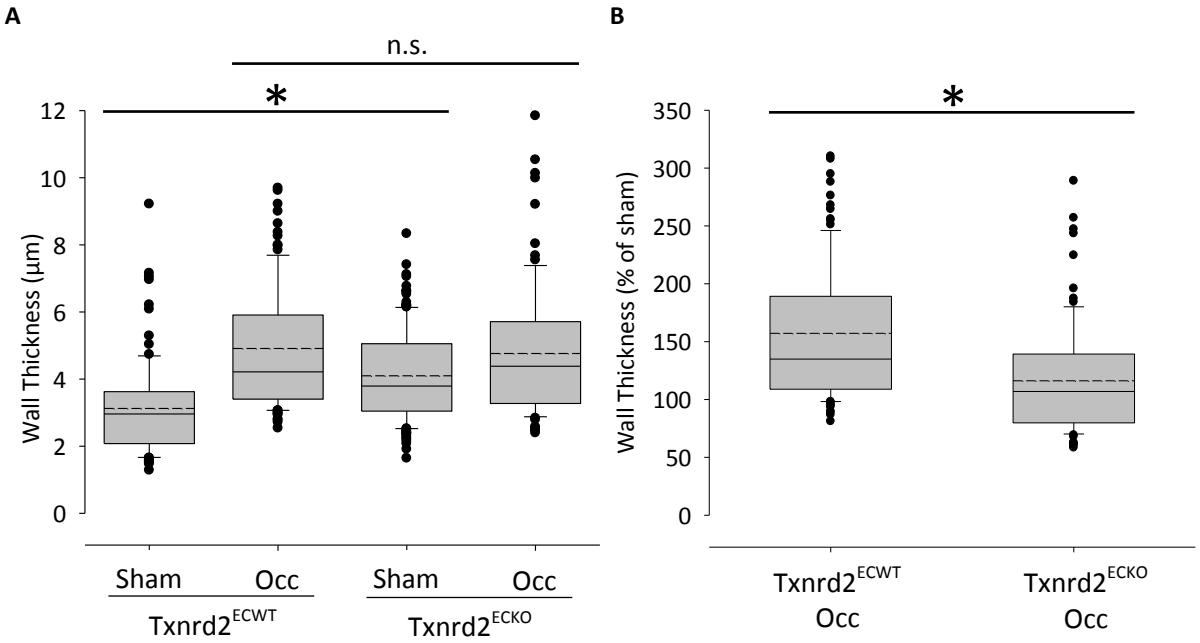

Figure 3-9: Collateral Vessel Wall Thickness. (A) At basal levels, collateral vessel wall thickness was increased in Txnrd2^{ECKO} mice. After seven days of hind-limb ischemia, wall thickness had increased in the occluded hind-limbs of both Txnrd2^{ECWT} and Txnrd2^{ECKO} mice and no difference was evident between the two experimental groups. (B) Normalised wall thickness was calculated from the inner and outer circumferences and values from the collaterals of the occluded hind-limb normalised to the thickness of the collateral vessels of the sham-operated hind-limb. *p <0.001, n.s.: not significant, Rank Sum Test; n = 3 (Txnrd2^{ECWT}) – 4 (Txnrd2^{ECKO}).

Finally, since the vascular wall parameters suggested that the remodelling of the collateral vessels in the occluded hind-limbs of the Txnrd2^{ECKO} mice were lagging behind those of the Txnrd2^{ECWT} mice, we compared the luminal diameters of the collateral vessels. As the previous data already alluded to, the lumen of the collateral vessels of the Txnrd2^{ECKO} mice was significantly smaller in diameter as in the controls (Txnrd2^{ECWT}: 44.36 µm; Txnrd2^{ECKO}: 37.31 µm (median); p < 0.001, Rank Sum test; Figure 3-10). No difference in the luminal diameter of the collateral vessels between Txnrd2^{ECWT} and Txnrd2^{ECKO} mice was evident in the sham-operated hind-limb.

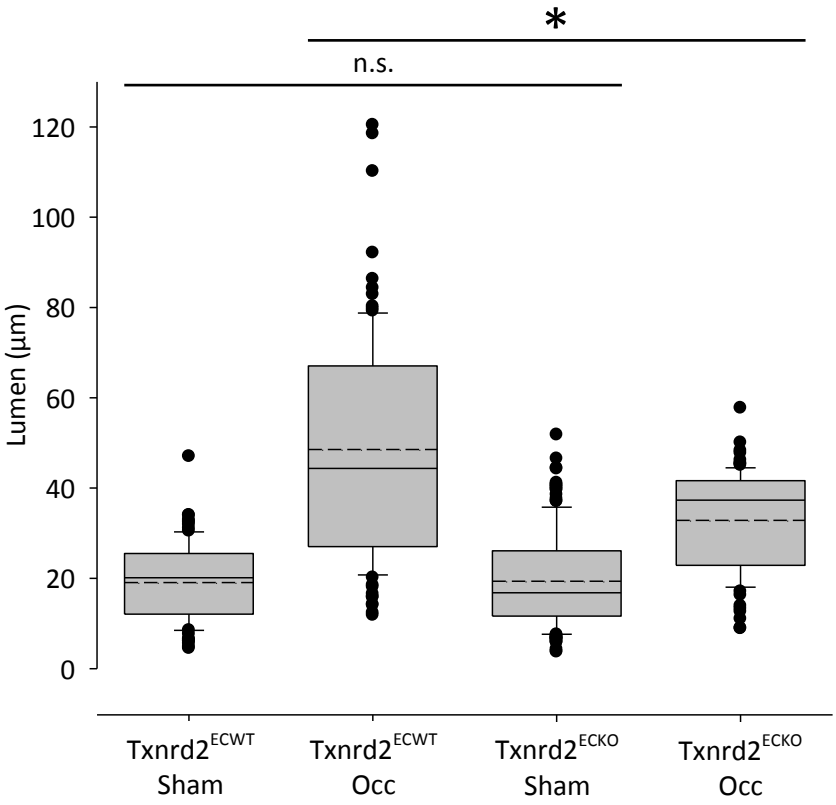

Figure 3-10: Assessment of luminal diameter in occluded and sham-operated hind-limbs seven days after surgery. Following the results obtained on vascular wall area and thickness, luminal diameter was significantly smaller in Txnrd2^{ECKO} mice than in Txnrd2^{ECWT} mice. No difference was observed in the sham-operated hind-limbs. Solid line: median, dotted line: mean; dots: outliers. *p < 0.001; Rank Sum Test; n = 3 (Txnrd2^{ECWT}) – 4 (Txnrd2^{ECKO}).

3.4 Possible pathways impaired in angiogenesis and arteriogenesis

To investigate the cause of the impairment in the remodelling of the collateral vessels in the occluded hind-limb of Txnrd2^{ECKO} mice, we assessed flow-mediated dilatation in isolated, unremodelled collaterals. This was achieved by increasing the pressure gradient across the vessel. Since the hydrostatic outflow pressure from the vessel remained unchanged, the increase in inflow pressure changed flow velocity. Unfortunately, no significant difference between Txnrd2^{ECKO} mice and their Txnrd2-expressing counterparts was detected (2-Way RM ANOVA and Holm-Sidak Post-Hoc test; Figure 3-11).

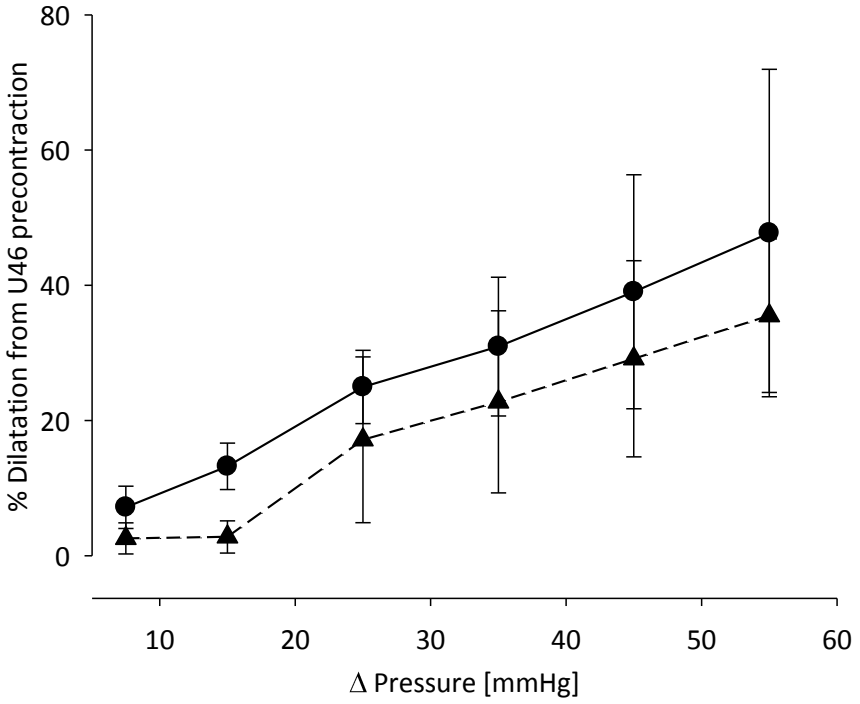

Figure 3-11: Flow-mediated dilatation of unremodelled collateral vessels. No significant difference in the vasodilatory response of collaterals from Txnrd2^{ECKO} mice compared to those obtained from Txnrd2^{ECWT} mice was detected. Circles: Txnrd2^{ECWT}; Triangles: Txnrd2^{ECKO}; n = 4 (Txnrd2^{ECWT}), 9 (Txnrd2^{ECKO}); 2-Way RM ANOVA and Holm-Sidak Post-Hoc test.

To investigate whether other FSS-independent, endothelium-mediated vasodilatory responses are impaired in vessels from Txnrd2^{ECKO} mice, the arterioles employed for the assessment of flow-mediated dilatation were also assessed for their vasodilatory capacity to Acetylcholine (ACh). As displayed in Figure 3-12 (A), collateral arterioles from Txnrd2^{ECKO} mice and their Txnrd2-expressing counterparts responded in a similar fashion to increasing concentrations of ACh.

Concentration-response-curves were also obtained from these vessels in response to the nitric oxide donor S-Nitroso-N-acetylpenicillamine (SNAP) to assess the extent of endothelium-independent vasodilatation. Similar to the results obtained in response to alterations in flow and ACh, no difference in the vasodilatory capacity of collateral arterioles from either Txnrd2^{ECWT} or Txnrd2^{ECKO} mice to various concentrations of SNAP were measured (Figure 3-12 B).

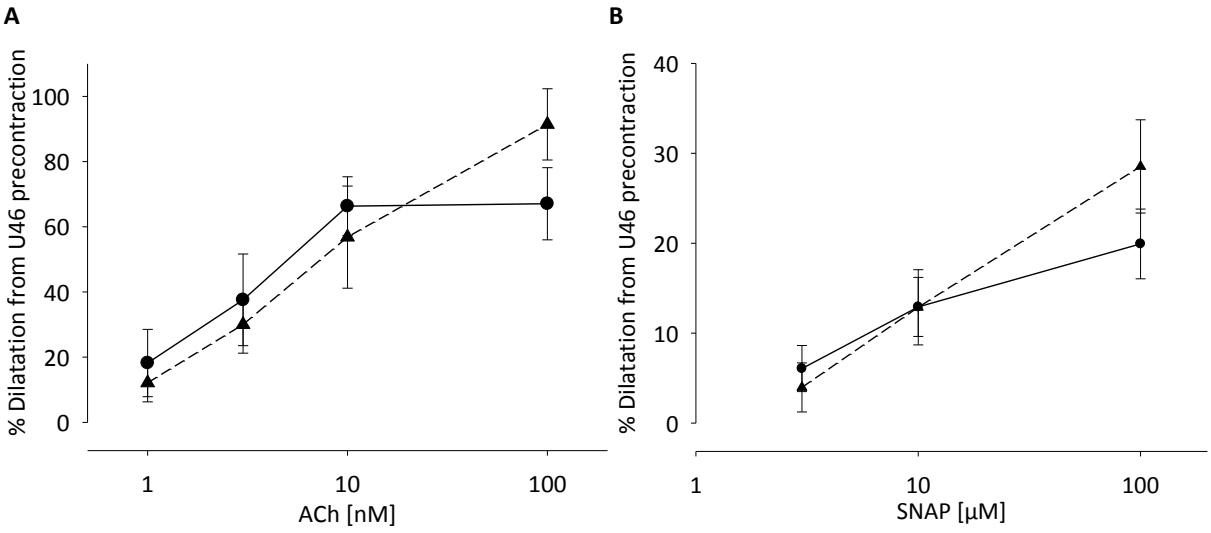

Figure 3-12: Vasodilation of unremodelled collateral vessels to exogenous vasodilators. (A) The vasodilatory responses of collaterals from Txnrd2^{ECKO} mice to increasing doses of ACh were not statistically different from those observed in Txnrd2^{ECWT} mice. (B) Similarly, the administration of SNAP did not reveal any statistically significant difference in the vasodilatory response of collateral arterioles from Txnrd2^{ECWT} or Txnrd2^{ECKO} mice. Circles: Txnrd2^{ECWT}, Triangles: Txnrd2^{ECKO}; n = 4 (Txnrd2^{ECWT}), 9 (Txnrd2^{ECKO}); 2-Way RM ANOVA and Holm-Sidak Post-Hoc test.

Since the impairment in both angiogenesis as well as arteriogenesis in the Txnrd2^{ECKO} mice should have its basis on a disruption of cellular signalling pathways, we investigated those associated with defects in these processes. In protein lysates obtained from eEPCs *in vitro*, western blots for PHD2, a protein implicated both in the control of HIF-1α stability as well as in the HIF-1α-independent regulation of EC proliferation, were prepared. As displayed in Figure 3-13, PHD2 expression was significantly increased at basal levels in Txnrd2$^{-/-}$ eEPCs compared to Txnrd2$^{+/+}$ eEPCs (Txnrd2$^{+/+}$: 1.00; Txnrd2$^{-/-}$: 1.27 (median fold expression); $p < 0.05$, Rank Sum test).

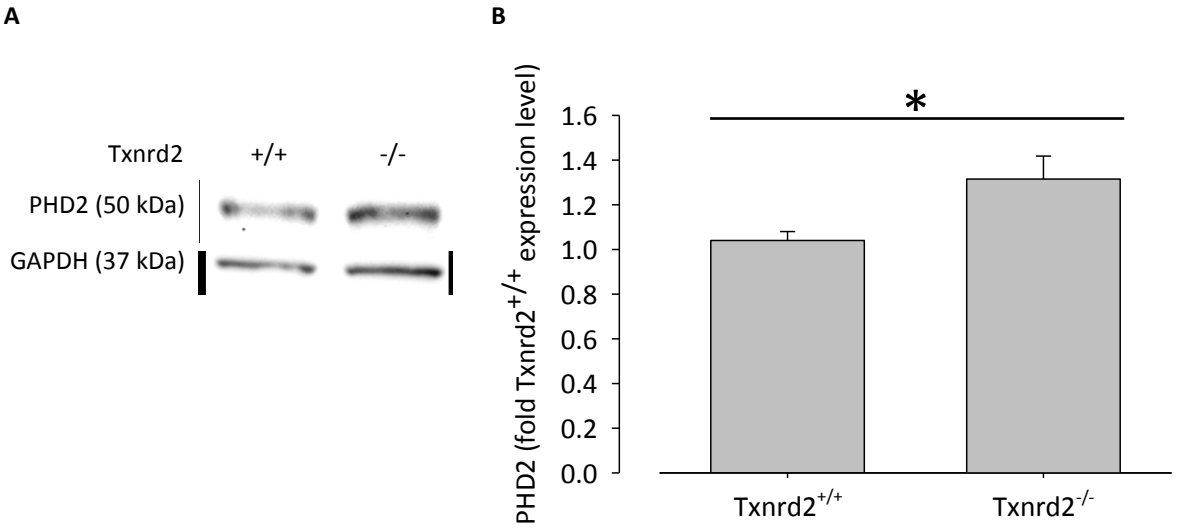

Figure 3-13: PHD2 expression is increased in Txnrd2$^{-/-}$ eEPCs. Protein lysates from Txnrd2$^{+/+}$ and Txnrd2$^{-/-}$ eEPCs were separated by SDS-Page and immunoblotted for PHD2. Semi-quantitative comparison revealed a significant increase in PHD2 protein expression in Txnrd2$^{-/-}$ eEPCs. (A) Representative immunoblot displaying an increase in PHD2 expression in Txnrd2$^{-/-}$ eEPCs. (B) Semi-quantitative comparison of PHD2 expression in Txnrd2$^{+/+}$ and Txnrd2$^{-/-}$ eEPCs from three western blots. n = 4; *p < 0.05, Rank Sum Test.

Increased ROS levels measured *in vitro* and the impaired remodelling observed *in vivo* led us to raise the question whether a reduction in NO bioavailability due to the sequestration of the vasodilatory gas by O_2^-• to form the toxic compound $ONOO^-$. Nitric oxide, O_2^-• and $ONOO^-$ are difficult to measure, so we attempted an indirect measurement of $ONOO^-$ damage by assessing the nitration of protein tyrosine residues in cell lysates prepared from eEPCs. However, as displayed in Figure 3-14 (A) no difference in the nitration of tyrosine residues was evident at baseline conditions between Txnrd2$^{+/+}$ and Txnrd2$^{-/-}$ eEPCs. Since ECs subjected to increased FSS *in vivo* would augment their NO production to elicit flow-mediated dilatation, we also assessed whether the administration of 10 µM sodium nitroprusside (SNAP), a NO donor, may increase protein nitrotyrosine. Again, no effect was evident in Txnrd2$^{-/-}$ eEPCs compared to their Txnrd2-expressing counterparts (Figure 3-14 B).

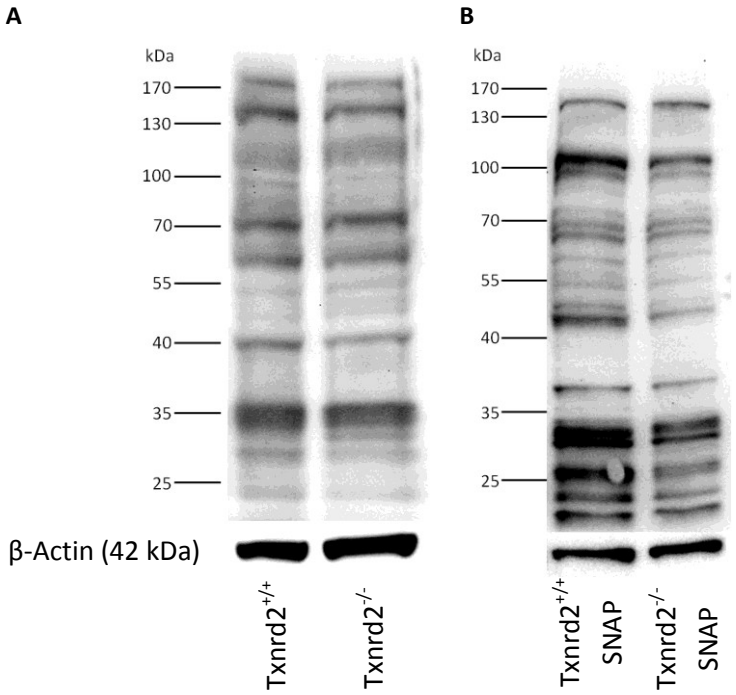

Figure 3-14: Tyrosine nitration in eEPCs. Nitration of tyrosine residues in proteins was assessed by immunoblot using an anti-nitrotyrosine antibody. (A) No difference the nitration of tyrosine residues of proteins was evident between Txnrd2$^{+/+}$ and Txnrd2$^{-/-}$ eEPCs. (B) To assess whether increased presence of NO would lead to an increase in the nitration of protein tyrosine residues, SNAP was administered to eEPCs prior to collecting the cell lysate. Again, no difference was observed between Txnrd2$^{+/+}$ and Txnrd2$^{-/-}$ eEPCs.

3.5 Additional consequences of Txnrd2 deletion

As the mitochondria can affect the function of the ER, for example by altering the Ca^{2+} resupply via the Na^{+}/Ca^{2+} exchanger, we were intrigued to find increased levels of the ER resident proteins Binding immunoglobulin Protein (BiP) and Protein Disulfide Isomerase (PDI), typically associated with ER stress (Figure 3-15) in Txnrd2-deficient eEPCs.

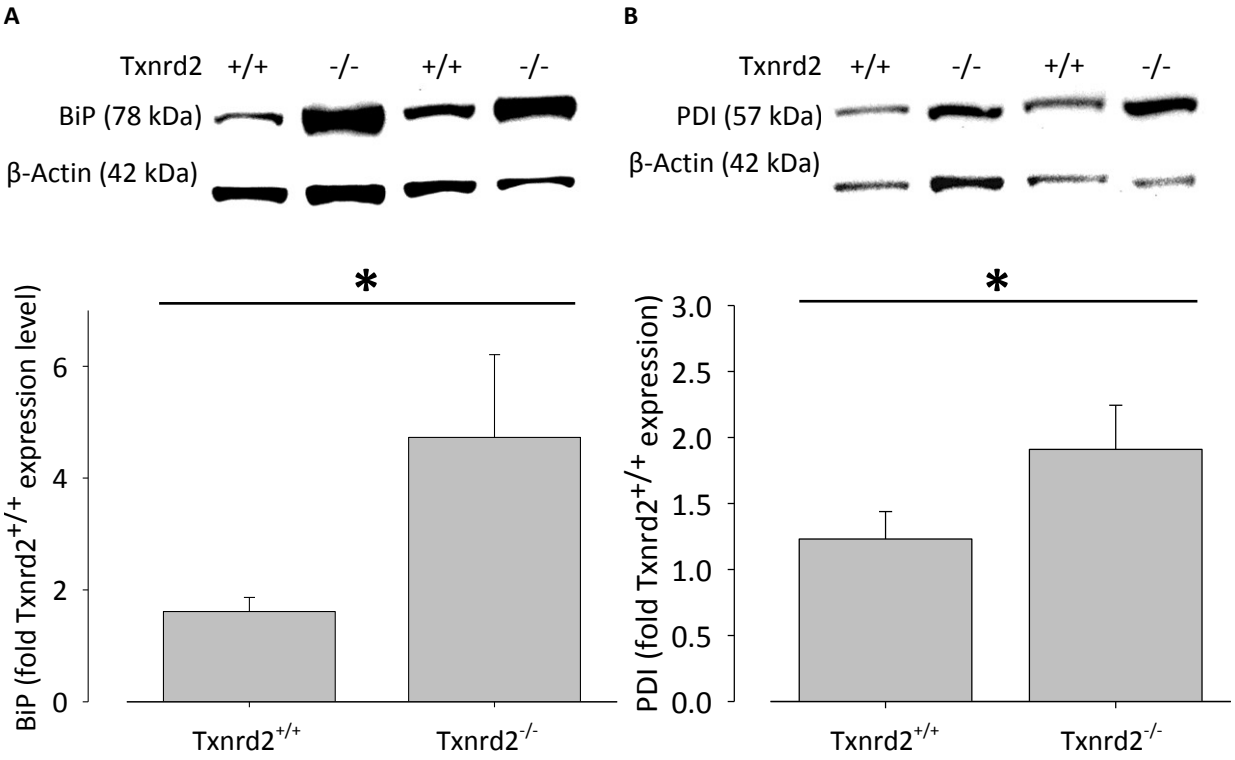

Figure 3-15: Txnrd2 deletion leads to increased levels of ER stress proteins. (A) Protein expression levels of BiP were assessed by immunoblot (upper panel). Semi-quantitative analysis of four western blots revealed a significant upregulation of BiP protein expression in Txnrd2$^{-/-}$ eEPCs (*p < 0.05, Rank Sum Test; lower panel). (B) PDI protein expression was also assessed by immunoblot (upper panel). Analogous to BiP, semi-quantitative analysis of five western blots confirmed a significant increase of PDI on the protein level in Txnrd2$^{-/-}$ eEPCs (*p < 0.05, Rank Sum Test; lower panel).

PDI can be released from ECs and has been implicated in the commencement of the coagulation cascade, possibly by activating tissue factor [122]. Thus, the finding on increased PDI protein levels in Txnrd2^{ECKO} mice led us to re-examine the paraffin sections of the collateral vessels in the adductor muscles. Indeed, in two of the four Txnrd2^{ECKO} mice from which paraffin sections had been prepared we found white thrombi in the collateral vessels and in the femoral artery (Figure 3-16). Furthermore, in paraffin sections stained for haematoxylin and the leukocyte marker CD45, we found atherosclerotic-like depositions in the femoral artery of a third Txnrd2^{ECKO} mouse (Figure 3-17). Neither thrombi nor atherosclerotic-like lesions were evident in the paraffin sections prepared from any of the three Txnrd2^{ECWT} mice.

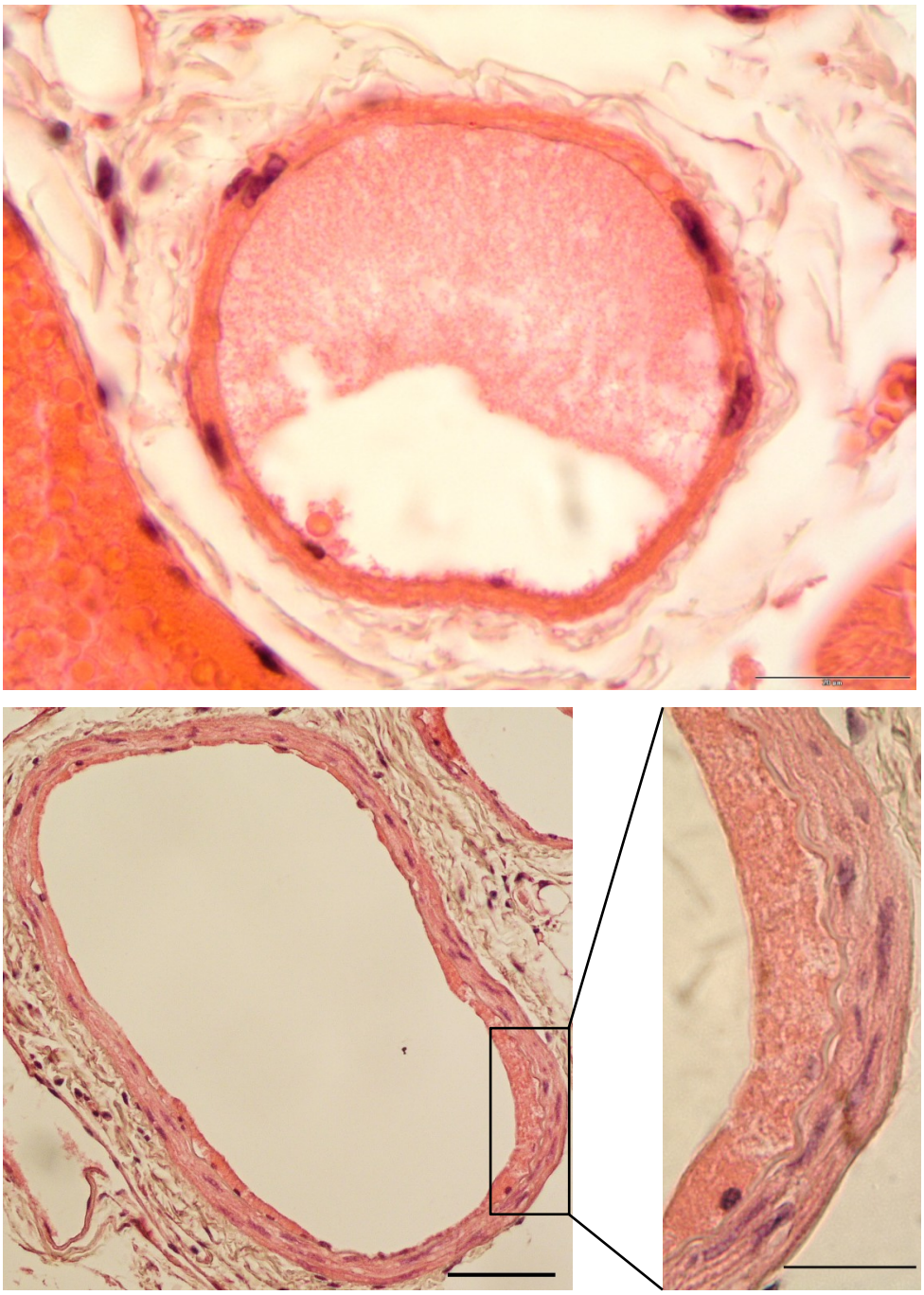

Figure 3-16: Depositions in the collateral arterioles and femoral artery of Txnrd2^{ECKO} mice. (Top panel) White thrombus-like depositions were found in the collateral arterioles of Txnrd2^{ECKO} mice from the hind-limb ischemia experiments. The blood-filled structure to the left of the arteriole is a corresponding venule and the nerve is displayed in the upper right corner of the image. Scale bar 20 µm. (Lower panel) Thrombotic depositions in the wall of the sham-operated femoral artery of a Txnrd2^{ECKO} mouse. Scale bar 50 µm (left), 20 µm (right).

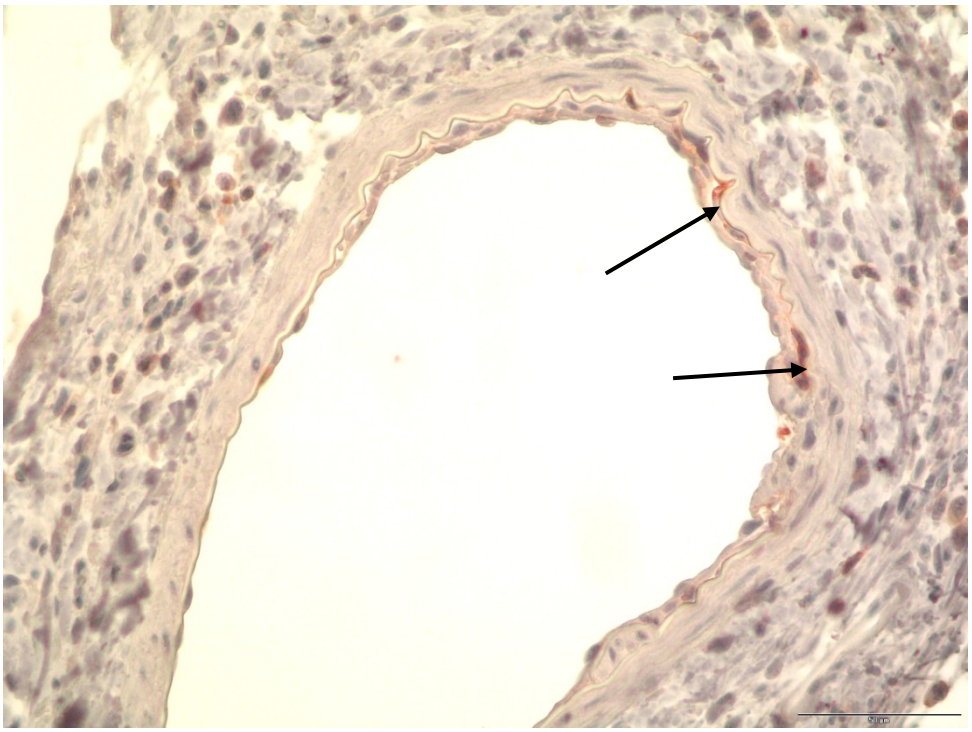

Figure 3-17: CD45-positive staining in femoral artery of Txnrd2^{ECKO} mouse. In the occluded femoral artery of a Txnrd2^{ECKO} mouse we found atherosclerotic-like depositions which were also positively stained for the leukocyte marker CD45 (red, indicated by arrows). Scale bar 50 µm.

4 Discussion

The precise regulation of cellular redox status is vital in controlling processes such as cellular proliferation or growth inhibition, and cellular activation or death [92, 123, 124]. The Txn system has been identified as one of the major regulators of cellular redox state and as such has begun to receive increasing interest [125]. As a result, the Txn system is now known to participate in the control of cellular function, proliferation, and redox-dependent signalling processes in addition to its antioxidative effects [23]. Txnrd1, for instance, is being considered as a target for anti-cancer therapeutics due to its effects on proliferation of tumour cells [126, 127]. Physiologically, Txnrd1 is relevant not only as an antioxidant but also, due to its wide substrate profile, in the regulation of cellular processes ranging from signalling pathways to the induction of apoptosis [36, 128]. In contrast to Txnrd1, however, the role of the mitochondrial thioredoxin reductase is still largely obscure.

In a previous study, an essential role in development could be ascribed to Txnrd2: a lack of the enzyme substantially impaired embryogenesis, and led to incomplete heart development and function as well as considerable defects in haematopoiesis [38]. Furthermore, we and others have shown that Txnrd2 can affect cellular proliferation and mitochondrial integrity as well as ROS levels *in vitro*, and can influence tumour growth and the angiogenic switch *in vivo* [37, 116, 129, 130]. The emergence of inducible, cell-specific knockout mice now circumvents the limitation of embryonic lethality in mice with a ubiquitous deletion of Txnrd2. Thus, a recent study which employed an inducible, cardiomyocyte-specific Txnrd2 deletion mouse has advanced our understanding on the role Txnrd2 plays in the progression of heart failure [39].

With a similar mouse in which the inducible deletion of Txnrd2 is under the control of the VE-cadherin promoter, we endeavoured to define the role of Txnrd2 specifically in the endothelium. Hind-limb ischemia in these mice allowed us to examine the *in vivo* effect of endothelial Txnrd2 ablation on angiogenesis and arteriogenesis, vascular processes both critically dependent on a functional endothelium. Since dysfunctional ECs are also implicated in several vascular diseases such as atherosclerosis, we also explored other phenotypical characteristics in these mice. Furthermore, with the use of eEPCs lacking Txnrd2, employed as substitutes due to the limited availability of adult ECs, we performed *in vitro* experiments to analyse the impact of Txnrd2 deletion on cellular ROS levels, mitochondrial integrity and potentially affected signalling pathways.

Indeed, we could show that Txnrd2 deletion leads to an increase in cellular ROS levels and impairs $\Delta\Psi m$ in eEPCs. In the living organism, EC-specific deletion of Txnrd2 significantly attenuated both

vascular remodelling processes investigated and our findings insinuate that these mice are prone to develop vascular wall depositions.

4.1 Txnrd2 deletion increases cellular ROS levels

Several well-known sources of radicals may contribute to the elevated levels of ROS observed in the Txnrd2$^{-/-}$ eEPCs. While the mitochondrial electron transport chain (ETC) is a substantial site of ROS production in many cell types including ECs, the roles of other sources are frequently reported. Especially the NAD(P)H oxidases have received increased attention and it is now well established that ECs are equipped with specific NAD(P)H oxidase isoforms, including the membrane-associated Nox2-containing subtype, which produces mainly O_2^-•, and Nox4, which primarily generates H_2O_2 [131-133]. However, ECs are also equipped with the Nox1 and Nox5 isoforms as well as other enzymes that contribute to the overall cytosolic levels of ROS, such as the xanthine-dependent system which consists of xanthine dehydrogenase, xanthine oxidoreductase and xanthine oxidase, capable of producing both O_2^-• and H_2O_2 [134, 135]. Finally, oxidation of tetrahydrobiopterin (BH_4), a cofactor for NOS, shifts the main product of NOS from NO to O_2^-• which, especially in the vasculature with its dependence on NO-mediated vasodilatation, can have detrimental effects [135, 136]. In order to balance the production of radicals from these sources, cells are equipped with a variety of enzymatic ROS detoxification systems, including the Txnrd2/Txn2/Prx3 axis which, together with glutathione, is considered the main line of defence in the maintenance of physiologic levels of mitochondrial H_2O_2 [115, 137]. Considering that the mitochondrial thioredoxin system can detoxify more than 60% of this organelle's total H_2O_2 production, it is not surprising that an increasing number of studies report a strong effect of impaired Txnrd2 activity on cellular H_2O_2 levels [138]. For example, the anti-rheumatoid and anti-cancer gold(I) compound, auranofin, a potent inhibitor of Txnrd2 enzymatic activity at low concentrations, has been shown to prevent Txn2 redox cycling, to increase the oxidation of Prx3, and lead to a significant increase in H_2O_2 emission from isolated mitochondria [139]. In line with these findings and previous examinations in our laboratory with mouse embryonic fibroblasts (MEFs) lacking the enzyme, we also measured a significant increase in ROS levels in Txnrd2$^{-/-}$ eEPCs. While the compound we used to detect ROS, CellROX, is unspecific for the exact nature of oxidants, an earlier study using H_2O_2-specific boronate-based fluorophores confirmed that the ablation of Txnrd2 in MEFs leads to an accumulation of H_2O_2 in the mitochondria and cytosol of these cells [116]. Data from this study also suggests that the increased accumulation of H_2O_2 is due to reduced detoxification rather than an increased mitochondrial production of this ROS as the expression of Prx3, which receives reducing equivalents from Txnrd2 via Trx2, is significantly

augmented in Txnrd2-deficient MEFs, an effect which is frequently observed in response to exogenous administration of H_2O_2 [116]. Considering that the eEPCs employed in this study are also impaired with regard to the Txnrd2/Txn2/Prx3 axis, it is likely that the increased levels of ROS we report here may reflect mainly an increased presence of H_2O_2; however, the contribution of the short-lived radical O_2^-• or other oxygen radicals to the measured ROS levels cannot be excluded using this general ROS sensor.

While the majority of H_2O_2 detoxification may occur via this process with only an indirect involvement of Txnrd2, a direct utilisation of H_2O_2 by Thioredoxin reductases, due to their broad substrate profile, has also been discussed. According to Zhong and Holmgren, the C-terminal Sec-containing active site in Txnrd1 could directly reduce H_2O_2, albeit at relatively high concentrations of the enzyme [140]. Considering the strong sequence homology between the different Txnrd isoforms and that particularly the Sec incorporation in the C-terminal active site is highly conserved between all Txnrds, it may well be that this affinity for H_2O_2 may also apply to Txnrd2, thereby adding another avenue for H_2O_2 accumulation in the Txnrd2$^{-/-}$ eEPCs employed in this study.

Extrapolating the reports in the literature, previous studies from our laboratory and the findings on elevated levels of ROS in eEPCs to the endothelium and taking into account that mitochondria in ECs are not the main site responsible for energy production – the main pathway in the synthesis of ATP is by anaerobic glycolysis – one must raise the question what an imbalance of mitochondrial-derived ROS may elicit in these cells [108]. Possibly, the impact of impaired H_2O_2 detoxification by the lack of Txnrd2 may be exacerbated by a "vicious circle" of oxidative damage resulting in increased production of additional ROS and subsequent exacerbation of oxidative stress [141, 142]. Taking this and the above mentioned variety of ROS sources into account as well as the recent suggestion that the main task of EC mitochondria and mitochondrial-derived ROS is the participation in cellular signalling events, for example by modifying, amongst others, Ca^{2+} dynamics, impaired control of mitochondrial ROS production and release, including the longer lived and lipid soluble radical H_2O_2, could restrict the signalling efficiency within a cell [110]. For example, ROS have been described to impact on angiogenesis by altering the activity of PHD2 via the oxidation of the cofactor Fe^{2+}, leading to HIF-1α stabilisation in response to hypoxia [84]. Additionally, an increase in ROS can activate a number of transcription factors, including NFκB and AP-1, leading to the expression of VEGF and favouring angiogenesis [74, 75]. The regulation of these pathways, however, pertains to cells with an otherwise normal redox status and possibly not to ECs experiencing basally elevated ROS.

In regard to the response of vessels to alterations in blood flow characteristics, changes in FSS induce the release of O_2^-• and H_2O_2 from the endothelium [58, 93, 143]. Basally elevated ROS could thus also interfere with the ROS-dependent signalling of FSS, especially taking into account that during exposure to FSS EC-derived H_2O_2 can act upon the underlying VSMC layer [94]. In addition, high

concentrations of H_2O_2 have also been shown to inhibit the activity of MMP-2 which could possibly interfere with outward remodelling of blood vessels [98]. Conditions with elevated ROS in the vasculature such as hypertension, diabetes, inflammation and aging suggest that a functional antioxidant defence is of substantial importance in the endothelium and our data implies the necessity of mitochondrial thioredoxin reductase in endothelial redox homeostasis.

At this stage one can only speculate whether and how the elevated concentrations of ROS measured in the Txnrd2-deficient eEPCs employed in this study lead to an impairment of signalling processes, in particular without having identified a precise signalling cascade for further investigation. And while we cannot directly measure levels of ROS in the Txnrd2-deficient endothelium, these data, together with the previous findings in other cell types described above, do suggest, however, that the ECs of $Txnrd2^{ECKO}$ mice bear an increased oxidative burden which may serve as the underlying cause for the subsequently discussed results.

4.2 Mitochondrial membrane potential is altered in Txnrd2$^{-/-}$ eEPCs.

Since the eEPCs employed in this study lack a major line of defence against mitochondrial H_2O_2 and as H_2O_2 has been shown to dissipate ΔΨm in a variety of cells, we investigated the effect Txnrd2 deletion in eEPCs on this transmembrane potential [114, 144]. Using a cell-permeable dye that locates specifically to the mitochondrial intermembrane space where its aggregation status-dependent fluorescence wavelength changes with the membrane potential, we measured a significant reduction of ΔΨm in $Txnrd2^{-/-}$ eEPCs [145]. Using the membrane potential disruptor CCCP as a positive control we could also observe that the potential was not completely lost. A complete dissipation of ΔΨm would result in the remodelling of the mitochondrial cristae, matrix condensation, the release of cytochrome C into the cytosol, and ultimately in apoptotic cell death which we did not observe [146]. In contrast, the eEPCs lacking $Txnrd2^{-/-}$ in our study displayed no apparent differences in proliferation or viability as would be the case for an enhanced rate of apoptosis in these cells.

While our results do not enable the determination of the exact reason for the reduction of ΔΨm, it has been described that its maintenance requires sufficient oxidisable substrates for the ETC, O_2, and a physiological cytosolic pH, amongst others [146]. It is therefore possible that the elevated levels of H_2O_2 in $Txnrd2^{-/-}$ eEPCs affected any of these determinants. Alternatively, ΔΨm dissipation may result from dysfunctional ETC complexes. H_2O_2 can react with transition metals to yield the highly toxic and DNA-damaging hydroxyl radical (HO•) via the Fenton reaction ($Fe^{2+} + H_2O_2 \leftrightarrow Fe^{3+} + OH + HO•$). HO•-induced damage to mitochondrial DNA which is transcribed to form the ETC complex proteins

may result in the transcription and expression of defective variants of these proteins, possibly resulting in the impairment of ΔΨm [147].

Dissipation of ΔΨm could result in a variety of consequences, the significance of which could not be assessed but may contribute to an additional functional impairment of the eEPCs lacking Txnrd2 in their mitochondria: molecular transport, including that of proteins and cations such as K^+ and Ca^{2+} into and out of the mitochondria requires an intact ΔΨm. Furthermore, the removal of cations from the mitochondrial matrix, e.g. via the Na^+/Ca^{2+} exchanger and the K^+/H^+ antiporter is also ΔΨm-dependent [110, 148]. Failure to correctly regulate the net movement of cations can lead to the influx of cytosolic water and subsequent mitochondrial swelling which can further hinder mitochondrial traffic [149]. Mitochondrial swelling may then affect both the function of this organelle as well as the entire cell. Thus, an increase in mitochondrial matrix volume can increase ATP production by activating the ETC, a process during which additional ROS are produced, resulting in a vicious circle [149]. Additionally, the increased space required by the swollen mitochondria may also impose mechanical constraints on other cellular structures [150]. Mitochondrial swelling has thus been shown to cause abnormal mitochondrial fusion in fibroblasts and cardiomyoblasts, resulting in a donut-shaped mitochondrial morphology. This abnormal morphology has also been demonstrated in mitochondria of human umbilical vein endothelial cells (HUVECs) and could explain the decrease in motility and deregulation of fusion and fission following the dissipation of ΔΨm [142]. Whether mitochondrial swelling also occurs in eEPCs or ECs lacking Txnrd2 will be investigated by transmission electron microscopy in future studies.

While the findings in eEPCs on ΔΨm serve as an indicative marker for mitochondrial function, we cannot conclude from this data alone how severe this may impact on the Txnrd2-deficient endothelial cells. However, the dissipation of ΔΨm in the eEPCs lacking Txnrd2 illustrates that the deletion of Txnrd2 results not only in increased ROS levels but that mitochondrial and thus also cellular integrity and function may also be affected. This is of particular importance when considering that impairments in mitochondrial and cellular integrity could potentially contribute to a variety of vascular diseases in which endothelial dysfunction is implicated, such as atherosclerosis, diabetes and ischemia/reperfusion injury.

4.3 A lack of endothelial Txnrd2 impairs vascular remodelling *in vivo*.

The *in vitro* results on the production of ROS and the dissipation of ΔΨm in eEPCs lacking Txnrd2 suggest that substantial impairments in the functionality of ECs in $Txnrd2^{ECKO}$ mice may also exist *in vivo*. We attempted to investigate the impact of Txnrd2 deletion in the endothelium on vascular remodelling processes by employing a model of ischemia- and hypoxia-induced remodelling in the

murine hind-limb. Both hypoxia and ischemia initiate compensatory, endothelium-dependent vascular remodelling processes, albeit by different mechanisms. While the lack of oxygen during hypoxia leads to angiogenesis in the calf muscle via increased HIF-1α stability and VEGF release, the altered haemodynamics following ischemic occlusion of the femoral artery initiate signalling pathways, including in the endothelium, in the non-ischemic pre-existing collateral vessels of the thigh muscle, leading to arteriogenesis [151].

Angiogenesis, the sprouting of new capillaries from an existing network, occurs in response to a lack of oxygen causing the inactivation of PHD2 and subsequent stabilisation of HIF-1α. The sensitivity of both PHD2 inactivation and HIF-1α stabilisation to ROS in hypoxic angiogenesis has frequently been reported [84, 152-155]. Likewise, the participation of ROS in FSS-dependent vasodilatation, activation of growth factors and infiltration of pro-arteriogenic monocytes, all processes governing arteriogenesis, i.e. the remodelling of existing arterioles in response to altered haemodynamics, have also been described [35, 58-60, 76, 80, 93, 95, 143]. Indeed, using LDI we could show that the perfusion recovery after occlusion of the femoral artery in Txnrd2^{ECKO} mice was significantly reduced compared to Txnrd2^{ECWT} mice after seven days, suggesting that either angiogenesis or arteriogenesis, or both could be impaired.

In response to ischemia, ROS levels have been reported to increase in the area in which the collateral arterioles undergo arteriogenesis, as well as in the hypoxic calf muscle [20, 132]. As long as this increase does not exceed the antioxidant defence capacity of the affected cells it is likely that the ROS partake in the ischemia-associated signalling and growth processes. However, when ROS are already basally elevated as in the Txnrd2^{ECKO} mice used in this study, the additional ischemia-induced increase may result in levels of ROS that impair the vascular compensation of ischemia. In support, in a study in which mice were exposed to cigarette smoke equivalent to levels experienced by heavy smokers and sufficient to elicit oxidative stress, LDI measurements revealed a significantly impaired recovery from ischemia [132]. Correspondingly, blocking ROS production or increasing the cellular antioxidative capacity has been shown to exert beneficial effects on the re-establishment of perfusion in response to ischemia. In the study in which mice were exposed to cigarette smoke, for instance, it was shown that recovery of blood flow and neovascularisation seven days after hind-limb ischemia was greater in transgenic mice lacking Nox2, a subunit of the ROS producing enzyme NADPH oxidase, compared to wildtype mice, both when exposed to smoke as well as under control conditions [132]. In support for the involvement of mitochondrial-derived ROS in the vascular response to hind-limb ischemia, the transgenic overexpression of Txn2 in ECs has also been shown to augment perfusion recovery via both arteriogenesis and angiogenesis as early as three days post-surgery [20]. Possibly the opposite holds true in the present study – a defective redox cycling of Txn2 due to the lack of Txnrd2 impairs reperfusion.

The beneficial effects of an increased antioxidative capacity can also be achieved by exogenous antioxidants or compounds that reverse ROS-induced damage such as the reduction in NO bioavailability. Thus, the administration of Vitamin C, BH_4 and $_L$-Arginine in the chow of mice prior to and during hind-limb ischemia significantly improved long-term recovery compared to mice receiving standard diet [156]. Despite the signalling roles ascribed to ROS in response to hind-limb ischemia, these data suggest that low basal levels of radicals provide a better foundation for vascular remodelling and that the boundary between signalling concentrations of ROS and toxic levels is narrow. A basal overabundance of vascular ROS, as is the case in the Txnrd2^{ECKO} mice, is thus even more likely to impair the recovery of perfusion.

4.3.1 Angiogenesis

Since the model of hind-limb ischemia employed in this study allows the analysis of both arteriogenesis and angiogenesis in the normoxic thigh and the hypoxic calf muscle of the same mouse, we analysed these muscles seven days after the ligation of the femoral artery to assess typical parameters of these adaptive processes.

In the calf muscle we found a significant reduction in the angiogenic response in Txnrd2^{ECKO} mice compared to their Txnrd2-expressing counterparts seven days after the occlusion of the femoral artery as assessed by capillary area. Interestingly, the remaining increase in capillary area fraction over that in the sham-operated hind-limb was not uniformly distributed throughout the muscle. In two of the three areas analysed, angiogenesis occurred but was depressed in the Txnrd2^{ECKO} mice compared to Txnrd2^{ECWT} mice. In the third area, no increase from the basal capillary area fraction as measured in the sham-operated limb was observed in either experimental group. We suspect that anoxia rather than hypoxia may have occurred in this area, either due to a steal effect of the vasculature in the other areas or of a higher local O_2 consumption due to the muscle fibre type. Indeed, H&E staining revealed tissue necrosis in the third analysed area of the gastrocnemius muscle of both Txnrd2^{ECWT} and Txnrd2^{ECKO} mice.

The acute occlusion of the femoral artery leads to an immediate and substantial decrease in perfusion of the calf muscle. Consequently, the lack of oxygen delivery results in tissue hypoxia which can be a considerable stimulus for angiogenic vessel growth. After all, angiogenesis is thought to improve perfusion conditions in the affected area and, consequently, of oxygen delivery. It is thus plausible that hypoxia and the subsequent activation of hypoxic signalling cascades function as major stimuli for capillary sprouting. Major participants in the hypoxic stimulation of angiogenesis are the hypoxia inducible transcription factor HIF-1α, its regulators PHD2 and FIH, and the products of HIF-1α target genes such as VEGF. This seemingly unambiguous link between hypoxia and angiogenesis,

however, is confounded by the regulation of the corresponding signalling cascades, and especially the involvement of ROS in the regulation of HIF-1α.

For long it was accepted that hypoxia but not anoxia leads to an increase in ROS which is required for the stabilisation of HIF-1α. A series of publications in 2005 as well as a recent follow-up study suggested that radicals from complex III of the ETC are necessary for the induction of hypoxic signalling via the stabilisation of HIF-1α [85, 153-155]. Furthermore, one of these studies as well as a recent report implicated especially H_2O_2 in the process of HIF-1α stabilisation either by exogenous administration of H_2O_2 or by increasing its scavenging via the administration of exogenous catalase [86, 155]. In these reports, ROS are commonly suggested to impair the hydroxylation of proline residues of HIF-1α by PHD2, most likely via the oxidation of the essential co-factor for PHD2, the non-heme Fe^{2+}.

Recently, however, this axiom of hypoxia-dependent ROS production has begun to falter. Oxygen is, by definition, required for the production of ROS. To increase the production of oxygen radicals while the essential ingredient, oxygen, is scarce appears contradictory. In line with this presumption, the mitochondrial production of H_2O_2 has been reported to be positively correlated to cellular oxygen levels, implying that a decrease in oxygen, as is the case during hypoxia, will actually decrease H_2O_2 production [157]. Accordingly and in contrast to the above reports, mitochondrial production of H_2O_2 has also been reported to decrease during hypoxia in cardiac myocytes from guinea pigs and in mitochondria isolated from rat hepatocytes [87, 158]. Furthermore, as early as 1996, the application of exogenous H_2O_2 was shown to decrease HIF-1α accumulation during experimental hypoxia *in vitro* [159]. Possibly, as proposed in a recent review, an actual hypoxia-induced production and release of ROS indeed increases HIF-1α levels which itself then acts upon the mitochondria in the fashion of a negative feedback loop to curtail ROS production [160]. This, however, does not exclude the possibility of reactive oxygen species production by other, non-mitochondrial systems. In line with the suggestion of a negative feedback loop curtailing mitochondrial ROS production, mitochondrial-derived ROS in response to acute hypoxia have been suggested to elicit an even greater production of ROS by NAD(P)H oxidase via MEK/ERK signalling pathways [161]. Furthermore, hypoxia can induce the activation of Xanthine Dehydrogenase and Xanthine Oxidase in a mitochondria-independent fashion, also resulting in the production of ROS [162-166]. It thus appears crucial to consider the timing when attempting to measure ROS levels in response to hypoxia.

Finally, a more critical review on this topic concluded that to date no consensus on the precise response of mitochondria to hypoxia in regard to ROS production can be reached and that, possibly, one should abandon the theory that mitochondria regulate HIF-1α stabilisation via the production of ROS and rather address whether mitochondria as a major consumer of oxygen can regulate HIF-1α stability by altering cellular oxygen concentrations [167].

Considering that our *in vitro* results revealed elevated basal levels of ROS and, as indicated by the decrease in ΔΨm, an impairment of mitochondrial function in cells lacking Txnrd2, it is somewhat irrelevant whether hypoxia increases or decreases mitochondrial ROS production and how this affects HIF-1α stability. Rather, the question must be how the elevated basal ROS levels can impair the cellular response to hypoxia and handle HIF-1α stabilisation. Or, if a negative-feedback loop from HIF-1α to the mitochondria to decrease the production of ROS indeed exists, whether the Txnrd2/Txn2/Prx3 axis, which is dysfunctional in the Txnrd2-deficient eEPCs (and in the endothelium of $Txnrd2^{ECKO}$ mice) employed in this study, is normally required to suppress a further increase of mitochondrial H_2O_2. A previous study by our group addressed this issue using Mouse Embryonic Fibroblasts lacking Txnrd2 and transformed with the pro-oncogenes c-myc and Ha-ras. Implanted subcutaneously into the flank of normal mice, tumour angiogenesis was significantly impaired relative to corresponding cells positive for Txnrd2, and this was accompanied by decreased protein levels of HIF-1α and VEGF [37]. In line, an attenuated tube formation capacity of $Txnrd2^{-/-}$ eEPCs was also demonstrated in that study. Hence, these results and the findings on impaired angiogenesis from the present study suggest that elevated basal levels of ROS indeed impair hypoxic signalling, including HIF-1α, *in vivo*.

The observation of significantly higher protein levels of PHD2 in $Txnrd2^{-/-}$ eEPCs may also indicate the contribution of PHD2 to the impairment of angiogenesis in $Txnrd2^{ECKO}$ mice. Unfortunately, information on the effects of increased PHD2 protein levels in vascular remodelling processes is scarce. However, the opposite – low levels of PHD2 protein – has been investigated more thoroughly, especially in the context of tumour angiogenesis but also in non-carcinogenic vessel maturation. Inducible, ubiquitous deletion of PHD2 in adult mice resulted in excessive angiogenesis, in which the vessels were perfusable and successfully recruited VSMC, suggesting that PHD2 is a negative regulator of vascular growth [168]. Using mice haplodeficient for PHD2, it was suggested that this protein can also affect the quality of newly formed tumour vessels [169]. In this study, ECs (and other cells) themselves expressed lower protein levels of PHD2 and while growth of implanted, PHD2-expressing tumours itself was not changed in $PHD2^{+/-}$ mice, perfusion was significantly augmented and metastasis reduced, indicating that the reduction in PHD2 expression favoured the maturation of tumour vessels [169]. In the aforementioned studies, however, the authors did not consider the assessment of HIF-1α signalling in response to reduced PHD2 protein expression. Chan and colleagues, on the other hand, showed not only that various cancer cell lines and tumours express lower levels of PHD2 and display an increase in the number of blood vessels, but also that silencing of PHD2 with short hairpin RNA (shRNA) further reduced PHD2 protein expression in tumours and resulted in even greater angiogenesis [170]. Most importantly, however, they demonstrated that the increase in angiogenesis remained even when both PHD2 and HIF-1α were silenced with shRNA in

tumour cells, indicating that PHD2 indeed exerts HIF-1α-independent effects on angiogenesis [170]. In support, Takeda and Fong showed that elevated PHD2 expression impaired EC proliferation *in vitro* [171]. By employing a recombinant PHD2 mutant lacking hydroxylase activity they also supported an inhibitory, HIF-1α-independent effect of PHD2 itself on EC proliferation [171]. Considering that to date the majority of publications focus on investigating the effect of reduced PHD2 expression on angiogenesis, it is intriguing to report that the Txnrd2$^{-/-}$ eEPCs, and thus possibly also the endothelium of Txnrd2^{ECKO} mice employed in this study, express elevated PHD2 protein levels despite the exact reason for this observation remaining elusive in this study. In light of the published literature, however, an elevation of PHD2 protein levels could serve as the major mechanism responsible for the impairment of the angiogenic response in the hypoxic calf muscle after femoral artery ligation by suppressing the proliferative capacity of the ECs.

In addition to the involvement of ROS, PHD2 and/or HIF-1α in the response to hypoxia, Txnrd2 or any of its substrates could potentially be more directly involved in the regulation of hypoxic signalling. Interestingly, the protein and mRNA levels of the cytoplasmic equivalent to Txnrd2, Txnrd1, are reduced during hypoxia, independently of HIF-1α stability in transformed fibroblasts and in a mouse breast cancer cell line [172]. Furthermore, hypoxia also caused a reduction in Txnrd1 activity in these cells which suggests further post-translational modifications of the enzyme. While the authors of this study observed a general increase in ROS levels in response to hypoxia, this increase was attenuated in cells lacking Txnrd1, suggesting that ROS are indeed required for hypoxic signalling – however, independent of HIF-1α signalling. Furthermore, these findings suggest that not an increased formation of ROS occurs in response to hypoxia but rather a decreased detoxification of H_2O_2. Possibly, so the authors speculated, the downregulation of Txnrd1 may also serve in the modification of transcription factors that are substrates for this enzyme, such as AP-1 or NFκB. However, this would inevitably also activate gene transcription of genes potentially counterproductive for angiogenesis such as ASK1, leading to pro-apoptotic signalling [89]. Obviously, the role of ROS production, removal, HIF stability and PHD activity still remains elusive albeit the substantial increase of efforts to elucidate the exact mechanisms. While the above excursion into possible pathways cannot be narrowed down to a decisive role of ROS in hypoxic angiogenic signalling, the findings on HIF-independent Txnrd1 sensitivity to hypoxia and the impact of Txnrd2 deletion on PHD2 expression and especially angiogenesis in both tumour growth and in the present study will provide alternative avenues that should be considered in the quest to gain a comprehensive and integrated understanding of these complex processes.

4.3.2 Arteriogenesis

As described above, hind-limb ischemia, induced by the surgical occlusion of the femoral artery, leads to both arteriogenesis and angiogenesis. Seven days after the occlusion of the femoral artery, the vessels of the lower limbs were maximally dilated and perfusion fixed with paraformaldehyde prior to excision of the adductor of the ischemic and the sham-operated hind-limb. Subsequently, the muscles were embedded in paraffin and sections cut in a plane allowing the evaluation of the cross-sectional area of the wall and lumen of the vessels. Following H&E staining of the sections, wall area of the same collateral arterioles was measured at the middle part of the thigh muscle and compared between the limbs (sham vs. occluded) and the genotype of the mice (Txnrd2^{ECWT} vs. Txnrd2^{ECKO}). As expected, occlusion of the femoral artery led to a significant increase in collateral arteriole wall area in the adductor muscle of the ischemic hind-limb regardless of the genotype. Importantly, this increase was significantly attenuated in Txnrd2^{ECKO} mice compared to their Txnrd2-expressing counterparts, indicating that the arteriogenic response is also blunted in mice lacking EC Txnrd2. Using the data from the inner and outer circumference of the collateral arterioles, vessel wall thickness and lumen were calculated using standard circle formulas. Since these parameters were also employed for the assessment of wall area, analogous results were achieved: Wall thickness was increased in collateral arterioles in the occluded hind-limbs while in the mice lacking EC Txnrd2 this increase was significantly blunted. Likewise, the luminal diameter was significantly smaller in Txnrd2^{ECKO} mice compared to the corresponding Txnrd2^{ECWT} mice.

Interestingly, both wall area and wall thickness but not the luminal diameter of the collateral arterioles were also significantly increased in Txnrd2^{ECKO} mice in the sham hind-limb, indicating that these vessels were larger at baseline. In the case of the wall thickness of the arterioles in the occluded limb, where no significant difference between Txnrd2-expressing mice and those lacking Txnrd2 in the ECs was detected when comparing the raw data, this could indicate that an additional increase of wall thickness in the Txnrd2^{ECKO} mice may not have been possible as a maximal size had been achieved. However, the fact that wall area and luminal diameter in the collaterals from the occluded hind-limbs of Txnrd2^{ECKO} mice were both impaired, also without normalising the data, demonstrates that the capacity of the vessels to remodel in these mice is indeed decreased.

The remodelling of the collateral arterioles is of substantial importance in this model; after all, hypoxia in the calf muscle will endure until adequate blood supply has been re-established via these upstream collaterals. Thus, a decrease in the arteriogenic capacity of the collateral vessels in the thigh muscle will ultimately also affect any potential positive effect on angiogenesis in the calf muscle. However, as discussed in the previous section, angiogenesis was attenuated in Txnrd2^{ECKO} mice, further supporting a substantial impairment of the endothelium of these animals.

Regarding the interplay of arteriogenesis and angiogenesis and in contrast to the latter, the mechanism driving the remodelling of the collateral arterioles is not induced by hypoxia [48, 52]. After all, the collateral vessels do transport blood, oxygen and nutrients to the thigh muscles. The exact stimuli responsible for the induction of collateral artery remodelling in this muscle remains a topic of considerable debate; however, the majority of publications propose that an increase in FSS in the collateral arterioles following the occlusion of the femoral artery serves as the inaugural signal [45, 53]. While several authors discuss arteriogenesis in the context of it being a FSS-driven process, it is often ignored that an increase in FSS in the collateral circulation following the occlusion of a main artery has not been measured as such yet. Furthermore, an increase in FSS leads to rapid collateral vasodilatation after acute occlusion of the femoral artery, as was demonstrated more than four decades ago by Rosenthal and Guyton [173]. And since vessel radius has a major impact on shear stress according to the formula $\tau = \frac{4\eta \times Q}{\pi \times r^3}$, where Q represents flow velocity and η viscosity, a rapid flow-mediated vasodilatation would tend to return FSS to normal levels, thereby decreasing the impact of FSS as an – at least continuously – contributing stimulus [55, 71, 174-177]. Nevertheless, that an increase in FSS can indeed induce collateral arteriole remodelling was elegantly demonstrated in two studies in which the hind-limb ischemia model employed here was extended by the creation of an arteriovenous shunt between the distal femoral artery stump and the femoral vein. This led to a substantial additional pressure drop across the length of the collateral arterioles and resulted in further arteriogenesis of the collateral arterioles above that observed in the 'classical' occlusion model [53, 71].

If FSS is considered as an integral stimulus for the remodelling of the hind-limb collateral arterioles, focus must centre on the constitution of the endothelium as these are the only cells that can sense this force. Accordingly, functional integrity of ECs is required to translate this biomechanical force into biochemical signals for the underlying structures such as the VSMCs. Fluid shear stress sensing and transmission occurs in a decentralised fashion and involves signalling from the luminal surface (including the glycocalyx, G-protein coupled receptors, ion channels and tyrosine kinase receptors), from intracellular structures (such as the cytoskeleton, focal adhesion and integrin-linked kinases, various adaptor proteins and the nuclear membrane), and from abluminal connectors, (e.g. integrins and their respective extracellular matrix proteins) [44, 178, 179]. An intact endothelium will integrate signals from these sources and translate changes in FSS to a biochemical signal, for example by increasing eNOS mRNA and/or activity, resulting in a sustained production and release of NO and subsequent relaxation of the underlying VSMCs [56, 180, 181]. Furthermore, the levels of adhesion molecules such as ICAM-1 and VCAM-1 are altered during increased FSS as is the activity of a range of transcription factors such as AP-1 and NFκB as well as growth factors like bFGF and platelet-

derived growth factor [60, 67-69, 182]. Importantly, FSS has been reported to alter the oxidative capacity of ECs, resulting in increased levels of ROS, including H_2O_2, both *in vitro* and *in vivo* [58, 59, 93, 94, 183]. A recent study demonstrated that different flow characteristics elicit specific effects on both the activity of sources of ROS (e.g. increased ROS from NAD(P)H oxidase) as well as of antioxidants such as glutathione peroxidase and catalase (decreased detoxification) [184]. The FSS-dependent reduction of catalase activity was shown to occur via decreased PKCδ activity, resulting in an accumulation of H_2O_2 [181]. By increasing Akt signalling, the elevated levels of H_2O_2 indirectly led to the phosphorylation of eNOS at the activity-enhancing Ser1177, thereby also increasing NO production [181]. Consequently, this and the possibility that one or more of the mechanosensors and –transmitters could potentially be modulated by ROS raises the question what occurs in response to increased FSS in dysfunctional ECs or those already struggling to curb oxidative stress at basal levels, such as the Txnrd2-deficient eEPCs or EC in the current study.

The results obtained *in vitro* with eEPCs and MEFs demonstrate that the deletion of Txnrd2 results in a significant increase in basal ROS levels, an effect likely to also occur in the endothelial cells of the $Txnrd2^{ECKO}$ mice *in vivo*. It is therefore possible that these ECs are incapable of responding adequately to the haemodynamic alterations they are exposed to after occlusion of the femoral artery, especially when one considers that both FSS as well as stretch result in increases in ROS [93, 185]. Excessive levels of ROS are implicated in numerous diseases affecting the vascular wall, such as hypertension and atherosclerosis as well as in vascular complications associated with increasing age. For example, the increase in luminal diameter of remodelling collateral arterioles in young rats is attenuated in aged rats; an effect that could be reversed by administration of antioxidants [101]. Furthermore, increasing age and the related rise in ROS impairs the activation of eNOS and thus FSS-induced vasodilatation [186]. The impairment in luminal expansion and FSS-induced arterial remodelling in aged rats has been suggested to be due to a decreased sensitivity of these ECs to subtle changes in FSS [102]. Furthermore, impaired vasodilatation due to elevated levels of ROS has also been described employing Txnrd1 inhibitors [35].

However, we could not detect an impairment in EC sensitivity to changes FSS in isolated collateral arterioles in this study. Whether this is due to experimental restrictions or a true result remains elusive and is under current investigation. Likewise we cannot deduce from our results whether the translation from the biomechanical stimulus of FSS to a biochemical signal relevant for vasodilatation and/or vascular wall remodelling is potentially derailed. Possibly, eNOS is uncoupled or NO scavenged rapidly by excess $O_2^-\bullet$, leading to the production of $ONOO^-$. Yet, we have been unable to detect an increase in protein tyrosine nitration, an indirect evaluation of $ONOO^-$ formation, neither in lysates from eEPCs or MEFs either untreated or stimulated with the NO donor SNAP, nor in lysates

from remodelled collateral arterioles of Txnrd2^{ECKO} mice. Possibly, though, results from lysates from the collaterals are confounded by other, Txnrd2-expressing, cells such as VSMCs or pericytes.

In continuation of the aforementioned association of thioredoxin systems and NO, another role for NO, the nitration of free cysteine thiol-groups in proteins, could possibly also contribute to the decrease in arteriogenesis observed in Txnrd2^{ECKO} mice [187]. Indeed, upon exposure to FSS, S-nitrosylation of free SH-groups of proteins, including Txn1, has been reported to increase [188]. Like the phosphorylation of specific residues as a method for post-transcriptional protein regulation, S-nitrosylation can alter the activity of proteins [189]. Similarly to the reduction of oxidised proteins by Txns, the vicinal dithiols of these disulfide oxidoreductases also enable them to function as denitrosylators [189]. In support, Txnrd1 and Txnrd2 have indeed been described to participate in the denitrosylation of proteins. In the mitochondria, for example, the presence and activity of Txnrd2 is essential for the activation of caspase-3 which is usually neutralised by constitutive S-nitrosylation to prevent the induction of apoptosis [189]. Without Txnrd2, caspase-3 cannot be activated, thereby preventing caspase-3-induced apoptosis. Since arteriogenesis requires a concerted activation and deactivation of specific proteins involved in processes such as signalling as well as controlled proliferation and intracellular communication, it would be possible that a lack of Txnrd2 could potentially result in a continuous S-nitrosylation and therefore deregulation of proteins critically involved in the process of arteriogenic vascular growth.

Another reason for the reduced arteriogenesis in Txnrd2^{ECKO} mice suggests itself from the dissipation of $\Delta\Psi m$ we observed in eEPCs. Since the $\Delta\Psi m$ is required for the movement of ions, including calcium, through the mitochondrial membranes, mitochondrial calcium handling may be impaired. Correct calcium signalling is required for the initiation of FSS-dependent eNOS activation in the endothelium [110]. Impaired EC mitochondrial calcium handling in the Txnrd2-deficient ECs could therefore possibly lead to a delayed activation of eNOS and thus NO production and consequent vasodilatation. Furthermore, the release of Ca^{2+} from the mitochondria to the ER to replenish its stores via the Ca^{2+}/Na^{+} exchanger is susceptible to modification by mitochondrial H_2O_2, an effect that could also blunt NO-dependent processes in the endothelium of Txnrd2^{ECKO} mice [111, 112].

In addition to the effects the deletion of Txnrd2 elicits in the endothelium, effects beyond these cells could possibly contribute to the blunted arteriogenic response in Txnrd2^{ECKO} mice. Especially H_2O_2, the oxidant normally detoxified by the thioredoxin systems, can move across certain membranes and H_2O_2 derived from endothelia has been shown to affect the underlying VSMCs where it influences arteriogenesis by the induction of PLGF production [94, 190].

Thus, the critical role of the endothelium in mediating FSS-dependent vasodilation implies that an impairment of these cells will ultimately impact on arteriogenesis. Since the only cell type affected the Txnrd2^{ECKO} mice is the endothelium, it is plausible that any of the mechanisms discussed above could be defective, resulting in a blunted arteriogenic response.

While we and others have shown that Txnrd2 deletion increases ROS levels and that this is most likely due to an impairment of the Txnrd2/Txn2/Prx3 axis, the lack of Txnrd2 itself or the resulting impaired function of Txn2 as well as other, possibly yet unidentified substrates for Txnrd2, may contribute to the compromised arteriogenic response to hind-limb ischemia observed in this study [37, 39, 116, 191].

Finally, evidence for the importance of the thioredoxin system in vascular homeostasis in the context of human disease can be deduced from the findings that hypertensive patients with impaired EC-dependent vasodilatation present significantly reduced plasma levels of selenium compared to other hypertensive patients with an intact EC-dependent vasodilatory response [192]. This finding is intriguing as selenium is essential in the maintenance of selenoproteins such as Txnrd2 and depletion of this trace element can lead to a loss of Txnrd2 activity [193].

4.3.3 Endoplasmic Reticulum Stress

Since mitochondria are in close proximity to the ER we also investigated the possibility of an impairment of ER function in cells lacking Txnrd2 [194, 195]. Indeed, mitochondria are tethered to the ER via mitofusin-2, thereby forming mitochondria-associated-membranes which are patches of ER membranes attached to the mitochondria [196]. These microdomains have been shown to comprise up to 5-20% of total mitochondrial network surface area, suggesting that mitochondrial and ER functions are closely linked [194, 197]. The main reason for the close proximity of these two organelles appears to be their involvement in Ca^{2+} signalling. The ER, in addition to the sarcoplasmic reticulum in myocytes, represents one of the major cellular stores of Ca^{2+} [198-200]. But the mitochondria can also take up Ca^{2+} and this ability implies the mitochondria as buffers of cytosolic Ca^{2+} levels [194, 195]. Furthermore, the close apposition of the mitochondria and the ER enables the mitochondria to sense the initiation of ER-dependent Ca^{2+} signalling directly at the points of origin, the ER Ca^{2+} channels; information which can be harvested directly, e.g. to alter the organelle's metabolism [194, 195]. Uptake of ions into the mitochondria, however, is dependent on their electrochemical gradient and requires the presence of a sufficient $\Delta\Psi m$ – which is, as discussed above, negatively affected by Txnrd2 deletion in eEPCs investigated in this study [110]. In addition to the mitochondria participating in Ca^{2+} signalling and in the regulation of cytosolic levels, these organelles are also required for the replenishment of ER Ca^{2+} stores via the Na^{+}/Ca^{2+} exchanger, a channel that is sensitive to regulation

by H_2O_2 [112]. Since Txnrd2 ablation leads to significantly increased levels of ROS, most likely via an increase in H_2O_2, we suspected that cells lacking Txnrd2 may also present impairments of the ER.

The lumen of the ER represents a unique oxidising environment, allowing the efficient formation of disulfide bonds in the folding of proteins mainly designated for secretion and membrane-bound expression [197, 198, 201, 202]. The redox reaction of disulfide bond formation is catalysed mainly by PDI, a protein that was predicted and then also confirmed more than two decades ago to exhibit sequence similarity to Txn and therefore may also be a substrate for Txnrds [24, 203, 204]. Similarly, two ER-resident, PDI-like proteins, now identified as P5 and ERp72, as well as other members of the expanding family of PDIs, also possess structural similarities with Txns and their activity could possibly also be regulated by Txnrds [25, 205]. The presence of Txnrd2 splice variants in cellular areas other than the mitochondria could thus potentially act as reductases for such PDIs [206]. Considering that the ER contributes to such vital cellular processes as calcium storage, release and signalling as well as the three-dimensional folding of proteins, it is evident that ER homeostasis must be maintained. The observation that Txnrd2 ablation leads to significantly increased levels of ROS, most likely via an increase in H_2O_2, and the dissipation of $\Delta\Psi m$, as well as the possibility of a direct involvement of the mitochondrial thioredoxin system in ER function, we speculated that the function of the ER may also be compromised in Txnrd2 knockout cells.

To investigate this, we analysed markers characteristic of ER stress. Derailed ER function, elicited either by insufficient Ca^{2+} levels or by the accumulation of misfolded proteins in the ER lumen, can initiate the unfolded protein response (UPR) [202, 207]. The UPR is initiated by the release of the ER-resident proteins PERK, IRE1α and ATF6 to re-establish ER homeostasis or, if this fails, to proceed to apoptotic cell death [207]. The transcriptional increase of UPR genes, including BiP (also known as 78 kDa glucose-regulated protein) and PDI, the reduction of cellular protein synthesis to decrease ER work load, as well as augmented ER-associated protein degradation are all aimed at re-establishing ER homeostasis [201, 202, 207]. BiP is considered the major regulator of the UPR and acts in a positive feedback manner: normally, this chaperone is bound to the transducers of the UPR listed above from where it observes the correct folding of proteins. In the case of excessive protein misfolding, e.g. by ineffective PDI, BiP binds to incorrectly folded proteins to inhibit their release from the ER and accordingly liberates PERK, IRE1α and ATF6 which can then initiate UPR signalling [207]. The resulting increase in BiP and PDI translation is then constructive to rectify incorrect disulfide bonds and prevent the release of misfolded proteins [201, 207]. The activity of many ER proteins, including BiP, is critically dependent on the rich levels of Ca^{2+} normally present in the ER lumen [202]. In order to maintain the Ca^{2+} levels within the ER in the µM to mM range (cf 100 nM in the cytosol), this organelle is equipped with Calcium-binding proteins such as calreticulin which can bind more than

50% of the total ER Ca^{2+} levels [199, 200, 208, 209]. Thus, one could hypothesize that ineffective replenishing of ER Ca^{2+} stores in Txnrd2 knockout cells could potentially impair correct protein processing, a point that could be addressed in future studies.

In the Txnrd2-deficient eEPCs and also in mouse embryonic fibroblasts protein levels of the ER stress markers BiP and PDI were indeed substantially upregulated. Whether this effect was due to the lack of Txnrd2 or due to oxidation of Txn2 remains elusive in this study. Apart from the effect the elevated ROS levels in Txnrd2 deficient cells may have on Ca^{2+} funnelling to the ER by mitochondrial-expressed Ca^{2+} channels, ROS may also elicit ER stress by inactivating ER-resident Ca^{2+} channels and protein folding enzymes [197]. Additionally, ROS-elicited ER stress may initiate a vicious cycle as deregulated oxidative protein folding itself also increase ROS [197, 203]. Finally, increases in H_2O_2, as occurs in the response to changes in FSS or during hypoxia *in vivo*, lead to the transcription of numerous genes and consequently also production of proteins requiring correct assembly in the ER of ECs [210]. Thus, the presence of an impaired ER as the elevated levels of BiP and PDI in Txnrd2-deficient cells imply, could possibly advance the already detrimental effects observed here.

In this study we could demonstrate that a lack of Txnrd2 not only leads to elevated levels of ROS and a loss of $\Delta\Psi m$ but is also associated with ER stress. ER stress could be both the consequence of Txnrd2 deficiency and could result in the incorrect folding of mediator proteins required for vascular remodelling, as well as a contributing and amplifying factor to the mitochondrial defect, e.g. by interfering with calcium homeostasis and signalling.

Considering the plethora of effects ER stress can elicit, especially when unresolved, it is not surprising that the UPR is associated with numerous pathological conditions including obesity, diabetes, viral infections, neurodegenerative disorders, inflammation, and cardiovascular disorders [202]. The manifestations of thrombi in blood vessels and the development of atherosclerosis have also been reported to occur increasingly when ER stress is present.

4.3.4 Thrombus formation, atherosclerosis and future prospects

We were intrigued to discover thrombi in the collateral arterioles of both the occluded and the sham-operated hind-limb while assessing the remodelling of the collateral vessels in the thigh muscles of $Txnrd2^{ECKO}$ mice following femoral artery occlusion. Especially in light of the *in vitro* findings on increased ROS levels and ER stress in eEPCs, we speculated whether these factors may also be associated in the formation of thrombi. Indeed, PDI is implicated in the activation of tissue factor, a protein expressed, amongst others, on the surface of ECs where it can increase the proteolytic activity of a number of factors involved in the coagulation cascade of fibrin and thrombus formation [211]. PDI, while normally contained in the ER, may be released from ECs where it

participates in the thiol-dependent regulation of tissue factor by the formation of disulfide bonds of key cysteine residues in its sequence, thereby rendering it procoagulant [122, 211, 212]. Indeed, recent studies have suggested that tissue factor activation by EC-released PDI is critical for the initiation of thrombus formation as PDI is detected prior to the onset of platelet and fibrin accumulation and inhibitors of PDI also inhibit the formation of fibrin at sites of vascular injury [122, 211, 212]. Whether this observation of white thrombi in Txnrd2^{ECKO} mice serves as an indication for aberrant activation of blood coagulation due to increased ER stress will be the focus of future studies as it is beyond the scope of this project.

Additionally, in the femoral artery of Txnrd2^{ECKO} mice we observed sub-intimal infiltrations in the vascular wall, leading us to speculate that these mice may be more susceptible to atherosclerosis compared to their wildtype counterparts. In atherosclerotic plaques, increased markers of ER stress have been reported in macrophages and VSMCs but also ECs [213]. The increase in ER stress markers in ECs occurs mainly at atherosusceptible regions *in vivo*, as has been exemplified by the expression of BiP and the UPR-associated proteins IRE1α and ATF6 at the inner aortic arch, the intercostal branch points of the thoracic aorta and the renal branches [214, 215]. While increased ER stress at these sites can augment the aptitude of the ER to fold proteins and thus serve as an adaptive and protective response by counteracting the pathological aggregation of misfolded proteins, the oxidative folding of proteins also generates ROS which, especially when increased ROS levels already exist, can cause inflammation. Inflammation, in turn is critically involved in the initiation and progression of atherosclerotic lesions [214]. Furthermore, chronic exposure to additional risk factors, including elevated levels of ROS, can tip the balance of adaptive ER stress to a terminal UPR, resulting in apoptosis and atherosusceptible EC phenotypes [213, 214].

While further evidence is required to support the suggestion of an increased susceptibility of Txnrd2-deficient ECs to the development of atherosclerosis, our results on impaired vascular remodelling, the presence of thrombi and the measurements of mitochondrial impairment, increased ROS and ER stress, and the numerous reports in the literature which implicate exactly these parameters in the formation of atherosclerotic lesions warrant further investigation of the mitochondrial thioredoxin system and other thiol reducing enzymes in the initiation and progression of atherosclerosis [105, 109, 213, 216-218].

5 Conclusion

The present study demonstrates that the mitochondrial enzyme Thioredoxin Reductase 2 (Txnrd2) can considerably affect endothelial cell (EC) function. The lack of this enzyme leads to elevated basal levels of reactive oxygen species (ROS), resulting in the depolarisation of the mitochondrial membrane and endoplasmic reticulum (ER) stress. These cellular effects impair the ability of the vascular system to adapt to severe flow reduction induced by the ligation of the femoral artery. The deficit in angiogenesis in the hypoxic calf muscle is likely due to enhanced HIF-1α degradation via elevated levels of PHD2 which itself is regulated by ROS. While Txnrd2 deletion also attenuated arteriogenesis, we could not detect a lack of endothelial sensitivity to shear stress or an impairment of NO availability, both requirements for the remodelling of collateral arterioles and typically affected by ROS. The precise mechanism, however, remained unclear. Besides these effects on vascular remodelling, an incidental observation also indicated that Txnrd2 deletion may also promote thrombus formation, possibly due to the release of thrombogenic ER stress proteins.

This project adds insight into the role of the mitochondrial thioredoxin system in the maintenance of endothelial integrity and extends the available knowledge on the participation of EC mitochondria and ROS derived thereof in vascular remodelling. Granting that this investigation only scratched the surface of the importance of Txnrd2 in mitochondrial and EC health, it demonstrates that further research into this field is indeed warranted.

6 Summary

In the mitochondria, numerous antioxidant systems act in concert to prevent the toxic accumulation of reactive oxygen species and resulting oxidative stress. The mitochondrial thioredoxin system, consisting of peroxiredoxin 3, Thioredoxin 2 and Thioredoxin Reductase 2 are critically involved in the detoxification of hydrogen peroxide in order to maintain cellular redox homeostasis.

Previous studies by our and other laboratories have demonstrated that an impairment of the mitochondrial thioredoxin system and recently, and also more specifically, the ablation of the mitochondrial Thioredoxin Reductase results in increased levels of ROS and affects cellular proliferation rates. Furthermore, studies in whole organisms have implicated the mitochondrial thioredoxin system in embryonic development, tumour growth, and heart function. While these findings critically contribute to solving the puzzle of the precise role of Thioredoxin Reductase 2, many pieces remain to be put together.

In this study we aimed to add specific information to the understanding of Thioredoxin Reductase 2 function in endothelial cells with respect to vascular remodelling processes. We chose to investigate this oxidoreductase in endothelial cells *in vivo* as their mitochondrial function differs from other cells which largely rely on aerobic glycolysis to meet their energy demands. The fact that endothelial cells generate ATP mainly via anaerobic glycolysis implies that the electron transport chain in the mitochondria of these cells may participate more in cellular signalling processes rather than in energy production. Accordingly, this study aimed to also investigate the involvement of Thioredoxin Reductase 2 in signalling processes and the regulation of angiogenic/arteriogenic endothelial cell function.

We could show that the deletion of mitochondrial Thioredoxin Reductase leads to an increase in the levels of reactive oxygen species in embryonic endothelial progenitor cells which were used in the course of this study as sufficiently available substitutes for endothelial cells. Furthermore, these cells presented a partial dissipation of the mitochondrial membrane potential which is indicative of impending mitochondrial dysfunction. Since the mitochondria and the endoplasmic reticulum are closely associated both spatially and in terms of their function, we also revealed that deletion of Thioredoxin Reductase 2 in these cells results in endoplasmic reticulum stress.

With the availability of a novel mouse model in which the deletion of Thioredoxin Reductase 2 can be induced specifically and exclusively in the endothelium we also investigated the role of this enzyme *in vivo*. Occlusion of the femoral artery in these mice exposed an impairment of the vascular remodelling responses in the collateral arterioles of the thigh which normally exhibit substantial

growth in order to form natural bypasses to re-establish blood perfusion to areas downstream of the femoral artery (arteriogenesis). Laser Doppler imaging revealed impaired reperfusion which mirrored the blunted increase in collateral arteriole wall area, wall thickness, and of the expansion of luminal diameter. Furthermore, in comparison to mice expressing Thioredoxin Reductase 2, the sprouting of capillaries (angiogenesis) in the hypoxic calf muscle was significantly impaired, possibly via increased PHD2 protein expression in the endothelium. Together with the *in vitro* results, these findings strongly suggest an important involvement of endothelial cell Thioredoxin Reductase 2, its substrates and the mitochondria in vascular remodelling.

Interestingly, while assessing the impact of Thioredoxin Reductase 2 deletion on endothelium-dependent vascular remodelling, we observed the presence of thrombi in some collateral arterioles in both the occluded limb as well as in the sham-operated limb. Furthermore, sub-intimal infiltrations in the wall of the femoral artery in endothelial cell Thioredoxin Reductase 2-defienct mice drew our attention to the possible involvement of this enzyme system in the susceptibility toward thrombosis and atherosclerosis, possibly via endoplasmic reticulum stress. This further supports our conclusion that the mitochondrial Thioredoxin Reductase plays an important role in vascular homeostasis.

7 Zusammenfassung

Als Nebenprodukt der Atmungskette entstehen in den Mitochondrien zahlreiche reaktive Sauerstoffspezies (ROS). Um deren toxische Akkumulation zu verhindern und die mitochondriale Redox-Homöostase aufrechtzuerhalten, verfügen Mitochondrien über ein umfangreiches Netzwerk an antioxidativen Schutzsystemen. Eines dieser mitochondrial lokalisierten antioxidativen Schutzsysteme ist das Thioredoxin-System, bestehend aus Peroxiredoxin 3, Thioredoxin 2 und Thioredoxin Reduktase 2, welches vor allem Wasserstoffperoxid entgiftet.

Bisherige Studien zeigten, dass eine Beeinträchtigung des mitochondrialen Thioredoxin Systems und speziell die Ablation der mitochondrialen Thioredoxin Reduktase, zu einer Akkumulation von ROS führt und hierdurch die zelluläre Proliferation beeinflusst wird. Darüber hinaus zeigt ein genetischer knockout der mitochondrialen Thioredoxin Reduktase im Mausmodell Störungen in der Embryonalentwicklung, im Tumorwachstum als auch in der Herzfunktion. Während diese Ergebnisse bereits einen wesentlichen Beitrag zu der Entschlüsselung der genauen Bedeutung der Thioredoxin Reduktase 2 leisten konnten, stehen weiterhin Antworten auf zahlreiche Fragen aus.

Ziel dieser Studie war es, die Funktion der Thioredoxin Reduktase 2 speziell in Endothelzellen hinsichtlich vaskulärer Homöostase sowie vaskulärer Umbauprozesse wie Angiogenese und Arteriogenese zu analysieren. Endothelzellen unterscheiden sich von vielen anderen Körperzellen dadurch, dass sie ihren Energiebedarf weitgehend durch Glykolyse und nicht über oxidative Phosphorylierung decken. Diese Tatsache deutet an, dass die mitochondriale Atmungskette dieser Zellen mehr an Prozessen innerhalb zellulärer Signalwege beteiligt sein könnte als an der Energieerzeugung. Dementsprechend soll diese Studie auch die Beteiligung von Thioredoxin Reduktase 2 in Signalprozessen und an der Regulation der Endothelzellfunktion in der Angiogenese und Arteriogenese untersuchen.

Wir konnten zeigen, dass die Deletion der mitochondrialen Thioredoxin Reduktase zu einem Konzentrationsanstieg der ROS in embryonalen endothelialen Vorläuferzellen führt, die im Rahmen dieser Studie als Ersatz für adulte Endothelzellen verwendet wurden. Außerdem konnten wir in diesen Zellen eine partielle Dissipation des mitochondrialen Membranpotentials nachweisen, welches Indikativ für eine drohende mitochondriale Dysfunktion ist. Da die Mitochondrien und das Endoplasmatische Retikulum sowohl räumlich als auch im Hinblick auf ihre Funktion eng verbunden sind, stellten wir auch fest, dass die Deletion der Thioredoxin Reduktase 2 in diesen Zellen zu einer Stressantwort des Endoplasmatischen Retikulums führt.

Mittels eines Mausmodells, in dem die Deletion der Thioredoxin Reduktase 2 spezifisch und ausschließlich im adulten Endothel induziert werden kann, untersuchten wir auch die Rolle dieses Enzyms *in vivo*. Okklusion der Arteria femoralis in diesen Mäusen zeigte eine Beeinträchtigung der vaskulären Umbaureaktionen in den Kollateralarteriolen des Oberschenkels, welche normalerweise durch deutliches Wachstum natürliche Bypässe bilden, um die Durchblutung der nachgelagerten Bereiche wieder herzustellen (Arteriogenese). Mittels Laser Doppler konnte eine Beeinträchtigung der Reperfusion gezeigt werden, welche den abgeschwächten Zuwachs der Wandfläche und -dicke als auch die verringerte Expansion des Lumendurchmessers der Kollateralarteriolen wiederspiegelte. Darüber hinaus war die Neubildung von Kapillaren (Angiogenese) im hypoxischen Wadenmuskel dieser Mäuse im Vergleich zu Mäusen, die Thioredoxin Reduktase 2 im Endothel exprimieren, signifikant beeinträchtigt, möglicherweise durch eine erhöhte PHD2 Proteinexpression im Endothel. Zusammen mit den *in vitro* Ergebnissen deuten diese Befunde auf eine wesentliche Beteiligung der Thioredoxin Reduktase 2, seinen Substraten und den Mitochondrien in Endothelzellen an vaskulären Umbauprozessen hin.

Interessanterweise beobachteten wir während der Beurteilung der Auswirkungen der Thioredoxin Reduktase 2 Deletion auf Endothel-abhängige Gefäßumbauprozesse das Vorhandensein von Thromben in einigen Kollateralarteriolen sowohl im okkludierten als auch im kontrolloperierten Hinterlauf dieser Mäuse. Subintimale Infiltrationen in der Wand der Arteria femoralis in Endothelzell-Thioredoxin Reduktase 2- defizienten Mäusen richteten unser Augenmerk auf die mögliche Beteiligung dieses Enzymsystems an der Anfälligkeit für Thrombose und Arteriosklerose, möglicherweise über eine Stressantwort des Endoplasmatisches Retikulums. Dies unterstützt unsere Schlussfolgerung, dass die mitochondriale Thioredoxin Reduktase eine wichtige Rolle in der vaskulären Homöostase spielt.

8 References

1. Valko M, Leibfritz D, Moncol J, Cronin MTD, Mazur M, Telser J. Free radicals and antioxidants in normal physiological functions and human disease. *The International Journal of Biochemistry & Cell Biology*. 2007;39:44-84
2. Sun Q-A, Kirnarsky L, Sherman S, Gladyshev VN. Selenoprotein oxidoreductase with specificity for thioredoxin and glutathione systems. *Proceedings of the National Academy of Sciences*. 2001;98:3673-3678
3. Holmgren A, Lu J. Thioredoxin and thioredoxin reductase: Current research with special reference to human disease. *Biochemical and Biophysical Research Communications*. 2010;396:120-124
4. Laurent TC, Moore EC, Reichard P. Enzymatic Synthesis of Deoxyribonucleotides. IV. Isolation and Characterization of Thioredoxin, the Hydrogen Donor from Escherichia Coli B. *Journal of Biological Chemistry*. 1964;239:3436-3444
5. Matsui M, Oshima M, Oshima H, Takaku K, Maruyama T, Yodoi J, Taketo MM. Early Embryonic Lethality Caused by Targeted Disruption of the Mouse Thioredoxin Gene. *Developmental Biology*. 1996;178:179-185
6. Nonn L, Williams RR, Erickson RP, Powis G. The Absence of Mitochondrial Thioredoxin 2 Causes Massive Apoptosis, Exencephaly, and Early Embryonic Lethality in Homozygous Mice. *Molecular and Cellular Biology*. 2003;23:916-922
7. Matthews JR, Wakasugi N, virelizier J-L, Yodoi J, Hay RT. Thioredoxin regulates the DNA binding activity of NF-χB by reduction of a disulphid bond involving cysteine 62. *Nucleic Acids Research*. 1992;20:3821-3830
8. Schenk H, Klein M, Erdbrügger W, Dröge W, Schulze-Osthoff K. Distinct effects of thioredoxin and antioxidants on the activation of transcription factors NF-kappa B and AP-1. *Proceedings of the National Academy of Sciences*. 1994;91:1672-1676
9. Grippo JF, Tienrungroj W, Dahmer MK, Housley PR, Pratt WB. Evidence that the endogenous heat-stable glucocorticoid receptor-activating factor is thioredoxin. *Journal of Biological Chemistry*. 1983;258:13658-13664
10. Makino Y, Okamoto K, Yoshikawa N, Aoshima M, Hirota K, Yodoi J, Umesono K, Makino I, Tanaka H. Thioredoxin: a redox-regulating cellular cofactor for glucocorticoid hormone action. Cross talk between endocrine control of stress response and cellular antioxidant defense system. *The Journal of Clinical Investigation*. 1996;98:2469-2477
11. Gasdaska J, Berggren M, Powis G. Cell growth stimulation by the redox protein thioredoxin occurs by a novel helper mechanism. *Cell Growth & Differentiation*. 1995;6:1643-1650

12. Baker A, Payne CM, Briehl MM, Powis G. Thioredoxin, a Gene Found Overexpressed in Human Cancer, Inhibits Apoptosis in Vitro and in Vivo. *Cancer Research*. 1997;57:5162-5167
13. Freemerman AJ, Powis G. A Redox-Inactive Thioredoxin Reduces Growth and Enhances Apoptosis in WEHI7.2 Cells. *Biochemical and Biophysical Research Communications*. 2000;274:136-141
14. Ago T, Sadoshima J. Thioredoxin and ventricular remodeling. *Journal of Molecular and Cellular Cardiology*. 2006;41:762-773
15. Turoczi T, Chang VW-H, Engelman RM, Maulik N, Ho Y-S, Das DK. Thioredoxin redox signaling in the ischemic heart: an insight with transgenic mice overexpressing Trx1. *Journal of Molecular and Cellular Cardiology*. 2003;35:695-704
16. Yamawaki H, Pan S, Lee RT, Berk BC. Fluid shear stress inhibits vascular inflammation by decreasing thioredoxin-interacting protein in endothelial cells. *The Journal of Clinical Investigation*. 2005;115:733-738
17. Wang X-Q, Nigro P, World C, Fujiwara K, Yan C, Berk BC. Thioredoxin Interacting Protein Promotes Endothelial Cell Inflammation in Response to Disturbed Flow by Increasing Leukocyte Adhesion and Repressing Kruppel-Like Factor 2. *Circulation Research*. 2012;110:560-568
18. Damdimopoulos AE, Miranda-Vizuete A, Pelto-Huikko M, Gustafsson J-Å, Spyrou G. Human Mitochondrial Thioredoxin: Involvement in Mitochondrial Membrane Potential and Cell Death. *Journal of Biological Chemistry*. 2002;277:33249-33257
19. Widder JD, Fraccarollo D, Galuppo P, Hansen JM, Jones DP, Ertl G, Bauersachs J. Attenuation of Angiotensin II–Induced Vascular Dysfunction and Hypertension by Overexpression of Thioredoxin 2. *Hypertension*. 2009;54:338-344
20. Dai S, He Y, Zhang H, Yu L, Wan T, Xu Z, Jones D, Chen H, Min W. Endothelial-Specific Expression of Mitochondrial Thioredoxin Promotes Ischemia-Mediated Arteriogenesis and Angiogenesis. *Arteriosclerosis, Thrombosis, and Vascular Biology*. 2009;29:495-502
21. Rackham O, Shearwood A-MJ, Thyer R, McNamara E, Davies SMK, Callus BA, Miranda-Vizuete A, Berners-Price SJ, Cheng Q, Arnér ESJ, Filipovska A. Substrate and inhibitor specificities differ between human cytosolic and mitochondrial thioredoxin reductases: Implications for development of specific inhibitors. *Free Radical Biology and Medicine*. 2011;50:689-699
22. Biterova EI, Turanov AA, Gladyshev VN, Barycki JJ. Crystal structures of oxidized and reduced mitochondrial thioredoxin reductase provide molecular details of the reaction mechanism. *Proceedings of the National Academy of Sciences of the United States of America*. 2005;102:15018-15023

23. Arnér ESJ. Focus on mammalian thioredoxin reductases — Important selenoproteins with versatile functions. *Biochimica et Biophysica Acta (BBA) - General Subjects*. 2009;1790:495-526

24. Lundström J, Holmgren A. Protein disulfide-isomerase is a substrate for thioredoxin reductase and has thioredoxin-like activity. *Journal of Biological Chemistry*. 1990;265:9114-9120

25. Lundström-Ljung J, Birnbach U, Rupp K, Söling H-D, Holmgren A. Two resident ER-proteins, CaBP1 and CaBP2, with thioredoxin domains, are substrates for thioredoxin reductase: comparison with protein disulfide isomerase. *FEBS Letters*. 1995;357:305-308

26. Jiménez A, Pelto-Huikko M, Gustafsson J-Å, Miranda-Vizuete A. Characterization of human thioredoxin-like-1: Potential involvement in the cellular response against glucose deprivation. *FEBS Letters*. 2006;580:960-967

27. Björkhem-Bergman L, Jönsson-Videsäter K, Paul C, Björnstedt M, Andersson M. Mammalian thioredoxin reductase alters cytolytic activity of an antibacterial peptide. *Peptides*. 2004;25:1849-1855

28. Xia L, Nordman T, Olsson JM, Damdimopoulos A, Björkhem-Bergman L, Nalvarte I, Eriksson LC, Arnér ESJ, Spyrou G, Björnstedt M. The Mammalian Cytosolic Selenoenzyme Thioredoxin Reductase Reduces Ubiquinone: A Novel Mechanism For Defense Against Oxidative Stress. *Journal of Biological Chemistry*. 2003;278:2141-2146

29. May JM, Mendiratta S, Hill KE, Burk RF. Reduction of Dehydroascorbate to Ascorbate by the Selenoenzyme Thioredoxin Reductase. *Journal of Biological Chemistry*. 1997;272:22607-22610

30. Nalvarte I, Damdimopoulos AE, Spyrou G. Human mitochondrial thioredoxin reductase reduces cytochrome c and confers resistance to complex III inhibition. *Free Radical Biology and Medicine*. 2004;36:1270-1278

31. Jakupoglu C, Przemeck GKH, Schneider M, Moreno SG, Mayr N, Hatzopoulos AK, de Angelis MH, Wurst W, Bornkamm GW, Brielmeier M, Conrad M. Cytoplasmic Thioredoxin Reductase Is Essential for Embryogenesis but Dispensable for Cardiac Development. *Molecular and Cellular Biology*. 2005;25:1980-1988

32. Yoo M-H, Xu X-M, Carlson BA, Gladyshev VN, Hatfield DL. Thioredoxin Reductase 1 Deficiency Reverses Tumor Phenotype and Tumorigenicity of Lung Carcinoma Cells. *Journal of Biological Chemistry*. 2006;281:13005-13008

33. Hamanaka RB, Chandel NS. Mitochondrial reactive oxygen species regulate hypoxic signaling. *Current Opinion in Cell Biology*. 2009;21:894-899

34. Carlson BA, Yoo M-H, Tobe R, Mueller C, Naranjo-Suarez S, Hoffmann VJ, Gladyshev VN, Hatfield DL. Thioredoxin reductase 1 protects against chemically induced hepatocarcinogenesis via control of cellular redox homeostasis. *Carcinogenesis*. 2012;33:1806-1813

35. Choi H, Tostes RC, Webb RC. Thioredoxin reductase inhibition reduces relaxation by increasing oxidative stress and s-nitrosylation in mouse aorta. *Journal of Cardiovascular Pharmacology*. 2011;58:522-527

36. Mustacich D, Powis G. Thioredoxin reductase. *Biochemical Journal*. 2000;346:1-8

37. Hellfritsch J. Loss of mitochondrial thioredoxin reductase delays angiogenic switch and impairs tumour growth. *Faculty of Chemistry and Pharmacy*. 2011; Dr. rer. nat.

38. Conrad M, Jakupoglu C, Moreno SG, Lippl S, Banjac A, Schneider M, Beck H, Hatzopoulos AK, Just U, Sinowatz F, Schmahl W, Chien KR, Wurst W, Bornkamm GW, Brielmeier M. Essential Role for Mitochondrial Thioredoxin Reductase in Hematopoiesis, Heart Development, and Heart Function. *Molecular and Cellular Biology*. 2004;24:9414-9423

39. Horstkotte J, Perisic T, Schneider M, Lange P, Schroeder M, Kiermayer C, Hinkel R, Ziegler T, Mandal PK, David R, Schulz S, Schmitt S, Widder J, Sinowatz F, Becker BF, Bauersachs J, Naebauer M, Franz WM, Jeremias I, Brielmeier M, Zischka H, Conrad M, Kupatt C. Mitochondrial Thioredoxin Reductase Is Essential for Early Postischemic Myocardial Protection / Clinical Perspective. *Circulation*. 2011;124:2892-2902

40. Sibbing D, Pfeufer A, Perisic T, Mannes AM, Fritz-Wolf K, Unwin S, Sinner MF, Gieger C, Gloeckner CJ, Wichmann H-E, Kremmer E, Schäfer Z, Walch A, Hinterseer M, Näbauer M, Kääb S, Kastrati A, Schömig A, Meitinger T, Bornkamm GW, Conrad M, von Beckerath N. Mutations in the mitochondrial thioredoxin reductase gene TXNRD2 cause dilated cardiomyopathy. *European Heart Journal*. 2011;32:1121-1133

41. Levick JR. *An Introduction to Cardiovascular Physiology*. Hodder Arnold; 2003

42. Rowley AH, Baker SC, Orenstein JM, Shulman ST. Searching for the cause of Kawasaki disease - cytoplasmic inclusion bodies provide new insight. *Nature Reviews Microbiology*. 2008;6:394-401

43. Sumpio BE, Timothy Riley J, Dardik A. Cells in focus: endothelial cell. *The International Journal of Biochemistry & Cell Biology*. 2002;34:1508-1512

44. Davies PF. Flow-mediated endothelial mechanotransduction. *Physiological Reviews*. 1995;75:519-560

45. Schaper W, Scholz D. Factors regulating arteriogenesis. *Arteriosclerosis, Thrombosis, and Vascular Biology*. 2003;23:1143-1151

46. Resnick N, Yahav H, Shay-Salit A, Shushy M, Schubert S, Zilberman LCM, Wofovitz E. Fluid shear stress and the vascular endothelium: for better and for worse. *Progress in Biophysics and Molecular Biology*. 2003;81:177-199

47. Owens GK. Regulation of differentiation of vascular smooth muscle cells. *Physiological Reviews*. 1995;75:487-517

48. Heil M, Eitenmüller I, Schmitz-Rixen T, Schaper W. Arteriogenesis versus angiogenesis: similarities and differences. *Journal of Cellular and Molecular Medicine*. 2006;10:45-55

49. Carmeliet P. Mechanisms of angiogenesis and arteriogenesis. *Nature Medicine*. 2000;6:389-395

50. Adams RH, Alitalo K. Molecular regulation of angiogenesis and lymphangiogenesis. *Nature Reviews Molecular Cell Biology*. 2007;8:464-478

51. Grundmann S, Piek JJ, Pasterkamp G, Hoefer IE. Arteriogenesis: basic mechanisms and therapeutic stimulation. *European Journal of Clinical Investigation*. 2007;37:755-766

52. Deindl E, Buschmann I, Hoefer IE, Podzuweit T, Boengler K, Vogel S, van Royen N, Fernandez B, Schaper W. Role of Ischemia and of Hypoxia-Inducible Genes in Arteriogenesis After Femoral Artery Occlusion in the Rabbit. *Circulation Research*. 2001;89:779-786

53. Pipp F, Boehm S, Cai WJ, Adili F, Ziegler B, Karanovic G, Ritter R, Balzer J, Scheler C, Schaper W, Schmitz-Rixen T. Elevated fluid shear stress enhances postocclusive collateral artery growth and gene expression in the pig hind limb. *Arteriosclerosis, Thrombosis, and Vascular Biology*. 2004;24:1664-1668

54. Hoefer IE, van Royen N, Buschmann IR, Piek JJ, Schaper W. Time course of arteriogenesis following femoral artery occlusion in the rabbit. *Cardiovascular Research*. 2001;49:609-617

55. Endlich K, Muller C, Barthelmebs M, Helwig J-J. Role of shear stress in nitric oxide-dependent modulation of renal angiotensin II vasoconstriction. *British Journal of Pharmacology*. 1999;127:1929-1935

56. Busse R, Fleming I. Regulation of endothelium-derived vasoactive autacoid production by hemodynamic forces. *Trends in pharmacological sciences*. 2003;24:24-29

57. Dimmeler S, Fleming I, Fisslthaler B, Hermann C, Busse R, Zeiher AM. Activation of nitric oxide synthase in endothelial cells by Akt-dependent phosphorylation. *Nature*. 1999;399:601-605

58. Liu Y, Zhao H, Li H, Kalyanaraman B, Nicolosi AC, Gutterman DD. Mitochondrial Sources of H_2O_2 Generation Play a Key Role in Flow-Mediated Dilation in Human Coronary Resistance Arteries. *Circulation Research*. 2003;93:573-580

59. Yang Z-w, Zhang A, Altura BT, Altura BM. Hydrogen peroxide-induced endothelium-dependent relaxation of rat aorta: Involvement of Ca^{2+} and other cellular metabolites. *General Pharmacology: The Vascular System*. 1999;33:325-336

60. Demicheva E, Hecker M, Korff T. Stretch-Induced Activation of the Transcription Factor Activator Protein-1 Controls Monocyte Chemoattractant Protein-1 Expression During Arteriogenesis. *Circulation Research*. 2008;103:477-484

61. Folkow B, Svanborg A. Physiology of cardiovascular aging. *Physiological Reviews*. 1993;73:725-764

62. Jacobsen JCB, Mulvany MJ, Holstein-Rathlou N-H. A mechanism for arteriolar remodeling based on maintenance of smooth muscle cell activation. *American Journal of Physiology - Regulatory, Integrative and Comparative Physiology*. 2008;294:R1379-R1389

63. Sorop O, Bakker ENTP, Pistea A, Spaan JAE, VanBavel E. Calcium channel blockade prevents pressure-dependent inward remodeling in isolated subendocardial resistance vessels. *American Journal of Physiology - Heart and Circulatory Physiology*. 2006;291:H1236-H1245

64. Unthank JL, Nixon JC, Burkhart HM, Fath SW, Dalsing MC. Early collateral and microvascular adaptations to intestinal artery occlusion in rat. *American Journal of Physiology - Heart and Circulatory Physiology*. 1996;271:H914-H923

65. Unthank JL, Fath SW, Burkhart HM, Miller SC, Dalsing MC. Wall Remodeling During Luminal Expansion of Mesenteric Arterial Collaterals in the Rat. *Circulation Research*. 1996;79:1015-1023

66. McCormick SM, Eskin SG, McIntire LV, Teng CL, Lu C-M, Russell CG, Chittur KK. DNA microarray reveals changes in gene expression of shear stressed human umbilical vein endothelial cells. *Proceedings of the National Academy of Sciences*. 2001;98:8955-8960

67. Scholz D, Ito W, Fleming I, Deindl E, Sauer A, Wiesnet M, Busse R, Schaper J, Schaper W. Ultrastructure and molecular histology of rabbit hind-limb collateral artery growth (arteriogenesis). *Virchows Archiv-an International Journal of Pathology*. 2000;436:257-270

68. Walpola PL, Gotlieb AI, Cybulsky MI, Langille BL. Expression of ICAM-1 and VCAM-1 and Monocyte Adherence in Arteries Exposed to Altered Shear Stress. *Arteriosclerosis, Thrombosis, and Vascular Biology*. 1995;15:2-10

69. Ohtsuka A, Ando J, Korenaga R, Kamiya A, Toyamasorimachi N, Miyasaka M. The Effect of Flow on the Expression of Vascular Adhesion Molecule-1 by Cultured Mouse Endothelial Cells. *Biochemical and Biophysical Research Communications*. 1993;193:303-310

70. Arras M, Ito WD, Scholz D, Winkler B, Schaper J, Schaper W. Monocyte activation in angiogenesis and collateral growth in the rabbit hindlimb. *The Journal of Clinical Investigation*. 1998;101:40-50

71. Eitenmuller I, Volger O, Kluge A, Troidl K, Barancik M, Cai WJ, Heil M, Pipp F, Fischer S, Horrevoets AJ, Schmitz-Rixen T, Schaper W. The range of adaptation by collateral vessels after femoral artery occlusion. *Circulation Research*. 2006;99:656-662

72. Haas TL, Doyle JL, Distasi MR, Norton LE, Sheridan KM, Unthank JL. Involvement of MMPs in the outward remodeling of collateral mesenteric arteries. *American Journal of Physiology - Heart and Circulatory Physiology*. 2007;293:H2429-H2437

73. Tronc F, Mallat Z, Lehoux S, Wassef M, Esposito B, Tedgui A. Role of Matrix Metalloproteinases in Blood Flow–Induced Arterial Enlargement: Interaction With NO. *Arteriosclerosis, Thrombosis, and Vascular Biology*. 2000;20:e120-e126

74. Barchowsky A, Munro SR, Morana SJ, Vincenti MP, Treadwell M. Oxidant-sensitive and phosphorylation-dependent activation of NF-kappa B and AP-1 in endothelial cells. *American Journal of Physiology - Lung Cellular and Molecular Physiology*. 1995;269:L829-L836

75. Yasuda M, Ohzeki Y, Shimizu S, Naito S, Ohtsuru A, Yamamoto T, Kuroiwa Y. Stimulation of in vitro angiogenesis by hydrogen peroxide and the relation with ETS-1 in endothelial cells. *Life Sciences*. 1999;64:249-258

76. Maulik N, Das DK. Redox signaling in vascular angiogenesis. *Free Radical Biology and Medicine*. 2002;33:1047-1060

77. Szatrowski TP, Nathan CF. Production of Large Amounts of Hydrogen Peroxide by Human Tumor Cells. *Cancer Research*. 1991;51:794-798

78. Ushio-Fukai M, Nakamura Y. Reactive oxygen species and angiogenesis: NADPH oxidase as target for cancer therapy. *Cancer Letters*. 2008;266:37-52

79. Connor KM, Subbaram S, Regan KJ, Nelson KK, Mazurkiewicz JE, Bartholomew PJ, Aplin AE, Tai Y-T, Aguirre-Ghiso J, Flores SC, Melendez JA. Mitochondrial H_2O_2 Regulates the Angiogenic Phenotype via PTEN Oxidation. *Journal of Biological Chemistry*. 2005;280:16916-16924

80. Cho M, Hunt TK, Hussain MZ. Hydrogen peroxide stimulates macrophage vascular endothelial growth factor release. *American Journal of Physiology - Heart and Circulatory Physiology*. 2001;280:H2357-H2363

81. Lee J-W, Bae S-H, Jeong J-W, Kim S-H, Kim K-W. Hypoxia-inducible factor (HIF-1)alpha: its protein stability and biological functions. *Experimental & Molecular Medicine*. 2004;36:1-12

82. Fong GH, Takeda K. Role and regulation of prolyl hydroxylase domain proteins. *Cell Death and Differentiation*. 2008;15:635-641

83. Manalo DJ, Rowan A, Lavoie T, Natarajan L, Kelly BD, Ye SQ, Garcia JGN, Semenza GL. Transcriptional regulation of vascular endothelial cell responses to hypoxia by HIF-1. *Blood*. 2005;105:659-669

84. Pan Y, Mansfield KD, Bertozzi CC, Rudenko V, Chan DA, Giaccia AJ, Simon MC. Multiple Factors Affecting Cellular Redox Status and Energy Metabolism Modulate Hypoxia-Inducible

Factor Prolyl Hydroxylase Activity In Vivo and In Vitro. *Molecular and Cellular Biology*. 2007;27:912-925

85. Calvani M, Comito G, Giannoni E, Chiarugi P. Time-dependent stabilization of hypoxia inducible factor-1alpha by different intracellular sources of reactive oxygen species. *PLoS One*. 2012;7:e38388
86. Masson N, Singleton RS, Sekirnik R, Trudgian DC, Ambrose LJ, Miranda MX, Tian Y-M, Kessler BM, Schofield CJ, Ratcliffe PJ. The FIH hydroxylase is a cellular peroxide sensor that modulates HIF transcriptional activity. *EMBO reports*. 2012;13:251-257
87. Hoffman DL, Salter JD, Brookes PS. Response of mitochondrial reactive oxygen species generation to steady-state oxygen tension: implications for hypoxic cell signaling. *American Journal of Physiology - Heart and Circulatory Physiology*. 2007;292:H101-H108
88. Dunn LL, Buckle AM, Cooke JP, Ng MKC. The Emerging Role of the Thioredoxin System in Angiogenesis. *Arteriosclerosis, Thrombosis, and Vascular Biology*. 2010;30:2089-2098
89. Saitoh M, Nishitoh H, Fujii M, Takeda K, Tobiume K, Sawada Y, Kawabata M, Miyazono K, Ichijo H. Mammalian thioredoxin is a direct inhibitor of apoptosis signal-regulating kinase (ASK) 1. *EMBO Journal*. 1998;17:2596-2606
90. Buechner N, Schroeder P, Jakob S, Kunze K, Maresch T, Calles C, Krutmann J, Haendeler J. Changes of MMP-1 and collagen type Iα1 by UVA, UVB and IRA are differentially regulated by Trx-1. *Experimental Gerontology*. 2008;43:633-637
91. Ott I, Qian X, Xu Y, Vlecken DHW, Marques IJ, Kubutat D, Will J, Sheldrick WS, Jesse P, Prokop A, Bagowski CP. A Gold(I) Phosphine Complex Containing a Naphthalimide Ligand Functions as a TrxR Inhibiting Antiproliferative Agent and Angiogenesis Inhibitor. *Journal of Medicinal Chemistry*. 2009;52:763-770
92. Bir SC, Kolluru GK, Fang K, Kevil CG. Redox balance dynamically regulates vascular growth and remodeling. *Seminars in Cell & Developmental Biology*. 2012;23:745-757
93. Laurindo FR, Pedro MdA, Barbeiro HV, Pileggi F, Carvalho MH, Augusto O, da Luz PL. Vascular free radical release. Ex vivo and in vivo evidence for a flow-dependent endothelial mechanism. *Circulation Research*. 1994;74:700-709
94. Shaw JH, Xiang L, Shah A, Yin W, Lloyd PG. Placenta growth factor expression is regulated by hydrogen peroxide in vascular smooth muscle cells. *American Journal of Physiology - Cell Physiology*. 2011;300:C349-C355
95. Luttun A, Tjwa M, Moons L, Wu Y, Angelillo-Scherrer A, Liao F, Nagy JA, Hooper A, Priller J, De Klerck B, Compernolle V, Daci E, Bohlen P, Dewerchin M, Herbert J-M, Fava R, Matthys P, Carmeliet G, Collen D, Dvorak HF, Hicklin DJ, Carmeliet P. Revascularization of ischemic

tissues by PlGF treatment, and inhibition of tumor angiogenesis, arthritis and atherosclerosis by anti-Flt1. *Nature Medicine*. 2002;8:831-840

96. Nelson KK, Melendez JA. Mitochondrial redox control of matrix metalloproteinases. *Free Radical Biology and Medicine*. 2004;37:768-784
97. Fortuño A, José GS, Moreno MU, Díez J, Zalba G. Oxidative stress and vascular remodelling. *Experimental Physiology*. 2005;90:457-462
98. Rajagopalan S, Meng XP, Ramasamy S, Harrison DG, Galis ZS. Reactive oxygen species produced by macrophage-derived foam cells regulate the activity of vascular matrix metalloproteinases in vitro. Implications for atherosclerotic plaque stability. *The Journal of Clinical Investigation*. 1996;98:2572-2579
99. Sohal RS, Orr WC. The redox stress hypothesis of aging. *Free Radical Biology and Medicine*. 2012;52:539-555
100. Sohal RS, Sohal BH. Hydrogen peroxide release by mitochondria increases during aging. *Mechanisms of Ageing and Development*. 1991;57:187-202
101. Miller SJ, Coppinger BJ, Zhou X, Unthank JL. Antioxidants Reverse Age-Related Collateral Growth Impairment. *Journal of Vascular Research*. 2010;47:108-114
102. Tuttle JL, Hahn TL, Sanders BM, Witzmann FA, Miller SJ, Dalsing MC, Unthank JL. Impaired collateral development in mature rats. *American Journal of Physiology - Heart and Circulatory Physiology*. 2002;283:H146-H155
103. Miller SJ, Norton LE, Murphy MP, Dalsing MC, Unthank JL. The role of the renin-angiotensin system and oxidative stress in spontaneously hypertensive rat mesenteric collateral growth impairment. *American Journal of Physiology - Heart and Circulatory Physiology*. 2007;292:H2523-H2531
104. Tuttle JL, Sanders BM, Burkhart HM, Fath SW, Kerr KA, Watson WC, Herring BP, Dalsing MC, Unthank JL. Impaired Collateral Artery Development in Spontaneously Hypertensive Rats. *Microcirculation*. 2002;9:343-351
105. Förstermann U. Nitric oxide and oxidative stress in vascular disease. *Pflügers Archiv European Journal of Physiology*. 2010;459:923-939
106. Milstien S, Katusic Z. Oxidation of Tetrahydrobiopterin by Peroxynitrite: Implications for Vascular Endothelial Function. *Biochemical and Biophysical Research Communications*. 1999;263:681-684
107. Zhang H, Luo Y, Zhang W, He Y, Dai S, Zhang R, Huang Y, Bernatchez P, Giordano FJ, Shadel G, Sessa WC, Min W. Endothelial-Specific Expression of Mitochondrial Thioredoxin Improves Endothelial Cell Function and Reduces Atherosclerotic Lesions. *The American Journal of Pathology*. 2007;170:1108-1120

108. Culic O, Gruwel ML, Schrader J. Energy turnover of vascular endothelial cells. *American Journal of Physiology - Cell Physiology*. 1997;273:C205-C213

109. Groschner L, Waldeck-Weiermair M, Malli R, Graier W. Endothelial mitochondria—less respiration, more integration. *Pflügers Archiv - European Journal of Physiology*. 2012;464:63-76

110. Davidson SM, Duchen MR. Endothelial Mitochondria. *Circulation Research*. 2007;100:1128-1141

111. Jornot L, Maechler P, Wollheim CB, Junod AF. Reactive oxygen metabolites increase mitochondrial calcium in endothelial cells: implication of the Ca^{2+}/Na^{+} exchanger. *Journal of Cell Science*. 1999;112:1013-1022

112. Malli R, Frieden M, Trenker M, Graier WF. The Role of Mitochondria for Ca^{2+} Refilling of the Endoplasmic Reticulum. *Journal of Biological Chemistry*. 2005;280:12114-12122

113. Perry SW, Norman JP, Barbieri J, Brown EB, Gelbard HA. Mitochondrial membrane potential probes and the proton gradient: a practical usage guide. *BioTechniques*. 2011;50:98-115

114. Han YW, Kim SZ, Kim SH, Park WH. The changes of intracellular H_2O_2 are an important factor maintaining mitochondria membrane potential of antimycin A-treated As4.1 juxtaglomerular cells. *Biochemical Pharmacology*. 2007;73:863-872

115. Zhang H, Go Y-M, Jones DP. Mitochondrial thioredoxin-2/peroxiredoxin-3 system functions in parallel with mitochondrial GSH system in protection against oxidative stress. *Archives of Biochemistry and Biophysics*. 2007;465:119-126

116. Perisic T. Addressing the Role of Mitochondrial Thioredoxin Reductase and xCT in the Maintenance of Redox Homeostasis. *Faculty of Biology*. 2009;Dr. rer. nat.

117. Heil M, Schaper W. Influence of mechanical, cellular, and molecular factors on collateral artery growth (arteriogenesis). *Circulation Research*. 2004;95:449-458

118. Limbourg A, Korff T, Napp LC, Schaper W, Drexler H, Limbourg FP. Evaluation of postnatal arteriogenesis and angiogenesis in a mouse model of hind-limb ischemia. *Nature Protocols*. 2009;4:1737-1748

119. Bolz SS, de Wit C, Pohl U. Endothelium-derived hyperpolarizing factor but not NO reduces smooth muscle Ca^{2+} during acetylcholine-induced dilation of microvessels. *British Journal of Pharmacology*. 1999;128:124-134

120. Hatzopoulos AK, Folkman J, Vasile E, Eiselen GK, Rosenberg RD. Isolation and characterization of endothelial progenitor cells from mouse embryos. *Development*. 1998;125:1457-1468

121. MacPhee DJ. Methodological considerations for improving Western blot analysis. *Journal of Pharmacological and Toxicological Methods*. 2010;61:171-177

122. Jasuja R, Furie B, Furie BC. Endothelium-derived but not platelet-derived protein disulfide isomerase is required for thrombus formation in vivo. *Blood*. 2010;116:4665-4674

123. Nakamura H, Nakamura K, Yodoi J. Redox regulation of cellular activation. *Annual Review of Immunology*. 1997;15:351-369

124. Powis G, Briehl M, Oblong J. Redox signalling and the control of cell growth and death. *Pharmacology & Therapeutics*. 1995;68:149-173

125. Arnér ESJ, Holmgren A. Physiological functions of thioredoxin and thioredoxin reductase. *European Journal of Biochemistry*. 2000;267:6102-6109

126. Becker K, Gromer S, Schirmer RH, Müller S. Thioredoxin reductase as a pathophysiological factor and drug target. *European Journal of Biochemistry*. 2000;267:6118-6125

127. Arnér ESJ, Holmgren A. The thioredoxin system in cancer. *Seminars in Cancer Biology*. 2006;16:420-426

128. Gromer S, Urig S, Becker K. The thioredoxin system—From science to clinic. *Medicinal Research Reviews*. 2004;24:40-89

129. Patenaude A, Murthy MRV, Mirault M-E. Mitochondrial Thioredoxin System: effects of TrxR2 overexpression on redox balance, cell growth, and apoptosis. *Journal of Biological Chemistry*. 2004;279:27302-27314

130. Kim M-R, Chang H-S, Kim B-H, Kim S, Baek S-H, Hye Kim J, Lee S-R, Kim J-R. Involvements of mitochondrial thioredoxin reductase (TrxR2) in cell proliferation. *Biochemical and Biophysical Research Communications*. 2003;304:119-124

131. Craige SM, Chen K, Pei Y, Li C, Huang X, Chen, C, Shibata R, Sato K, Walsh K, Keaney JF. NADPH Oxidase 4 Promotes Endothelial Angiogenesis Through Endothelial Nitric Oxide Synthase Activation. *Circulation*. 2011;124:731-740

132. Haddad P, Dussault S, Groleau J, Turgeon J, Michaud S-E, Ménard C, Perez G, Maingrette F, Rivard A. Nox2-Containing NADPH Oxidase Deficiency Confers Protection From Hindlimb Ischemia in Conditions of Increased Oxidative Stress. *Arteriosclerosis, Thrombosis, and Vascular Biology*. 2009;29:1522-1528

133. Martyn KD, Frederick LM, von Loehneysen K, Dinauer MC, Knaus UG. Functional analysis of Nox4 reveals unique characteristics compared to other NADPH oxidases. *Cellular Signalling*. 2006;18:69-82

134. BelAiba RS, Djordjevic T, Petry A, Diemer K, Bonello S, Banfi B, Hess J, Pogrebniak A, Bickel C, Gorlach A. NOX5 variants are functionally active in endothelial cells. *Free Radical Biology and Medicine*. 2007;42:446-459

135. McNally JS, Davis ME, Giddens DP, Saha A, Hwang J, Dikalov S, Jo H, Harrison DG. Role of xanthine oxidoreductase and NAD(P)H oxidase in endothelial superoxide production in

response to oscillatory shear stress. *American Journal of Physiology - Heart and Circulatory Physiology*. 2003;285:H2290-H2297

136. Landmesser U, Dikalov S, Price SR, McCann L, Fukai T, Holland SM, Mitch WE, Harrison DG. Oxidation of tetrahydrobiopterin leads to uncoupling of endothelial cell nitric oxide synthase in hypertension. *The Journal of Clinical Investigation*. 2003;111:1201-1209
137. Aon MA, Stanley BA, Sivakumaran V, Kembro JM, O'Rourke B, Paolocci N, Cortassa S. Glutathione/thioredoxin systems modulate mitochondrial H_2O_2 emission: An experimental-computational study. *The Journal of General Physiology*. 2012;139:479-491
138. Kudin AP, Augustynek B, Lehmann AK, Kovács R, Kunz WS. The contribution of thioredoxin-2 reductase and glutathione peroxidase to H_2O_2 detoxification of rat brain mitochondria. *Biochimica et Biophysica Acta (BBA) - Bioenergetics*. 2012;1817:1901-1906
139. Stanley BA, Sivakumaran V, Shi S, McDonald I, Lloyd D, Watson WH, Aon MA, Paolocci N. Thioredoxin Reductase-2 Is Essential for Keeping Low Levels of H_2O_2 Emission from Isolated Heart Mitochondria. *Journal of Biological Chemistry*. 2011;286:33669-33677
140. Zhong L, Holmgren A. Essential Role of Selenium in the Catalytic Activities of Mammalian Thioredoxin Reductase Revealed by Characterization of Recombinant Enzymes with Selenocysteine Mutations. *Journal of Biological Chemistry*. 2000;275:18121-18128
141. Andreyev AY, Kushnareva YE, Starkov AA. Mitochondrial metabolism of reactive oxygen species. *Biochemistry (Mosc)*. 2005;70:200-214
142. Giedt R, Pfeiffer D, Matzavinos A, Kao C-Y, Alevriadou BR. Mitochondrial Dynamics and Motility Inside Living Vascular Endothelial Cells: Role of Bioenergetics. *Annals of Biomedical Engineering*. 2012;40:1903-1916
143. Liu Y, Bubolz AH, Mendoza S, Zhang DX, Gutterman DD. H_2O_2 Is the Transferrable Factor Mediating Flow-Induced Dilation in Human Coronary Arterioles. *Circulation Research*. 2011;108:566-573
144. Mizutani H, Tada-Oikawa S, Hiraku Y, Kojima M, Kawanishi S. Mechanism of apoptosis induced by doxorubicin through the generation of hydrogen peroxide. *Life Sciences*. 2005;76:1439-1453
145. Smiley ST, Reers M, Mottola-Hartshorn C, Lin M, Chen A, Smith TW, Steele GD, Chen LB. Intracellular heterogeneity in mitochondrial membrane potentials revealed by a J-aggregate-forming lipophilic cation JC-1. *Proceedings of the National Academy of Sciences*. 1991;88:3671-3675
146. Gottlieb E, Armour SM, Harris MH, Thompson CB. Mitochondrial membrane potential regulates matrix configuration and cytochrome c release during apoptosis. *Cell Death and Differentiation*. 2003;10:709-717

147. Kirkinezos IG, Moraes CT. Reactive oxygen species and mitochondrial diseases. *Seminars in Cell & Developmental Biology*. 2001;12:449-457

148. Safiulina D, Veksler V, Zharkovsky A, Kaasik A. Loss of mitochondrial membrane potential is associated with increase in mitochondrial volume: Physiological role in neurones. *Journal of Cellular Physiology*. 2006;206:347-353

149. Kaasik A, Safiulina D, Zharkovsky A, Veksler V. Regulation of mitochondrial matrix volume. *American Journal of Physiology - Cell Physiology*. 2007;292:C157-C163

150. Kaasik A, Joubert F, Ventura-Clapier R, Veksler V. A novel mechanism of regulation of cardiac contractility by mitochondrial functional state. *FASEB Journal*. 2004;18:1219-1227

151. Heil M, Schaper W. Insights into pathways of arteriogenesis. *Current Pharmaceutical Biotechnology*. 2007;8:35-42

152. Semenza GL. Hypoxia-Inducible Factor 1 (HIF-1) Pathway. *Science's STKE*. 2007;2007:cm8

153. Brunelle JK, Bell EL, Quesada NM, Vercauteren K, Tiranti V, Zeviani M, Scarpulla RC, Chandel NS. Oxygen sensing requires mitochondrial ROS but not oxidative phosphorylation. *Cell metabolism*. 2005;1:409-414

154. Guzy RD, Hoyos B, Robin E, Chen H, Liu L, Mansfield KD, Simon MC, Hammerling U, Schumacker PT. Mitochondrial complex III is required for hypoxia-induced ROS production and cellular oxygen sensing. *Cell metabolism*. 2005;1:401-408

155. Mansfield KD, Guzy RD, Pan Y, Young RM, Cash TP, Schumacker PT, Simon MC. Mitochondrial dysfunction resulting from loss of cytochrome c impairs cellular oxygen sensing and hypoxic HIF-± activation. *Cell metabolism*. 2005;1:393-399

156. Yan J, Tie G, Messina LM. Tetrahydrobiopterin, L-arginine and vitamin C actsynergistically to decrease oxidative stress, increase nitricoxide and improve blood flow after induction of hindlimb ischemia in the rat. *Mol Med*. 2012;18:676-684

157. Munns SE, Lui JKC, Arthur PG. Mitochondrial hydrogen peroxide production alters oxygen consumption in an oxygen-concentration-dependent manner. *Free Radical Biology and Medicine*. 2005;38:1594-1603

158. Hool LC, Arthur PG. Decreasing Cellular Hydrogen Peroxide With Catalase Mimics the Effects of Hypoxia on the Sensitivity of the L-Type Ca^{2+} Channel to β-Adrenergic Receptor Stimulation in Cardiac Myocytes. *Circulation Research*. 2002;91:601-609

159. Huang LE, Arany Z, Livingston DM, Bunn HF. Activation of Hypoxia-inducible Transcription Factor Depends Primarily upon Redox-sensitive Stabilization of its α Subunit. *Journal of Biological Chemistry*. 1996;271:32253-32259

160. Finkel T. Signal Transduction by Mitochondrial Oxidants. *Journal of Biological Chemistry*. 2012;287:4434-4440

161. Schäfer M, Schäfer C, Ewald N, Piper HM, Noll T. Role of Redox Signaling in the Autonomous Proliferative Response of Endothelial Cells to Hypoxia. *Circulation Research*. 2003;92:1010-1015

162. Berry CE, Hare JM. Xanthine oxidoreductase and cardiovascular disease: molecular mechanisms and pathophysiological implications. *The Journal of Physiology*. 2004;555:589-606

163. Wiezorek JS, Brown DH, Kupperman DE, Brass CA. Rapid conversion to high xanthine oxidase activity in viable Kupffer cells during hypoxia. *The Journal of Clinical Investigation*. 1994;94:2224-2230

164. Poss WB, Huecksteadt TP, Panus PC, Freeman BA, Hoidal JR. Regulation of xanthine dehydrogenase and xanthine oxidase activity by hypoxia. *American Journal of Physiology - Lung Cellular and Molecular Physiology*. 1996;270:L941-L946

165. Terada LS, Guidot DM, Leff JA, Willingham IR, Hanley ME, Piermattei D, Repine JE. Hypoxia injures endothelial cells by increasing endogenous xanthine oxidase activity. *Proceedings of the National Academy of Sciences*. 1992;89:3362-3366

166. Terada LS, Piermattei D, Shibao GN, McManaman JL, Wright RM. Hypoxia Regulates Xanthine Dehydrogenase Activity at Pre- and Posttranslational Levels. *Archives of Biochemistry and Biophysics*. 1997;348:163-168

167. Hagen T. Oxygen versus Reactive Oxygen in the Regulation of HIF-1: The Balance Tips. *Biochemistry Research International*. 2012;2012:Article ID 436981

168. Takeda K, Cowan A, Fong G-H. Essential Role for Prolyl Hydroxylase Domain Protein 2 in Oxygen Homeostasis of the Adult Vascular System. *Circulation*. 2007;116:774-781

169. Mazzone M, Dettori D, Leite de Oliveira R, Loges S, Schmidt T, Jonckx B, Tian Y-M, Lanahan AA, Pollard P, Ruiz de Almodovar C, De Smet F, Vinckier S, Aragonés J, Debackere K, Luttun A, Wyns S, Jordan B, Pisacane A, Gallez B, Lampugnani MG, Dejana E, Simons M, Ratcliffe P, Maxwell P, Carmeliet P. Heterozygous Deficiency of PHD2 Restores Tumor Oxygenation and Inhibits Metastasis via Endothelial Normalization. *Cell*. 2009;136:839-851

170. Chan DA, Kawahara TLA, Sutphin PD, Chang HY, Chi J-T, Giaccia AJ. Tumor Vasculature Is Regulated by PHD2-Mediated Angiogenesis and Bone Marrow-Derived Cell Recruitment. *Cancer Cell*. 2009;15:527-538

171. Takeda K, Fong G-H. Prolyl Hydroxylase Domain 2 Protein Suppresses Hypoxia-Induced Endothelial Cell Proliferation. *Hypertension*. 2007;49:178-184

172. Naranjo-Suarez S, Carlson BA, Tsuji PA, Yoo M-H, Gladyshev VN, Hatfield DL. HIF-Independent Regulation of Thioredoxin Reductase 1 Contributes to the High Levels of Reactive Oxygen Species Induced by Hypoxia. *PLoS One*. 2012;7:e30470

173. Rosenthal SL, Guyton AC. Hemodynamics of Collateral Vasodilatation following Femoral Artery Occlusion in Anesthetized Dogs. *Circulation Research*. 1968;23:239-248

174. Schauf CL, Moffett DF, Moffett SB. *Human physiology : foundations & frontiers*. St. Louis: Times Mirror/Mosby College Pub.; 1990

175. Sirs JA. The flow of human blood through capillary tubes. *Journal of Physiology*. 1991;442:569-583

176. Koller A, Kaley G. Endothelial regulation of wall shear stress and blood flow in skeletal muscle microcirculation. *American Journal of Physiology - Heart and Circulatory Physiology*. 1991;260:H862-H868

177. de Wit C, Schäfer C, von Bismarck P, Bolz S-S, Pohl U. Elevation of plasma viscosity induces sustained NO-mediated dilation in the hamster cremaster microcirculation in vivo. *Pflügers Archiv European Journal of Physiology*. 1997;434:354-361

178. Davies P, Spaan J, Krams R. Shear Stress Biology of the Endothelium. *Annals of Biomedical Engineering*. 2005;33:1714-1718

179. Zaragoza C, Marquez S, Saura M. Endothelial mechanosensors of shear stress as regulators of atherogenesis. *Current Opinion in Lipidology*. 2012;23:446-452

180. Duerrschmidt N, Stielow C, Muller G, Pagano PJ, Morawietz H. NO-mediated regulation of NAD(P)H oxidase by laminar shear stress in human endothelial cells. *The Journal of Physiology*. 2006;576:557-567

181. Kumar S, Sud N, Fonseca FV, Hou Y, Black SM. Shear stress stimulates nitric oxide signaling in pulmonary arterial endothelial cells via a reduction in catalase activity: role of protein kinase Cδ. *American Journal of Physiology - Lung Cellular and Molecular Physiology*. 2010;298:L105-L116

182. Chien S, Li S, Shyy JY-J. Effects of Mechanical Forces on Signal Transduction and Gene Expression in Endothelial Cells. *Hypertension*. 1998;31:162-169

183. De Keulenaer GW, Chappell DC, Ishizaka N, Nerem RM, Alexander RW, Griendling KK. Oscillatory and steady laminar shear stress differentially affect human endothelial redox state: role of a superoxide-producing NADH oxidase. *Circulation Research*. 1998;82:1094-1101

184. Jones CI, 3rd, Zhu H, Martin SF, Han Z, Li Y, Alevriadou BR. Regulation of antioxidants and phase 2 enzymes by shear-induced reactive oxygen species in endothelial cells. *Annals of Biomedical Engineering*. 2007;35:683-693

185. Birukov KG. Cyclic stretch, reactive oxygen species, and vascular remodeling. *Antioxidants & Redox Signaling*. 2009;11:1651-1667

186. Sun D, Huang A, Yan EH, Wu Z, Yan C, Kaminski PM, Oury TD, Wolin MS, Kaley G. Reduced release of nitric oxide to shear stress in mesenteric arteries of aged rats. *American Journal of Physiology - Heart and Circulatory Physiology*. 2004;286:H2249-H2256

187. Stamler JS, Lamas S, Fang FC. Nitrosylation: The Prototypic Redox-Based Signaling Mechanism. *Cell*. 2001;106:675-683

188. Hoffmann J, Dimmeler S, Haendeler J. Shear stress increases the amount of S-nitrosylated molecules in endothelial cells: important role for signal transduction. *FEBS Letters*. 2003;551:153-158

189. Benhar M, Forrester MT, Hess DT, Stamler JS. Regulated Protein Denitrosylation by Cytosolic and Mitochondrial Thioredoxins. *Science*. 2008;320:1050-1054

190. Bienert GP, Schjoerring JK, Jahn TP. Membrane transport of hydrogen peroxide. *Biochimica et Biophysica Acta (BBA) - Biomembranes*. 2006;1758:994-1003

191. Sugiyama T, Michel T. Thiol-metabolizing proteins and endothelial redox state: differential modulation of eNOS and biopterin pathways. *American Journal of Physiology - Heart and Circulatory Physiology*. 2010;298:H194-H201

192. de la Sierra A, Larrousse M. Endothelial dysfunction is associated with increased levels of biomarkers in essential hypertension. *Journal of Human Hypertension*. 2010;24:373-379

193. Kiermayer C, Michalke B, Schmidt J, Brielmeier M. Effect of selenium on thioredoxin reductase activity in Txnrd1 or Txnrd2 hemizygous mice. *Biological Chemistry*. 2007;388:1091–1097

194. Rizzuto R, Pinton P, Carrington W, Fay FS, Fogarty KE, Lifshitz LM, Tuft RA, Pozzan T. Close Contacts with the Endoplasmic Reticulum as Determinants of Mitochondrial Ca^{2+} Responses. *Science*. 1998;280:1763-1766

195. Rizzuto R, Pozzan T. Microdomains of Intracellular Ca^{2+}: Molecular Determinants and Functional Consequences. *Physiological Reviews*. 2006;86:369-408

196. de Brito OM, Scorrano L. Mitofusin 2 tethers endoplasmic reticulum to mitochondria. *Nature*. 2008;456:605-610

197. Zhang K. Integration of ER stress, oxidative stress and the inflammatory response in health and disease. *International Journal of Clinical and Experimental Medicine*. 2010;3:33-40

198. Xu C, Bailly-Maitre B, Reed JC. Endoplasmic reticulum stress: cell life and death decisions. *The Journal of Clinical Investigation*. 2005;115:2656-2664

199. Michalak M, Groenendyk J, Szabo E, Gold LI, Opas M. Calreticulin, a multi-process calcium-buffering chaperone of the endoplasmic reticulum. *Biochemical Journal*. 2009;417:651-666

200. Schröder M, Kaufman RJ. ER stress and the unfolded protein response. *Mutation Research/Fundamental and Molecular Mechanisms of Mutagenesis*. 2005;569:29-63

201. Shen X, Zhang K, Kaufman RJ. The unfolded protein response—a stress signaling pathway of the endoplasmic reticulum. *Journal of Chemical Neuroanatomy*. 2004;28:79-92

202. Basha B, Samuel SM, Triggle CR, Ding H. Endothelial dysfunction in diabetes mellitus: possible involvement of endoplasmic reticulum stress? *Experimental Diabetes Research*. 2012;vol 2012:Article ID 481840

203. Tu BP, Weissman JS. Oxidative protein folding in eukaryotes: mechanisms and consequences. *The Journal of Cell Biology*. 2004;164:341-346

204. Edman JC, Ellis L, Blacher RW, Roth RA, Rutter WJ. Sequence of protein disulphide isomerase and implications of its relationship to thioredoxin. *Nature*. 1985;317:267-270

205. Ferrari DM, Söling HD. The protein disulphide-isomerase family: unravelling a string of folds. *Biochemical Journal*. 1999;339:1-10

206. Turanov AA, Su D, Gladyshev VN. Characterization of Alternative Cytosolic Forms and Cellular Targets of Mouse Mitochondrial Thioredoxin Reductase. *Journal of Biological Chemistry*. 2006;281:22953-22963

207. Liu CY, Kaufman RJ. The unfolded protein response. *Journal of Cell Science*. 2003;116:1861-1862

208. Michalak M, Milner RE, Burns K, Opas M. Calreticulin. *Biochemical Journal*. 1992;285 (Pt 3):681-692

209. Orrenius S, Zhivotovsky B, Nicotera P. Regulation of cell death: the calcium-apoptosis link. *Nature Reviews Molecular Cell Biology*. 2003;4:552-565

210. Ha MK, Chung KY, Bang D, Park YK, Lee KH. Proteomic analysis of the proteins expressed by hydrogen peroxide treated cultured human dermal microvascular endothelial cells. *PROTEOMICS*. 2005;5:1507-1519

211. Reinhardt C, von Brühl M-L, Manukyan D, Grahl L, Lorenz M, Altmann B, Dlugai S, Hess S, Konrad I, Orschiedt L, Mackman N, Ruddock L, Massberg S, Engelmann B. Protein disulfide isomerase acts as an injury response signal that enhances fibrin generation via tissue factor activation. *The Journal of Clinical Investigation*. 2008;118:1110-1122

212. Cho J, Furie BC, Coughlin SR, Furie B. A critical role for extracellular protein disulfide isomerase during thrombus formation in mice. *The Journal of Clinical Investigation*. 2008;118:1123-1131

213. Scull CM, Tabas I. Mechanisms of ER Stress-Induced Apoptosis in Atherosclerosis. *Arteriosclerosis, Thrombosis, and Vascular Biology*. 2011;31:2792-2797

214. Civelek M, Manduchi E, Riley RJ, Stoeckert CJ, Davies PF. Chronic Endoplasmic Reticulum Stress Activates Unfolded Protein Response in Arterial Endothelium in Regions of Susceptibility to Atherosclerosis. *Circulation Research*. 2009;105:453-461

215. Feaver RE, Hastings NE, Pryor A, Blackman BR. GRP78 Upregulation by Atheroprone Shear Stress Via p38-, α2β1-Dependent Mechanism in Endothelial Cells. *Arteriosclerosis, Thrombosis, and Vascular Biology*. 2008;28:1534-1541

216. Li J-M, Shah AM. Endothelial cell superoxide generation: regulation and relevance for cardiovascular pathophysiology. *American Journal of Physiology - Regulatory, Integrative and Comparative Physiology*. 2004;287:R1014-R1030

217. Madamanchi NR, Runge MS. Mitochondrial Dysfunction in Atherosclerosis. *Circulation Research*. 2007;100:460-473

218. Tabas I. The Role of Endoplasmic Reticulum Stress in the Progression of Atherosclerosis. *Circulation Research*. 2010;107:839-850

9 Abbreviations

Ang1	Angiopoietin 1
ANOVA	Analysis of variance
AP-1	Activator protein 1
ASK1	Apoptosis signal-regulating kinase 1
ATP	Adenosine triphosphate
bFGF	Basic fibroblast growth factor
BH_4	Tetrahydrobiopterin
BiP	Binding immunoglobulin Protein
BSA	Bovine serum albumin
Ca^{2+}	Calcium ion
CCCP	carbonyl cyanide 3-chlorophenylhydrazone
cDNA	Complementary DNA
cGMP	Cyclic guanosine monophosphate
Cre	Cre recombinase
ΔΨm	Mitochondrial membrane potential
DMEM	Dulbecco´s modified eagle´s medium
DMSO	Dimethyl sulfoxide
DNA	Desoxyribonucleic acid
dNTP	Desoxynucleoside triphosphate
EC	Endothelial cell
EDHF	Endothelium-derived hyperpolarising factor
EDTA	Ethylenediaminetetraacetic acid
eEPC	Embryonic endothelial progenitor cell
eNOS	Endothelial nitric oxide synthase
ER	Endoplasmic reticulum
ETS	Electron transport chain
FAD	Flavin adenine dinucleotide
FCS	Fetal calf serum
Fe	Iron
FIH	HIF asparaginyl hydroxylase Factor inhibiting HIF
Flox	LoxP-flanked
FSC	Forward scatter
FSS	Fluid shear stress
H&E stain	Hematoxylin and eosin stain
H_2O_2	Hydrogen peroxide
HIF-1α	Hypoxia-inducible factor 1α
HO•	Hydroxyl radical
HRP	Horseradish peroxidase
HUVEC	Human umbilical vein endothelial cell

ICAM-1	Intercellular adhesion molecule-1
JC-1	5',6,6'-tetrachloro-1,1',3,3'-tetraethylbenzimidazolylcarbocyanine iodide
LDI	Laser Doppler Imaging
MCP-1	Monocyte chemotactic protein-1
MEF	Mouse embryonic fibroblast
mmHg	Millimetres of mercury
MMP	Matrix metalloproteinase
MOPS	3-morpholinopropanesulphonic acid
mRNA	Messenger ribonucleic acid
Na	Sodium
NADPH	Nicotinamide adenine dinucleotide phospate
NFκB	Nuclear factor κB
NO	Nitric oxide
O_2	Oxygen
O_2^-•	Superoxide anion
Occ	Occluded
$ONOO^-$	Peroxynitrite
PBS	Phosphate buffered saline
PCR	Polymerase Chain Reaction
PDI	Protein Disulfide Isomerase
PHD2	prolyl hydroxylase 2
PLGF	Placenta growth factor
Prx	Peroxiredoxin
pVHL	von Hippel-Landau tumour suppressor protein
RNA	Ribonucleic acid
ROS	Reactive oxygen species
SD	Standard deviation
SDS	Sodium dodecyl sulfate
SDS-Page	Sodium dodecyl sulfate-polyacrylamide gel electrophoresis
Sec	Selenocysteine
SEM	Standard error of the mean
shRNA	Short hairpin RNA
siRNA	Small interfering RNA
SNAP	Sodium nitroprusside
SOD	Superoxide dismutase
SSC	Side scatter
TAE buffer	Tris-acetic acid-EDTA buffer
TBST	Tris-buffered saline with Tween
TE buffer	Tris-EDTA buffer

TNF-α	Tumour necrosis factor-α
Txn	Thioredoxin
Txn1	(cytosolic) Thioredoxin 1
Txn2	(mitochondrial) Thioredoxin 2
TXNIP	Thioredoxin-interacting protein
Txnrd	Thioredoxin reductase
Txnrd1	(cytosolic) Thioredoxin reductase 2
Txnrd2	(mitochondrial) Thioredoxin reductase 2
$Txnrd2^{ECKO}$ mouse	Mouse lacking Txnrd2 in the endothelium
$Txnrd2^{ECWT}$ mouse	Mouse expressing Txnrd2 in the endothelium
UPR	Unfolded protein response
VCAM-1	Vascular cell adhesion molecule-1
VEGF	Vascular endothelial growth factor
VSMC	Vascular smooth muscle cell

Acknowledgements

I have received great support throughout my doctoral studies from many people who have helped me commence, persist and complete this thesis.

Foremost I wish to thank Prof. Dr. Ulrich Pohl for providing me not only with a position in which I could work on this project but also for all the suggestions, his support and for sharing his knowledge, both scientifically and academically.

I also wish to thank Dr. Heike Beck for accepting me as a group member, for providing laboratory space and resources. I am grateful for her patience and enthusiasm, for keeping me on track and for the numerous scientific and casual conversations.

I would like to thank PD Dr. Elisabeth Deindl as well as her group members Judith Pagel and Omary Chillo for teaching me the hind-limb ischemia model and collaborating for a significant part of this project. I am very grateful for all the help and the fruitful discussions, and for including me in group meetings and the new-year dinners.

I am very appreciative of the help provided by our group technicians Dorothee Gössel, Dora Kiesl and Matthias Semisch as well as for the lab spirit. They always offered a hand when things got difficult and a lot of this work could not have been performed in time without their help.
I am also indebted to Michael Schubert and Dr. Holger Schneider for their expertise and for investigating the vasoresponses of small arterioles from mice employed in this study.

All colleagues at the Walter-Brendel-Centre have been of importance to me throughout my doctoral studies, either scientifically, academically or by extending their friendship. I am greatly appreciative to previous and ongoing doctoral colleagues, especially and foremost those with whom I shared an office, numerous hours, some frustration but mostly happiness in this stage of life: Dr. Theres Fey, Markus Wortmann, Dr. Juliane Hellfritsch, Fabian Kellner, Philipp Franke, Laurentia Tanase, Alessia Fraccaroli, Bernd Uhl, Stefan Schmitt, Miriam Singer and Dr. Joachim Pircher. I would also like to thank Prof. Dr. Andreas Dendorfer, Dr. Petra Kameritsch, PD Dr. Markus Rehberg, PD Dr. Steffen Dietzel and Dr. Michael Thormann for their help.

I have been lucky to participate in a Marie Curie Initial Training Network. For this opportunity I am immensely grateful and would like to acknowledge all members of the network.

I would also like to thank my close friends for their encouragement and understanding.

Acknowledgements

To my family – thank you Anja and Nina for your reassurance and support whenever needed. To my parents – thank you for always believing in me, for pointing me in the right direction and for your unconditional support. Without you I would not have done this. Finally, I am immensely thankful to my wife Carina. Your patience, encouragement, understanding and love always kept me going. To them I dedicate this thesis.

Eidesstattliche Versicherung

Kirsch, Julian

Name, Vorname

Ich erkläre hiermit an Eides statt,

dass ich die vorliegende Dissertation mit dem Thema

Endothelial cell-specific deletion of the mitochondrial thioredoxin reductase impairs vascular remodelling

selbständig verfasst, mich außer der angegebenen keiner weiteren Hilfsmittel bedient und alle Erkenntnisse, die aus dem Schrifttum ganz oder annähernd übernommen sind, als solche kenntlich gemacht und nach ihrer Herkunft unter Bezeichnung der Fundstelle einzeln nachgewiesen habe.

Ich erkläre des Weiteren, dass die hier vorgelegte Dissertation nicht in gleicher oder in ähnlicher Form bei einer anderen Stelle zur Erlangung eines akademischen Grades eingereicht wurde.

München, den 28.05.2014

Ort, Datum

Unterschrift Doktorandin/Doktorand